Nutrient and energy recovery from urine

Philipp Kuntke

Nutrient and energy recovery from urine

Philipp Kuntke

Thesis
submitted in fulfilment of the requirements for the degree of doctor
at Wageningen University
by the authority of the Rector Magnificus
Prof. dr. M.J. Kropff,
in the presence of the
Thesis Committee appointed by the Academic Board
to be defended in public
on Friday 26 April 2013
at 1:30 p.m. in the New York Hall of the WTC Leeuwarden

für meine Eltern

Abstract

In conventional wastewater treatment plants large amounts of energy are required for the removal and recovery of nutrients (i.e. nitrogen and phosphorus). Nitrogen (N) compounds are removed as inert nitrogen gas and phosphorus (P) is for example removed as iron phosphate. About 80% of the N and 50% of the P in wastewater originate from urine[1], but urine only contributes about 1% to the volume of this wastewater. High nutrient concentrations can be found in urine when it is collected separately from other wastewater streams. In this thesis, the nutrient and energy recovery from urine was investigated. At first, urine samples were analyzed for their composition. This characterization showed that the composition of the organic fraction in these samples was always similar. The differences between the concentrations of specific organic compounds were caused by dilution, due to individual consumption patterns of people. Two alternatives to the state-of-the-art nutrient recovery concepts are evaluated. These alternatives are on the one hand membrane capacitive deionization (MCDI) and on the other hand struvite precipitation combined with a microbial fuel cell (MFC). The evaluation of the MCDI system showed that nutrients can be concentrated from diluted urine. With its relatively low energy demand, MCDI could be an alternative to electrodialysis. The evaluation of the phosphate recovery by struvite precipitation combined with ammonium recovery and energy production by an MFC showed that this concept is most promising. The highest ammonium recovery rate achieved was 9.57 g_N m^{-2} d^{-1} at a current density of 2.6 A m^{-2} (0.67 W m^{-2}) using real undiluted urine. The ammonium recovery and energy production by an MFC (-10 kJ g_N^{-1}) can be considered a breakthrough, as usually energy is needed to recover (i.e. ammonia stripping 32.5 kJ g_N^{-1})[1] or convert (i.e. Sharon-Anammox 16 kJ g_N^{-1})[1] ammonium. Predictions show that approximately 5.1 kg struvite and 7.3 kg ammonia-nitrogen can be recovered from one cubic meter of urine, while producing approximately 20 kWh. A comparison to state-of-the-art technology showed that this process can be a good alternative for nutrient recovery from urine. Furthermore, ammonium recovery and energy production by an MFC can possibly be applied to other wastewater streams.

Keywords: urine, urine treatment, nutrient recovery, microbial fuel cells, energy production from urine, membrane capacitive deionization

---

[1] According to M. Maurer, P. Schwegler, and T.A. Larsen, Water Science and Technology 48 (1), 37 (2003)

Contents

1

General Introduction

1.1 Introduction

1.1.1 Background

Since its dawn, humanity has thrived. The growth rate of the human population has been dramatically accelerated fueled by developments during and following the industrial revolution [100]. As of 2012, over 7 billion people live on earth [2]. As a result, the impact of human activities on the environment has reached a critical point, not just for humanity [74]. Three out of nine planetary boundaries - proposed thresholds for a 'safe operation space of humanity' - have been breached, namely 'climate change', 'biodiversity loss' and 'nitrogen cycle'[1]. Furthermore, others, such as the 'phosphorus cycle', are reaching the proposed boundary conditions [74]. This shows that humanity needs to reconsider its current strategies and change its behavior to prevent dramatic changes.

1.1.2 Essential nutrients

Nitrogen and phosphorus in their biologically available form are essential nutrients for living organisms and are often limiting factors for growth. Their respective cycles and human interference with them are presented in the following two paragraphs.

Nitrogen cycle

Nitrogen (N) has several essential functions for living organisms [54]; as amino acids (i.e. $NH_2CHRCOOH$ [2]), nitrogen is present in proteins, DNA and RNA. In chlorophyll, nitrogen is needed for binding and entrapment of the magnesium ion.

Inert N_2 gas is found abundantly in the atmosphere, where it represents approximately 78% of the present gasses. However, nitrogen is not available to most living organisms in its N_2 form and needs to be converted to more reactive forms. The nitrogen-cycle relies on biological, chemical and physical processes which transform nitrogen compounds. Natural nitrogen-fixation - transformation of inert N_2 to reactive NH_3 - is carried out by some bacteria (e.g. *Azotobacter spp., Klebsiella, various cyanobacteria, Rhizobium*) using the nitrogenase enzyme [54]. Subsequently, nitrogen

---

[1]as part of the geochemical flow boundary with the phosphorus cycle
[2]generic form of an alpha amino acid with R as an organic substitute

is available to other living organisms. Figure 1.1 shows a simplified scheme of the biological nitrogen-cycle.
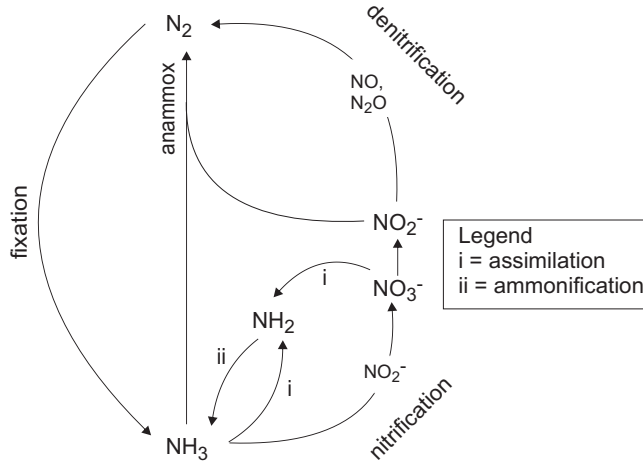
Figure 1.1: Simplified nitrogen-cycle showing the different processes involved in the conversion of the different nitrogen forms (adapted from Madigan et al. [54] to include the Anammox process).

Nowadays, humanity severely interferes with the nitrogen-cycle as large amounts (120-160 Mt yr^{-1}) of inert N_2 are transformed into reactive N-compounds [41, 74]. The Haber-Bosch process is used for the fixation of inert N_2 with H_2 as reactive NH_3 on an industrial scale, but the NH_3 synthesis requires a large amount of energy: 37 kJ g_N^{-1} [55]. Approximately 1% of the worlds energy production is used for ammonia synthesis by the Haber-Bosch process, but recent published research shows that this energy consumption can be lowered by using novel catalysts [41]. Most of the produced ammonia is used as fertilizer [41, 74]. In 2011 approximately 10 Mt of nitrogen based fertilizers per year were used in the European Union (EU) [18].

Phosphorus cycle

Phosphorus (P) is the 11th most abundant element in the earth crust. Phosphorus has an important role for life as it is involved in the metabolic energy transfer[3]

---

[3] ATP $\longrightarrow$ ADP + P
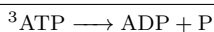
and is present in DNA and RNA as the backbone of sugar and phosphate groups. Phosphorus occurs in different forms and concentrations in the environment. Its concentration ranges from less than 0.001 wt% in sea water up to 15 wt% in phosphate rock [101]. Figure 1.2 shows a simplified scheme of the phosphorus-cycle without human interference.
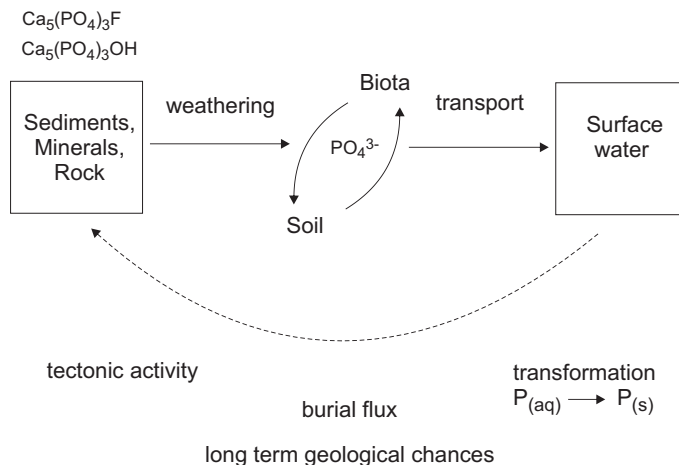
Figure 1.2: Simplified scheme of the P-cycle without human interference adapted from Valsami-Jones [101].

According to Valsami-Jones [101], this P-cycle compromises the erosion (weathering) of P containing solids (rock, sediment, minerals), which is followed by cycling between soil and biota with a consequent release to surface waters. Once in surface waters (i.e. rivers) phosphorus is transported to oceans and seas. In oceans and seas, phosphate transforms into P-containing solids due to burial flux, which is followed by long term geological changes (i.e. tectonic activities) closing this cycle.

Human activities interfere with this cycle as large amounts of phosphate rock are used to produce artificial fertilizers and the cycling capacity in the soil is reduced due to deforestation and soil loss. In 2011 approximately 1.5 Mt of P-fertilizers were used in the EU, which are applied in agriculture [18]. Therefore, a surplus of phosphate enters surface waters directly (wash-out from farmland) or indirectly (over the human/animal food chain) in addition to the natural phosphate loads [74, 101].

In course of the long time frame of the phosphorus-cycle and the current rate of mining, available resources of phosphate-rock are at risk of depletion: "...once resources begin to be depleted: there is no substitute."[3]. Based on proven reserves it is estimated that phosphorus reserves will be depleted within 50 to 100 years [17]. However, a recent phosphorous deposit study [65] suggests that available phosphate-rock deposits were underestimated in earlier studies and therefore phosphorus reserves will not be depleted as rapidly as predicted in earlier studies by Driver et al. [17]. Nontheless, at the same time the quality of the phosphorous ore is decreasing due to heavy metal contamination [14, 17]. Furthermore, rich phosphate-rock deposits are mainly found in a few countries such as Morocco (including Western Sahara), Iraq, China and Algeria [65].

1.1.3 Wastewater treatment

Due to the intensive use of phosphorus-products (i.e. fertilizers, anti-scalants, etc.) and nitrogen-products (i.e. fertilizers), these compounds can end up in wastewater. In wastewater P and N compounds were until recently considered as pollutants, as they increase the risk of eutrophication of receiving water bodies when released in large quantities. Therefore, these nutrients need to be removed or recovered from wastewater [3]. Currently, P and N compounds are largely lost during treatment in conventional wastewater treatment plants (WWTPs).

Nitrogen in WWTPs

Nitrogen is mainly removed by sequential biological nitrification and denitrifcation processes, after which it is released as N_2-gas to the atmosphere. Therefore, the valuable reactive nitrogen compounds (i.e. NO_3^-, NO_2^-, NH_4^+) are lost and additional processes are necessary to recover nitrogen in a useful form. The energy consumption of the nitrification and denitrifcation process is about 45 kJ g_N^{-1}-removed (without additional carbon source) and 109 kJ g_N^{-1}-removed (with methanol as carbon source) [55]. The Haber-Bosch process is applied globally for the recovery of nitrogen from the atmosphere in the form of ammonia (NH_3) using fossil fuels.

Anammox (Anaerobic Ammonium Oxidation) is a more energy efficient alternative to the conventional nitrification and denitrification process. Anammox relies on the biological conversion of ammonium and nitrite to nitrogen gas by specialized bacteria

(Planctomycete-like) [37]. Part of the ammonium needs to be converted to nitrite in a pretreatment step. Therefore, Anammox is combined with for example the Sharon process (single reactor system for high ammonium removal over nitrite) [102, 103]. According to Maurer et al. [55] the elimination of ammonium-nitrogen via the Sharon/Anammox process requires 16-19 kJ g_N^{-1}-removed.

P in WWTPs

Phosphorus can be immobilized in the wastewater sludge by precipitation with iron (II,III) salts (i.e. $FeCl_2$, $FeSO_4$, $FeCl_3$) or aluminium (III) salt ($AlCl_3$) [67]. However, the sludge from WWTPs is not suitable for direct re-use due to its large volume and also because other contaminants are immobilized in the sludge. The sludge can be biologically digested, de-watered and incinerated to reduce its volume and to remove organic contaminants. The remaining ash is rich in P, but also in heavy metals [63]. Furthermore, the solubility of these aluminium and iron phosphates is too low to be used directly as a fertilizer. The P-recovery by $FeSO_4$ requires 49 kJ g_P^{-1}-recovered [55]. The recovered P from wastewater still needs further processing before it can be used as a fertilizer (i.e. Triple Super Phosphate - TSP - $Ca(H_2PO_4)_2 \cdot H_2O$).

Alternatively, the Enhanced Biological Phosphate Removal (EBPR) process [57] can be used for a biological recovery of phosphates. So called polyphosphate accumulating organisms (PAOs) accumulate polyphosphates in their cells under aerobic conditions and break down these polyphosphates to phosphates under anaerobic conditions. The PAOs use two types of biopolymeres (polyphosphates and carbon storage polymeres) for this process. Under anaerobic conditions PAOs break down polyphosphates to phosphate and store short chain fatty acids as carbon storage polymeres (poly-β-hydroxybutyrate and poly-β-hydroxyvalerate). Under aerobic conditions PAOs degrade these carbon storage polymeres to take up phosphates and store them as polyphosphates. This allows for recovery of phosphorus from the excess sludge via precipitation as struvite ($MgNH_4PO_4 \cdot 6H_2O$) and hydroxyapatite ($Ca_5(PO_4)_3OH$) or incineration (which requires dewatering). According to Maurer et al. [55] the EBPR process combined with incineration requires about 28 kJ g_P^{-1}-recovered.

1.2 Urine

1.2.1 Urine separation

Urine contributes only 1% to the volume stream of conventional domestic wastewater. However, it contributes about 80% of the N-load [109] and 50% of the P-load [48]. One person produces on average 1.5 L of urine per day, which contains approximately 9.1 g_N L^{-1} and 1 g_P L^{-1} [56]. Figure 1.3 shows the different wastewater streams which can be collected in households with their respective nutrient and COD load. Nutrient and COD load were calculated based on data presented by Kujawa-Roeleveld and Zeeman [44], excluding the kitchen refuse waste stream.
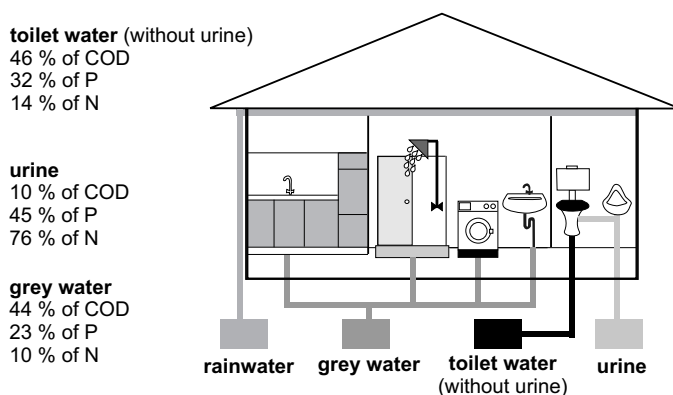
Figure 1.3: Overview of different types of source separated wastewater with their nutrient and COD loads. The nutrient and COD loads were recalculated from reported data [44], excluding the kitchen refuse stream.

The high nutrient concentrations in undiluted urine make it possible to develop more effective and energy efficient recovery technologies. Therefore, a separation of urine from other wastewater streams is an interesting option to keep these valuable nutrients concentrated and to develop a suitable nutrient recovery concept. Based

on this knowledge, European research groups started investigating treatment options for so called 'source separated urine' in the 1990s [40, 48] in order to promote sustainability of wastewater management. The term 'source separated urine' means that urine is separated at source (toilet) from other wastewater streams in order to prevent a dilution. Urine can be source separated by usage of urine separation toilets and (waterfree) urinals (Figure 1.4).

(a)   (b)
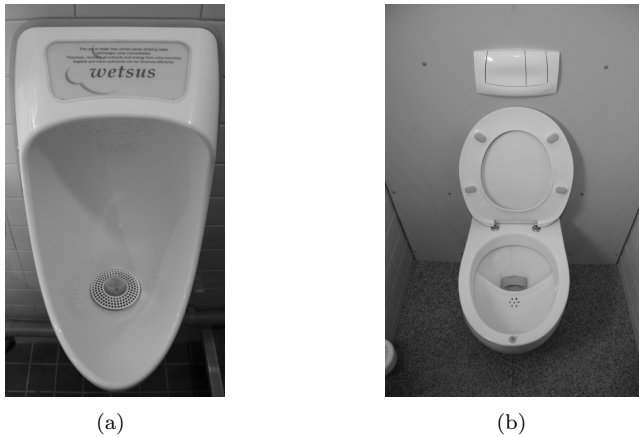
Figure 1.4: (a) Waterfree urinal type Urimat®-ECO (BioCompact Environmental Technology B.V., The Netherlands) and (b) separation toilet type Roediger No-mix (Roediger Vacuum GmbH, Germany).

1.2.2 Urine as a resource

Currently 10 Mt of nitrogen fertilizers and 1.5 Mt phosphorous fertilizers are used yearly in the EU [18]. The European food production is currently heavily dependent on phosphorous ore and fossil fuel imports for fertilizer production. Depletion of these primary raw materials and the potential political intervention by exporting countries would directly threaten EU food security. Direct and energy-efficient N and P recovery technologies will reduce those threats. Nutrient recovery from urine can provide 18% of the needed phosphorus and 25% of the needed nitrogen (details in Table 1.1).

Table 1.1: Possible coverage of N and P fertilizer from urine.

		Phosphorus	Nitrogen
Used Fertilizer [18]	(Mt yr^{-1})	1.5	10.0
Inhabitants EU [19]	(Million)	502.5	502.5
Excrete nutrients [15]	(Mt yr^{-1})	0.275[a]	2.476[b]
Expected coverage	(%)	18.3	24.8

[a] 1.5 L urine with 1 g_P L^{-1}, [b] 1.5 L urine with 9 g_N L^{-1}

1.2.3 Urine treatment

A detailed overview of different treatment processes for urine was presented by Maurer et al. [56]. Maurer et al. [56] reviewed reported methods for urine treatment and categorized them in hygenisation (Storage), volume reduction (Evaporation, Freeze-thaw, Reverse Osmosis), stabilisation (Acidification, Microfiltration, Nitrification), P-recovery (Struvite), N-recovery (Ion-exchange, Struvite, NH_3-stripping, Urea complexation), nutrient removal (Anammox) and micropollutant removal (Electrodialysis, Nanofiltration, Ozonation). Most of these processes were tested and evaluated under laboratory conditions. In the following paragraph nutrient recovery processes and proposed techniques are explained in detail.

1.2.4 Recovery of nutrients

Struvite precipitation

Struvite precipitation is a convenient choice for the simultaneous recovery of P and part of N from urine [75]. The pH of urine after urea hydrolysis[4] is sufficiently high (pH $\geq$ 9) and triggers the precipitation of struvite [97, 98]. Struvite from urine can occur in two main forms: $MgNH_4PO_4 \cdot 6\,H_2O$ (MAP) and $MgKPO_4 \cdot 6\,H_2O$ (MKP) [87, 88]. Therefore, a recovery of either ammonium or potassium struvite from urine is possible under the right conditions [111].

---

[4]Urea $((NH_2)_2CO)$ is hydrolyzed by the bacterial enzyme urease to NH_3 and carbamate (NH_2COOH), whereas carbamate hydrolyzes further to NH_3 and bicarbonate [58].

Ion-exchange

The application of ion-exchange materials such as resins or natural occurring zeolites (e.g. clinoptilolite and others) have been tested for the recovery of ammonium from wastewater [38] and urine [51]. Lind et al. [51] reported that the combination of zeolite treatment in combination with addition of MgO for struvite precipitation results in a good recovery of nutrients. The product (struvite and zeolite) can be used as soil conditioner.

NH_3-stripping

Ammonia (NH_3) can be recovered from urine by NH_3-stripping [4]. For this process additional chemicals (e.g. CaO, NaOH, etc.) are necessary to increase the pH to $\geq$ 9.3. Energy is required to heat the installation and potentially also for the applied vacuum [4, 55, 56]. The recovered product is a liquid solution of ammonium salt (e.g. with Cl^-, SO_4^{2-} or NO_3^- as the counter ions). The energy requirement for N-recovery by NH_3-stripping is 32.5 kJ g_N^{-1}-recovered [55].

1.2.5 Treatment processes

The large number of different treatment options means that various treatment concepts can be developed for urine. In the following two paragraphs two treatment concepts for urine are explained in detail.

Treatment concept as envisioned by DHV

Recently, a new process was proposed by Hemmes et al. [32], which combines struvite precipitation with energy production in a so called solid oxide fuel cell (SOFC). A SOFC is a fuel cell which operates at high temperature and usually uses natural gas or propane as a fuel [85]. The principle of the process is illustrated in Figure 1.5.

In the proposed process, ammonium is recovered from wastewater as struvite. Consequently, the struvite is thermally decomposed according to reaction 1.1 [5]:

$$MgNH_4PO_4 \cdot 6\,H_2O \xrightarrow{\text{heat}} NH_3 + MgHPO_4 + 6\,H_2O \qquad (1.1)$$

The released NH_3-gas is converted to electricity, N_2-gas and water in a modified SOFC (the then called NH_3-fuel cell [21, 62]). The remaining $MgHPO_4$ can be reused
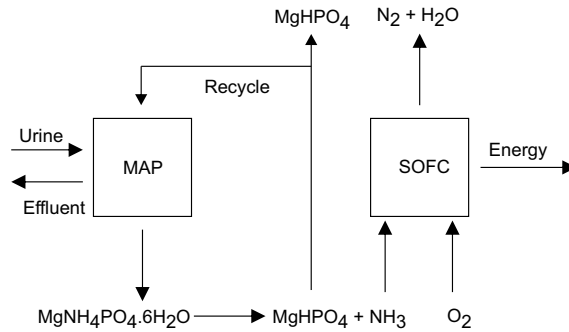
Figure 1.5: The envisioned DHV concept, adapted scheme from Hemmes et al. [32]

for the struvite precipitation as the magnesium and phosphate source. The process was envisioned for the treatment of wastewater from a WWTP as well as from urine to remove nitrogen and produce electricity. For the treatment of urine, this process is also known as the 'Gele stroom' ('Yellow current') process [24].

Recovery processes in practice by GMB

Currently, there is only one operational recovery system for nutrients from urine on a large scale [25]. The so called SaNiPhos® process was designed to produce struvite and ammonia-liquid (i.e. $2\,NH_4^+(aq) + SO_4^{2-}(aq)$). The centralized SaNiPhos® installation is situated at the WWTP near to Zutphen (GMB, The Netherlands), which requires the transport of urine from various locations to the installation. The process includes 8 steps in total [8, 25].

1. Buffer tank; controlled hydrolysis of urea at pH 6-7 with acid dosing

2. Filter unit; removal of larger unwanted particles

3. CO_2-stripper; removal of CO_2 at pH of 4 and aeration

4. MAP precipitation; recovery of MAP by dosage of $Mg(OH)_2$ and NaOH

5. NH_3-stripping; removal of NH_3 at pH of 10-11 by dosage of caustic, increased temperature (60°C) and aeration with process air (closed circuit)

6. Heat exchanger; heat recovery

7. Ammonia adsorption; NH_3 is recovered from the process air leaving the NH_3-stripper

The high energy, chemicals and heat demand of this system requires a centralized treatment facility. Therefore, it is necessary to transport large amounts of urine by motor lorries from various collection locations to the central treatment system, which results in additional costs and pollution (CO_2 emissions).

1.2.6 Criteria for an optimal process

Criteria for an optimal process included the recovery of nutrients (nitrogen and phosphorus) in a useful form (e.g. as fertilizers). A decentralized concept is preferred over a centralized system, in order to minimize the need to transport large amounts of water. Usually this transport would need additional infrastructure or a transport by motor lorries, which results in additional costs and emission of pollution. The energy requirement of the recovery process should be low. An energy production step - from for example the organic compounds - should be considered. An energy production could lower the demand for additional energy input and therefore lower the operational costs. Furthermore, the process should be compact and robust in design, so it can be operated in a decentralized setting. Both processes presented earlier do not fulfill all of these requirements. A summary of the advantages and disadvantages of the respective technologies is shown in table 1.2.

Table 1.2: Advantages and disadvantages of the DHV and GMB process.

Treatment Process	Advantages	Disadvantages
DHV 'Gele stroom'	energy production P-recovery $MgHPO_4$ re-use	no N-recovery
GMB 'SaNiPhos®'	N-recovery P-recovery	energy consumption chemical usage transport of urine

1.3 Scope and outline of this thesis

The state-of-the-art nutrient recovery from urine technology is energy intensive and/or requires large amounts of chemicals. Therefore, the scope of this thesis is to evaluate alternatives for the recovery of nutrients and energy from urine. In Chapter 2, the organic and inorganic fractions of urine from a large sample group were characterized to investigate their compositions and variations. This is essential for the development and optimization of a suitable treatment strategy. The application of membrane capacitive deionization (MCDI) as tool to concentrate and recover nutrients from urine was investigated in Chapter 3. Chapters 4 and 5 focus on the application of a bio-electrochemical system (BES) for the recovery of nitrogen with the possibility of simultaneous energy production from synthetic and real urine/wastewater. The applicability of BES for wastewater treatment containing high NH_4^+ concentrations is evaluated in Chapter 4 using synthetic wastewater. A concept for a future nitrogen recovery and energy production system is presented in Chapter 5, in which real undiluted urine is treated. Chapter 6 presents a treatment concept based on results of Chapter 5 in combination with phosphate recovery by Struvite (MAP) precipitation. A scenario analysis is presented based on these results and on literature. Finally, Chapter 7 gives a broader reflection of the presented work in this thesis. Furthermore, the proposed recovery concept from Chapter 6 is compared with the GMB 'SaNiPhos®' process and the envisioned DHV 'Gele stroom' process with respect to energy requirements and nutrient recovery prospects.

2

Urine characterization with special emphasis on the composition of the organic fraction

Abstract

In this study, the organic and inorganic fractions of urine samples were characterized to investigate their compositions and study their variations. In total 92 urine samples from healthy persons and 14 samples from persons in a hospital were analyzed. The inorganic fraction was analyzed for the most abundant components. The organic fraction was analyzed in terms of the chemical oxygen demand and in terms of functional groups of organic compounds commonly found in urine by ^{1}H-NMR. Theoretical COD values were calculated from the results of the ^{1}H-NMR analysis and compared to the actual measured COD values in the respective urine samples. Additionally, the total nitrogen content of the samples was measured. The results show that although a broad spectrum of urine samples was taken, the composition of the organic compounds was similar in these samples. However, relatively large fluctuations in the concentrations of organic compounds and measured COD in the urine samples were observed. This difference is caused by dilution, due to the individual water consumption of the sample donors. Over 73% of the COD in non-hospital samples is aliphatic and can be considered biodegradable. No direct correlation between the total nitrogen concentration and the measured COD was found.

Authors P. Kuntke, H. Bruning, G. Zeeman and C.J.N. Buisman

2.1 Introduction

Urine contributes less than 1% to the volume of domestic wastewater. However, 80% of the nitrogen (N), 70% of the potassium (K) and 50% of the phosphorus (P) load to a wastewater treatment plant originates from urine [108]. Urine contains on average 1 g_P L^{-1} phosphorus, 9 g_N L^{-1} nitrogen and 2 g_K L^{-1} potassium. Therefore, urine can be considered as a valuable source for the recovery of nutrients and numerous technologies have been developed to recover these nutrients [46, 56].

In addition to these nutrients, a high chemical oxygen demand (COD) of 10 g_{O_2} L^{-1} [48, 56, 99] has been reported. This indicates a considerable amount of oxidizable organic compounds, which can be used for energy production by biological processes (e.g. bio-electrochemical systems [27]). This energy could be used to recover nutrients. A broad overview of commonly found organic compounds in urine and excreted amounts are given in the Documenta Geigy [15]. In this book, various literature sources (mostly medical studies) are used, but nothing is reported about measured COD. Therefore, little to nothing is known about the origin and variation of the COD in urine samples. Furthermore, little attention has been given to explain the relatively high COD values which are measured in urine compared to the measured concentrations of organic compounds.

In this study, the organic and inorganic fraction of urine was characterized to investigate the compositions and study their variations. This characterization could be useful for the development and optimization of a suitable recovery strategy using the potential energy contained in the organic compounds. The inorganic fraction was analyzed for the most abundant components. The organic fraction was analyzed in terms of most abundant components based on functional groups and COD. The urine samples were analyzed by ^{1}H-NMR on the basis of functional groups of organic compounds commonly found in urine. Theoretical COD values were calculated from the results and compared to the actual measured COD values in the respective urine samples.

2.2 Materials and Methods

2.2.1 Urine samples

Two sets of urine samples were collected. The first urine sample set was collected from colleagues at Wetsus (Leeuwarden, The Netherlands) and the second sample set was collected from patients at the hospital MCL (Medisch Centrum Leeuwarden, The Netherlands). The Wetsus samples consists of morning and afternoon urine samples. In total 92 Wetsus urine samples (54 from male donors, 34 from female donors and 4 from unknown gender donors, age group between 18 and 65 years) were collected anonymously. The MCL samples (total of 14 samples, unknown gender) were collected from hospital patients. The samples were directly analyzed for the concentration of cations, anions, COD, total nitrogen and ammonium. Small aliquots (3 × 1.5 mL) of each sample were directly frozen at -80 ˚C until ^{1}H-NMR analysis.

2.2.2 ^{1}H-NMR measurements

Unfrozen sample aliquots (1.5 mL) were vortexed for 60 seconds to homogenize the samples. Afterwards solids and proteins were separated[1] by centrifugation for 10 minutes at 10,000 *g*. 200 µL of the supernatant was transferred to a clean PCR vial. In the PCR vial the sample was mixed with 200 µL buffer solution (0.1 M pH 7 sodium phosphate buffer, 10 volume % D_2O, and 25 µM TSP). From this mixture 200 µL was transferred to a 3 mm NMR tube and the samples were analyzed directly after preparation.

The ^{1}H-NMR measurements were performed using an Avance III 600 MHz spectrometer (H-frequency 600.45 MHz, 14.1T, Bruker, Germany). The sample measurements were fully automated (sample transfer, temperature control 300 K, tuning and matching, 90˚ pulse determination). The following conditions were used for the 1 dimensional ^{1}H-NMR experiments: pulse sequence, noesygppr1d; ~ 9 µs a 90˚ ^{1}H-NMR pulse; 4 seconds relaxation delay; 1.8 seconds acquisition time; 4 dummy scans; 256 total scans; spectral width: 18,000 Hz.

---

[1]Proteins were analyzed according to Bradford [9] see chemical analysis, page 20.

2.2.3 ^{1}H-NMR data analysis

Each NMR spectrum was segmented into 0.05 ppm pieces in the spectral region (σ) from 10 to 0.05 ppm with the Topspin software (Version 3.0.a, Bruker, Germany). The water peak region ($\sigma = 4.5$ - 4.8) and the urea peak region ($\sigma = 5.3$ - 5.9) were excluded from the analysis, since water and urea do not contribute to the measured COD of a sample. The remaining integrals from the defined segments were analyzed further on basis of the Bruker NMR table (see supporting information Table 2.4, page 28) for ^{1}H chemical shifts in organic compounds (Bruker, Germany) [11]. Where functional groups were overlapping in their spectral region, the overlapping parts of these integrals were equally divided among these functional groups. The specific regions and example compounds found in urine are shown in Figure 2.1.
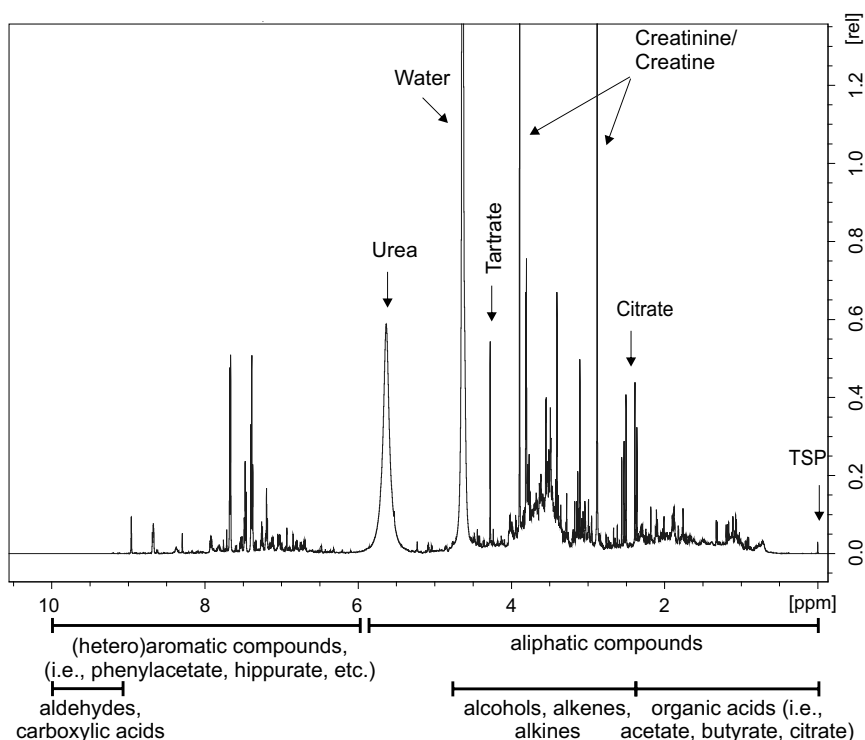
Figure 2.1: An overview of a representative urine sample analyzed with ^{1}H-NMR. The arrows indicate specific regions and compounds.

Since creatinine and creatine are the most abundant organic components in urine, their respective peak regions were excluded from the routine analysis and their signals were analyzed separately. For the COD calculations no distinction was made between creatine (reaction 2.1) and creatinine (reaction 2.2), since their oxidation requires the same amount of oxygen according to:

$$C_4H_9N_3O_2 + 3\,O_2 \longrightarrow 4\,CO_2 + 3\,NH_3 \tag{2.1}$$

$$C_4H_7N_3O + 3\,O_2 + H_2O \longrightarrow 4\,CO_2 + 3\,NH_3 \tag{2.2}$$
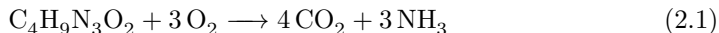
The ^{1}H concentration in a sample (excluding the water and urea regions) was calculated from the sums of the integrals $\left(\sum \left(\int\,^1H_i\,(\sigma)\right)\right)$. The amount of oxygen (mol) needed for the oxidation of a functional group was determined by setting up the redox-equation for the oxidation of the functional group (e.g. -CH$_3$ $+1\frac{3}{4}\,O_2 \longrightarrow CO_2 + 1\frac{1}{2}\,H_2O$). Afterwards the COD was calculated according to:

$$COD_{calc.} = \sum (COD_i \cdot n_i) \tag{2.3}$$

Where $COD_{calc.}$ (g L^{-1}) is the calculated total COD, COD_i (g mol^{-1}) is the COD of functional group i and n_i (mol L^{-1}) is the concentration of the functional group i. Additionally, a theoretical COD was calculated based on the reported concentrations from Documenta Geigy [15]. The Documenta Geigy lists average excreted amounts (mg d^{-1}) and concentrations (mg L^{-1}) originating from various literature sources. When excreted amounts per day were reported, the concentration was determined assuming an excretion of 1.5 L urine per day. The theoretical COD was calculated on basis of the sum formula of the reported compounds and their average concentrations (similar to Equation 2.3).

2.2.4 Analysis and measurements

Samples were analyzed for the concentration of cations, anions, chemical oxygen demand (COD), total nitrogen (T$_N$) and total ammonium nitrogen (NH$_4^+$-N). The cation concentrations were determined using an ICP-OES, type Perkin Elmer Optima 3000 DV (Waltham, Massachusetts, USA). The anion concentrations were determined using an ion chromatography system, type Metrohm IC Compact 761 (Schiedam, The

Netherlands). NH_4^+-N was analyzed using test kit LCK 303; T_N was analyzed using test kit LCK 338 and COD was analyzed using test kit LCK 314 (all Dr. Lange, HACH, Loveland, Colorado, USA) in a spectrophotometer HACH XION 500 (HACH, Loveland, Colorado, USA). Proteins were analyzed by the Bradford method [9]. All samples were analyzed in duplicate. Samples for determination of anion and cation concentrations were filtered through 0.45 µm filters prior to analysis. The BOD_5 was determined using the OxiTop® system (WTW, Germany) over a period of 5 days at 20°C.

2.3 Results and discussion

2.3.1 Overview of urine samples

An overview of the measured sample parameters is shown in Table 2.1. For comparison reported literature values are given in the same table.

Table 2.1: Average concentrations and standard deviations obtained from the 106 analyzed urine samples and reported literature values.

Compound (g L^{-1})	This study			literature[a] [15]	literature[a] [99]
COD	9.0	$\pm$	4.1	n.r.[b]	10.0
T_N	8.6	$\pm$	3.7	8.83	9.2
Cl^-	3.8	$\pm$	2.1	4.97	3.8
P_{total}	0.7	$\pm$	0.5	0.8-2.0	0.54
PO_4^{3-}	2.00	$\pm$	1.62	n.r.[b]	n.r.[b]
S_{total}	0.6	$\pm$	0.3	1.315	0.5
SO_4^{2-}	1.18	$\pm$	0.69	n.r.[b]	n.r.[b]
Na^+	2.41	$\pm$	1.43	3.45	2.60
K^+	1.89	$\pm$	1.16	2.737	2.20
Mg^{2+}	0.078	$\pm$	0.051	0.119	0.0
Ca^{2+}	0.106	$\pm$	0.073	0.233	0.0
NH_4^+-N/NH_3-N	0.431	$\pm$	0.192	0.463	8.1

[a] Standard deviation not available; [b]not reported

The measured concentrations in the analyzed samples are similar to concentrations

reported in literature [15, 99]. Only the NH_4^+/NH_3 concentration reported by Udert et al. [99] was significantly higher. This difference can be explained by the hydrolysis of urea $((NH_2)_2CO)$ to ammonia and carbamate followed by the subsequent carbamate decomposition, which leads to the formation of NH_3, NH_4^+ and CO_2 [58, 96]. The high standard deviation determined from the measured urine samples presented in this work reflects the individual diet and consumption patterns (food and water) of the individual persons who provided the urine samples. No information about standard deviations were available for the literature sources [15, 99]. The measured concentrations are similar to the literature values, which shows that representative urine samples were taken for the analysis of the COD content of urine in this study.

2.3.2 COD composition derived from literature

An extensive overview of various compounds commonly found in urine is presented in the Documenta Geigy [15]. A theoretical COD was calculated based on the reported average concentrations (g L^{-1}) or excreted amounts (g d^{-1}) of organic compounds according to the procedure explained in Materials and Methods (page 19). Table 2.2 shows the calculated COD from the various compound groups as reported in the Documenta Geigy [15].

Table 2.2: Calculated COD based on compound groups reported in the Documenta Geigy[15]

Compound Group	COD (g L^{-1})
Proteins	0.019
Amino acids	0.802
other N-Containing	3.887
Carbohydrates	0.498
Organic acids	0.770
Lipids	0.034
Sum	6.009

It has to be mentioned that the reported concentrations or excreted amounts originate from various literature sources and that those studies usually focus on one specific group of compounds. Therefore, these results show an incomplete picture of the COD composition. Furthermore, most of these studies do not report COD values,

as they have a medical background. Therefore, Table 2.2 only represents an approximation based on reported literature and further research on the COD composition is necessary. Also the calculated average COD differs from the average COD measured in various studies [56, 99] and the results presented in this study (see Table 2.1).

2.3.3 Characterization of COD by NMR

First the feasibility of using a functional group based analysis to characterize the COD composition as described in the Material and Method section 2.2.3 (page 19) was investigated. Therefore, the relation between the measured COD and the ^{1}H concentration in the analyzed functional groups was determined using linear regression analysis. Figure 2.2a shows the relation between the measured COD and ^{1}H concentration of the 106 urine samples.
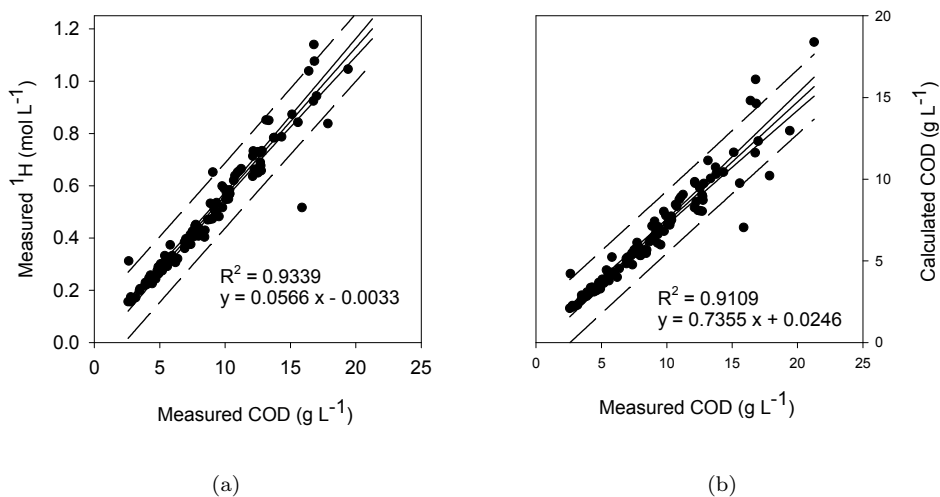
Figure 2.2: Linear regression analysis between the measured COD ^{1}H concentration of the functional groups (a) and the calculated COD (b) including for both 95% prediction band (dashed line) and 95% confidence band (solid line)

A good correlation ($R^2 = 0.9339$) was found between the ^{1}H concentration in the analyzed functional groups and the measured COD values. This proves that the ^{1}H-

NMR measurements provide a good overview of the organic compounds present in these urine samples, except for proteins which were removed prior to analysis.

As a next step, the relation between the calculated COD[2] and the measured COD was investigated by linear regression analysis. Figure 2.2b shows the relation between the measured COD and calculated COD of the urine samples. A correlation factor (R^2) of 0.9109 was found between the calculated COD and the measured COD. In general, the calculated COD values were 26% lower than the measured COD values. This difference can be explained by two factors: 1) The calculated COD does not include the COD of the protein content and 2) The sum formulas of the functional groups are only an approximation for organic compounds present. Both factors lead to an underestimation of the calculated COD. However, the good linear correlation between measured COD and measured ^{1}H concentration also shows that the composition of organic compounds is relatively stable (over the samples measured COD range) which indicates that the differences in COD are mainly caused by dilution.

Additionally, the relation between the measured total nitrogen (T_N) as well as the measured ion concentration and the measured COD was investigated. No direct correlation was found between the measured COD and those parameters (supporting information in Table 2.5 on page 29).

2.3.4 Differences between sample sets

The differences between sample sets were determined for further investigations. Therefore, the samples were grouped by their sampling time and gender of the persons. The hospital samples were a separated group. The samples were analyzed using a box-and-whisker diagram for the differences in COD, total nitrogen and ionic strength of the sample sets. The ionic strength was calculated from the dominant anions and cations as presented in Table 2.1 according to Equation 2.4.

$$\text{Ionic Strength} \, (\text{mol L}^{-1}) = \frac{1}{2} \cdot \sum_{i=1}^{n} \left(c_i z_i^2 \right) \tag{2.4}$$

Where c_i is the measured concentration of an ion and z_i is the charge of the respective ions. No significant differences were found between the various groups, only the hospital sample set showed minor differences compared to the other samples (see

---

[2]determined according to Equation 2.3 and Table 2.4

supporting information in Figure 2.4 on page 30). The results of the linear regression analysis of the calculated COD and measured COD of the respective sample sets are presented in Table 2.3. All sample sets collected at Wetsus show a good correlation, only the hospital sample set shows a lower correlation factor, which probably is due to pathological reasons.

Table 2.3: Results of the linear regression analysis of the different sample sets calculated COD vs measured COD

	R^2	Slope	Intercept
Morning	0.9408	0.820	-0.436
Afternoon	0.9770	0.746	-0.045
Male	0.9572	0.788	-0.322
Female	0.9528	0.789	-0.205
Hospital	0.8111	0.586	0.735

2.3.5 Relative contributions of the functional groups to the COD

Further analysis was performed to identify the relative contribution of the organic compounds to the calculated COD. Therefore, the specific COD of the organic compounds and proteins in the urine samples were divided by the total calculated COD (including the calculated COD of the protein content) of the respective samples. The relative contribution to the calculated COD of the different functional groups and protein content is shown in Figure 2.3. Although high standard deviations were found for the measured COD (9.0 ± 4.1 g L^{-1}) and calculated COD (6.6 ± 3.1 g L^{-1}), based on the 106 samples, very little variation was found in the relative contributions to the COD. For the Wetsus sample set most of the COD originates from aliphatic compounds (73.2%) and creatinine/creatine (20.7%). The remaining COD originates from aromatic and hetero aromatic compounds (3.4%) and proteins (2.7%). The hospital samples show a relatively high COD contribution from the proteins (11.8%) and therefore a respectively lower COD contribution by creatinine/creatine (14%) and aliphatic compounds (69.9%), which is a result of their medical condition.

The high amount of aliphatic compounds indicates a high biodegradability of the organic compounds found in urine. The biodegradability was determined by measuring the biological oxygen demand (BOD$_5$) of 10 representative urine samples. A
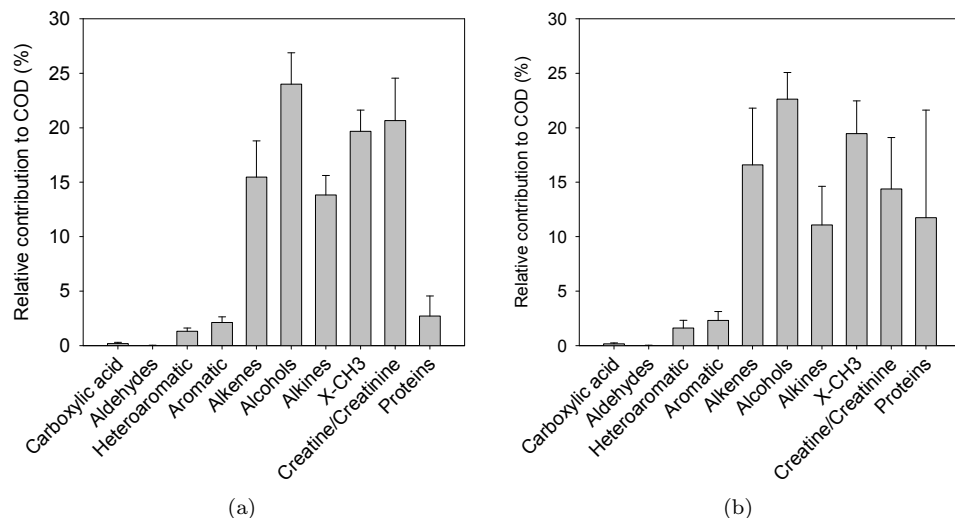
Figure 2.3: Relative contributions of the organic compounds to the calculated COD for (a) the Wetsus sample set and (b) the Hospital sample set.

BOD_5 of $67 \pm 2\%$ of the measured COD was found. This relatively high BOD_5 indicates a high biodegradability of the organic compounds found in urine. In literature, an even higher aerobic biodegradability of 85% was reported for the organic compounds in urine [95].

2.4 Conclusions

This work shows that although a broad spectrum of urine samples was taken, the composition of the organic compounds was similar in these samples. However, relatively large fluctuations in the concentration of total organic compounds and measured COD in the urine samples were observed. This difference in the measured COD of the urine samples is caused by dilution. This shows that urine is a relatively stable wastewater stream without major differences in the COD composition. Therefore, a conversion of chemical energy stored in these compounds into electrical energy by a bio-electrochemical system (i.e. MFC) can be an interesting option to consider for future research. The higher protein content in the hospital urine samples com-

pared to the other samples makes this urine more complex. Over 73% of the COD in non-hospital samples was aliphatic and can be considered biodegradable. No direct correlation between the total nitrogen concentration and the measured COD was found.

Acknowledgements

Supporting Information

Table 2.4: Overview of the spectral region (σ) for ^{1}H chemical shifts (ppm) in organic compounds

Functional Group	Sum-formula	σ (ppm)		
Carboxylic acid	COOH	10.0	$\rightarrow$	8.95
Aldehydes	COH	10.0	$\rightarrow$	9.45
Heteroaromatic	C_5H_5N	8.9	$\rightarrow$	8.05
	C_5H_5N	7.4	$\rightarrow$	6.45
Aromatic	C_6H_6	8.5	$\rightarrow$	6.45
Alkenes	=CH-	8.0	$\rightarrow$	4.45
	$=CH_2$	6.4	$\rightarrow$	4.45
Alcohols	=HC-O-	5.3	$\rightarrow$	3.75
	$-H_2C-O-$	4.5	$\rightarrow$	3.5
	H_3C-O-	4.0	$\rightarrow$	3.25
Alkines	-CCH	3.0	$\rightarrow$	2.35
X-CH3	$=N-CH_3$	3.45	$\rightarrow$	2.25
	$-S-CH_3$	2.85	$\rightarrow$	2.1
	H_3C-	2.6	$\rightarrow$	2.1
	$-OC-CH_2-$	2.6	$\rightarrow$	2.1
	$H_2C=$	1.8	$\rightarrow$	1.1
	$-OC-CH_3$	2.6	$\rightarrow$	1.75
	$C-CH_3$	2.0	$\rightarrow$	0.05
	$X-C-CH_3$	2.0	$\rightarrow$	0.8

Table 2.5: Correlation factor (R^2) of various parameters obtained by linear regression analysis.

R^2	Cl^-	PO_4^{3-}	SO_4^{2-}	Na^+	K^+	Mg^{2+}	Ca^{2+}	NH_4^+	COD	T_N
Cl^-	1.00	0.05	0.09	0.60	0.35	0.15	0.14	0.14	0.08	0.15
PO_4^{3-}		1.00	0.71	0.12	0.06	0.26	0.04	0.48	0.45	0.47
SO_4^{2-}			1.00	0.12	0.10	0.33	0.11	0.74	0.52	0.76
Na^+				1.00	0.31	0.16	0.16	0.18	0.14	0.18
K^+					1.00	0.08	0.09	0.10	0.10	0.11
Mg^{2+}						1.00	0.16	0.26	0.27	0.31
Ca^{2+}							1.00	0.07	0.08	0.11
NH_4^+								1.00	0.58	0.88
COD									1.00	0.59
T_N										1.00

(a)

(b)

(c)
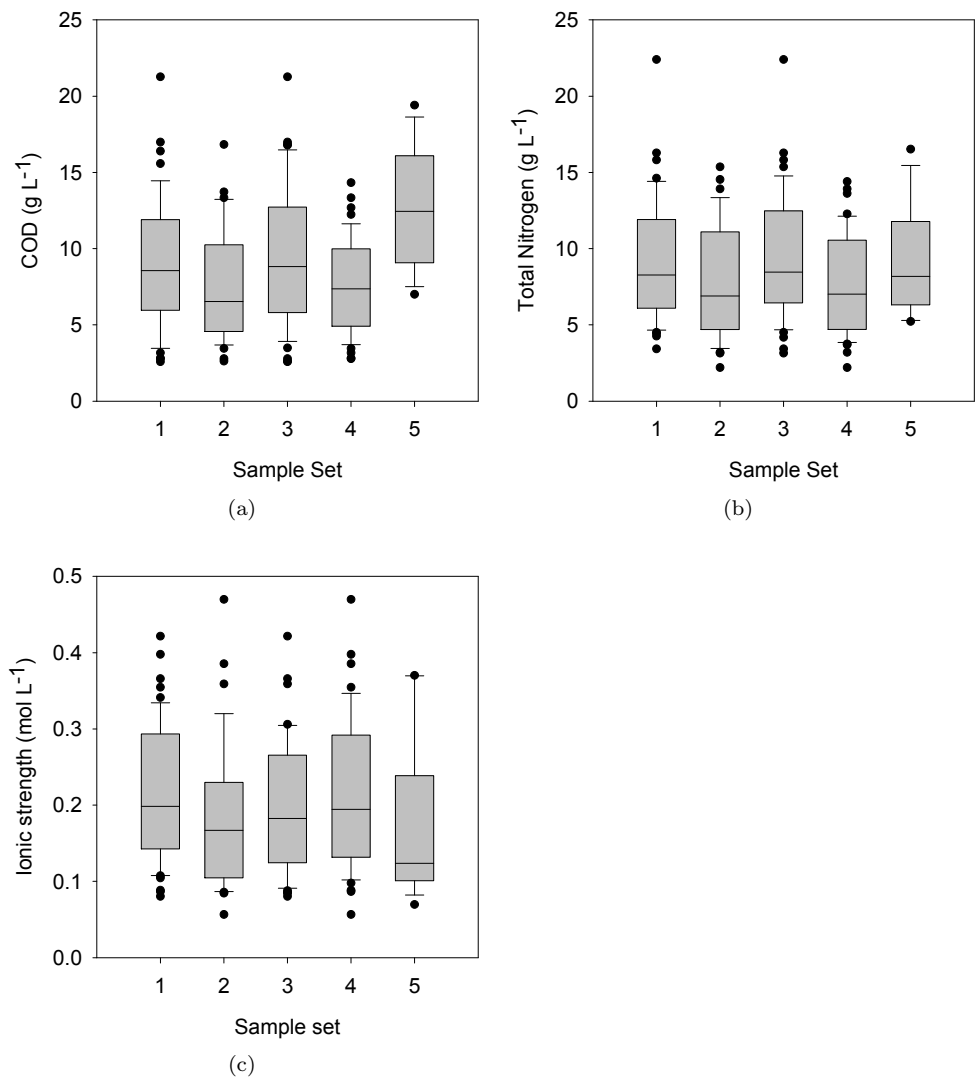
Figure 2.4: Box-and-whisker diagrams of the different sample sets for (a) COD, (b) Total nitrogen and (c) ionic strength. Where 1 are samples from male donors, 2 are samples from female donors, 3 are samples from morning, 4 are samples from afternoon and 5 are samples from hospital.

3

Membrane capacitive deionization as a novel tool to concentrate nutrients from urine

Abstract

This work describes the application of membrane capacitive deionization (MCDI) as a tool to concentrate and recover nutrients from urine. Concentrating nutrients is important for their recovery from diluted waste streams. The results obtained with model urine show that the applied flow rate has an effect on the concentration efficiency and recovery of nutrients. Higher flow rates led to high recoveries, whereas lower flow rates led to higher concentration efficiencies. Using MCDI it was possible to recover 99.3% of the potassium, 98.5% of the phosphate and 98.2% of the ammonium-nitrogen from diluted real urine. The low energy requirements (14.21 to 16.77 kJ L^{-1}) make MCDI an alternative to electrodialysis. Furthermore, MCDI allows for the separation of urea from ions.

Authors P. Kuntke, H. Bruning, G. Zeeman and C.J.N. Buisman

3.1 Introduction

Urine contributes, with a production of 1 - 1.5 L per person per day, only 1% to the total volume of domestic wastewater. Nonetheless, it contains approximately 80% of the nitrogen (N), 70% of the potassium (K) and 50% of the phosphorus (P) found in domestic wastewater [111]. Urine also contains a considerable amount of organic compounds [15, 56]. Therefore, urine can be considered as a valuable source for nutrients and energy [110]. Yet, the use of flushing toilets and urinals often results in dilution with considerable amounts of water and other waste streams which prevents efficient recovery of nutrients and energy. Lately, intensive studies were conducted by various research groups on effective and efficient treatment methods for separately collected urine [31, 34, 52, 56, 71, 72, 75, 97, 110]. It has been concluded that further research is needed to find promising process combinations for urine treatment and recovery of nutrients [56].

Capacitive deionization (CDI) can be seen as a potential technology for the treatment of urine. CDI or electrosorption is a process which removes ions from aqueous solutions with lower energy consumption compared to other desalination techniques (i.e. reverse osmosis, electrodialysis) [107]. The CDI principle is based on the electric double layer formed at the surface of two electrodes when a voltage is applied. Ion adsorption occurs when an aqueous solution flows through the electrodes while a potential is present. This results in a deionized stream. When the potential difference is equalized, stored ions are rapidly released to the solution, leading to a highly concentrated stream [6, 107, 113]. Recent studies have shown strong benefits when modifying the conventional CDI system by addition of ion-exchange membranes [7, 49, 50]. A membrane capacitive deionization (MCDI) stack consists of a cation exchange membrane (CEM) and an anion exchange membrane (AEM) applied with the electrodes, leading to a higher salt removal efficiency. MCDI has so far been studied and applied as a desalination technology, in which the focus lies on the production of deionized water [7, 22, 49, 50, 114].

This study investigates the application of MCDI as a concentration tool for a complex electrolyte solution, such as urine. The hypothesis is that MCDI is able to recover nutrients from urine in a concentrate stream. Furthermore, the separation of urea (a neutral organic compound) from other nutrients (i.e. P and K) is investigated by MCDI.

3.2 Materials and Methods

3.2.1 Membrane capacitive deionization unit

A commercially available MCDI stack was provided by Voltea LTD (Vlaardingen, The Netherlands). The MCDI stack contained 31 cells. Figure 3.1 presents the MCDI cell configuration.
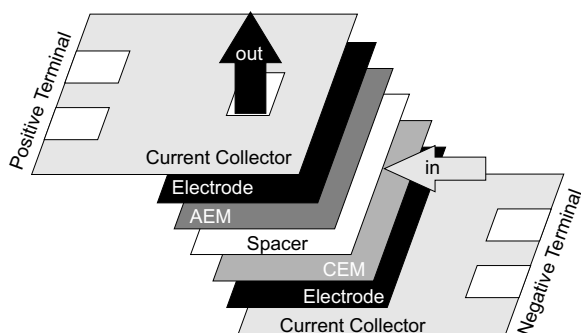
Figure 3.1: MCDI cell design including a current collector, activated carbon electrode, anion exchange membrane (AEM), a feed spacer, a cation exchange membrane (CEM), activated carbon electrode, a current collector.

Each cell was composed of two graphite current collectors, two carbon based electrodes (each 256 cm^2), one feed spacer, one AEM and one CEM. The layout of the experimental setup is presented in Figure 3.2.

The MCDI stack was connected to a power supply (Voltacraft 1560 PFC, Conrad Electronic SE, Hirschau, Germany). A 60 mV/ 100 A DIN-shunt (Weigel, Conrad Electronic SE, Hirschau, Germany) was placed in series with the power supply to record the applied current by measuring the voltage drop over the resistor (0.6 mΩ). The conductivity (σ) was measured using a conductivity electrode QC281x and a controller P 862 (ProSense BV - QiS, Oosterhout, The Netherlands). A peristaltic pump (Masterflex, Cole-Parmer, Vernon Hills, USA) was used for controlling the flow from the stirred reservoir. The conductivity and applied current were recorded on an Ecograph T RSG30 (Endress+Hauser B.V., Naarden, The Netherlands).
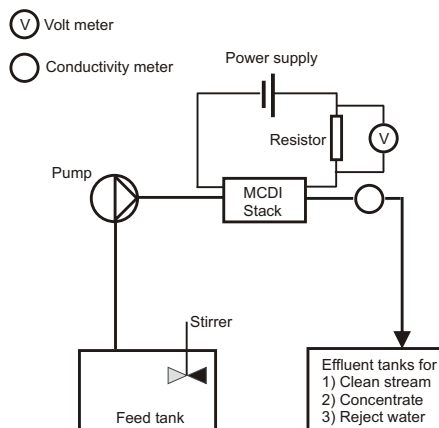
Figure 3.2: Schematics of the MCDI setup consisting of a feed tank with stirrer, pump, MCDI unit, power supply, and conductivity meter.

A diluted model urine solution, which composition was derived from literature [111], was used for the optimization of the flow rate. The model urine consisted of Milli-Q water and various salts. Table 3.1 presents its composition compared to the literature values [111].

All chemicals were purchased in analytical grade at Boom (Meppel, The Netherlands). Milli-Q water was produced using a Millipore system (Millipore, Billerica, MA, USA). HCl was added to stabilize the model urine and prevent precipitation of salts (i.e. hydroxyapatite, struvite) [31, 75]. It should be noted that the model solution only contained salts, no urea and organic compounds were added. A diluted model solution was chosen for the experiments, based on the expected dilution of urine with flushing water [56] from flushing urinals (for details see Table 3.2).

3.2.2 Urine solution

Morning urine samples from 5 male co-workers were collected, mixed and stabilized (pH $\leq$ 3) [31]) using concentrated sulfuric acid (97%) (Boom, Meppel, The Netherlands). In total, a volume of 4 L was collected and diluted to 10 L using Milli-Q water. This dilution (0.4) is similar to dilutions reported in literature [56]. Stabi-

Table 3.1: Diluted model urine solution used during optimization experiments and the reported literature values[111].

Compound/ Parameter	Model urine		Literature value [111]	
	Amount	Unit	Amount	Unit
KH_2PO_4	2.1	g L^{-1}	4.2	g L^{-1}
$MgCl_2 \cdot 2\,H_2O$	0.325	g L^{-1}	0.65	g L^{-1}
$CaCl_2 \cdot 6\,H_2O$	0.325	g L^{-1}	0.65	g L^{-1}
NH_4Cl	0.5	g L^{-1}	1	g L^{-1}
NaCl	2.3	g L^{-1}	4.6	g L^{-1}
Na_2SO_4	1.15	g L^{-1}	2.3	g L^{-1}
KCl	0.8	g L^{-1}	1.6	g L^{-1}
HCl (37%)	0.1	mL L^{-1}	– [a]	
σ	9.85	mS cm^{-1}	– [b]	

[a] not added; [b] not reportet

lization was performed to prevent hydrolysis of urea [58] and precipitation of salts. This diluted and stabilized urine was stored at room temperature for a period of 7 days and was afterwards filtered (0.45 µm) to remove any particulate matter (e.g. denatured proteins). Table 3.2 presents the measured concentrations of the diluted and stabilized urine solution after filtration.

3.2.3 MCDI operation

The MCDI stack was operated in cycles at a fixed cell potential. One cycle consisted of a charging step with a cell potential of 1.4 V followed by a discharging step with a cell potential of 0 V. 1.4 V was chosen for the desalination step following the recommendation of published work [50]. The MCDI setup was operated manually. The operational time for each step depended on the in situ measured effluent conductivity. For experiments using model urine, the chosen limit for the clean stream was ≤ 1 mS cm^{-1}, whereas the chosen limit for the concentrate stream was ≥13 mS cm^{-1}. After the power supply was switched on and the conductivity reached the set conductivity level (≤ 1 mS cm^{-1}), the clean stream was collected. Once the conductivity exceeded the set limit (breakthrough) the power was switched off and the cell potentials were equalized. The resulting concentrate stream ≥13 mS cm^{-1} was collected. After a

Table 3.2: Measured concentrations and parameters of the urine solution and model urine.

Compound/	Urine solution		Model urine	
Parameter	Amount	Unit	Amount	Unit
Mg^{2+}	6.9±0.5	mg L^{-1}	39.5±0.9	mg L^{-1}
Ca^{2+}	10.3±0.4	mg L^{-1}	91.3±1.8	mg L^{-1}
Na^+	1040±14	mg L^{-1}	1303±57	mg L^{-1}
K^+	588±11	mg L^{-1}	1103±50	mg L^{-1}
PO_4^{3-}	270±12	mg L^{-1}	1555±37	mg L^{-1}
Cl^-	1680±35	mg L^{-1}	2333±79	mg L^{-1}
SO_4^{2-}	1320±21	mg L^{-1}	779±24	mg L^{-1}
T_N	1840±6	mg L^{-1}	n.a.[b]	
NH_4^+-N	82±5	mg L^{-1}	123.7±2.4	mg L^{-1}
COD	1620±11	mg L^{-1}	n.a.[b]	
σ	8.45	mS cm^{-1}	8.95	mS cm^{-1}
Dilution[a]	0.4		0.5	

[a] dilution = $\frac{V_{urine}}{V_{urine}+V_{water}}$; [b] not analyzed

defined threshold value was reached (11.5 mS cm^{-1}) the next cycle was started by switching on the power supply.

For experiments using the urine solution, the set limit for the clean stream was ≤1 mS cm^{-1}, whereas the set limit for the concentrate stream was ≥10.5 mS cm^{-1}. The threshold value for starting the next cycle was chosen as 10 mS cm^{-1}. Figure 3.3 shows the effluent conductivity recorded from a representative experiment (two cycles) with model urine to indicate the concentrate stream and the clean stream.

Effluent which did not meet the set limits of the clean stream or concentrate stream was discarded as reject water. In real applications, this reject water can be recycled as a feed stream for the MCDI stack. Four cycles were performed for each experiment with model urine. The first cycle was not used for analysis to ensure a steady state system and therefore reproducible results. Samples from the clean stream and concentrate stream were taken for each cycle. For the experiment with real urine, the different effluent streams (clean, reject and concentrate stream) were collected over the 5 applied cycles. Samples were taken from the collected streams for analysis.
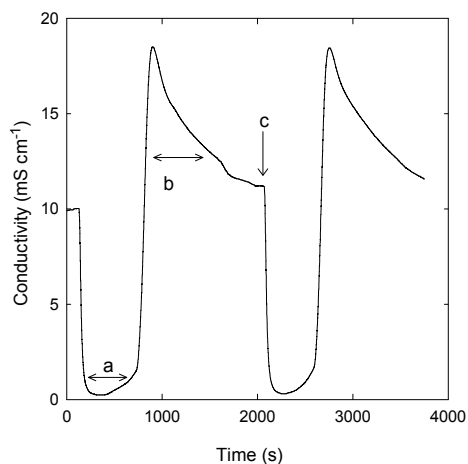
Figure 3.3: Measured effluent conductivity of a representative experiment to illustrate a clean stream (a), a concentrate stream (b) and the end of the cycle (c).

3.2.4 Analytical Methods

Samples from the experiments were analyzed for the concentration of cations, anions, chemical oxygen demand (COD), total nitrogen (T_N) and ammonium-nitrogen (NH_4^+-N). The cation concentrations were determined using an ICP-OES, type Perkin Elmer Optima 3000 DV (Waltham, Massachusetts, USA). The anion concentrations were determined using an ion chromatography system, type Metrohm IC Compact 761 (Schiedam, The Netherlands). NH_4^+-N was analyzed using test kit LCK 303; T_N was analyzed using test kit LCK 338 and COD was analyzed using test kit LCK 314 (all Dr. Lange, HACH, Loveland, Colorado, USA) in a spectrophotometer HACH XION 500 (HACH, Loveland, Colorado, USA). All samples were filtered through 0.45 μm filters (PTFE syringe filters, VWR, Amsterdam, The Netherlands) and analyzed in duplicate. Precipitated crystals were analyzed using an ATR-FTIR spectrometer, type Shimadzu 4800 (Shimadzu Benelux, s-Hertogenbosch, Netherlands).

3.2.5 Calculations

Recoveries (%) of ions were calculated using Equation 3.1.

$$\text{Recovery (\%)} = \frac{C_2 \cdot \text{Vol}_2}{(C_1 \cdot \text{Vol}_1 + C_2 \cdot \text{Vol}_2)} \cdot 100\% \tag{3.1}$$

C_1 refers to the concentration of a specific ion (g L^{-1}) in the clean stream, while Vol_1 refers to the volume (L) of the clean stream. C_2 refers to the concentration of a specific ion (g L^{-1}) in the concentrate stream, while Vol_2 refers to the volume (L) of the concentrate stream. Concentration efficiencies ($\eta_{\text{Concentration}}$ (%)) of ions were calculated using Equation 3.2.

$$\eta_{\text{Concentration}} \text{ (\%)} = \frac{C_2 - C_0}{C_0} \cdot 100\% \tag{3.2}$$

C_0 refers to the concentration of a specific ion (g L^{-1}) in the influent. C_2 refers to the concentration of a specific ion (g L^{-1}) in the concentrate stream.

The Energy_i (J) consumption for each cycle was calculated according to Equation 3.3.

$$\text{Energy}_i \text{ (J)} = V \cdot \int_0^t I \, dt \tag{3.3}$$

Where I is the measured current (A), V is the applied potential (V) and t is the time interval (s) for a specific desalination step. The energy demand (kJ L^{-1}) needed in each desalination step to process one liter of model urine or urine solution was calculated using Equation 3.4.

$$\text{Energy demand (kJ } L^{-1}) = \frac{\text{Energy}_i}{Vol_i} \tag{3.4}$$

Vol_i is the volume (L) of influent measured during a specific desalination step at a specific flow rate and Energy_i is the energy (J) used in the corresponding desalination step calculated according to Equation 3.3.

3.3 Results and Discussion

3.3.1 Flow rate optimization for model urine

The effect of the applied flow rate on the recovery (%) and concentration efficiency of ions (%) was investigated. The chosen flow rates were 25, 50, 75, and 100 mL min^{-1}. In situ measured parameters (volume and conductivity) were used for a general assessment of the process. Table 3.3 shows the measured volume and conductivity of the produced clean and concentrate streams.

Table 3.3: Characteristics of the produced clean streams and concentrate streams including standard deviations at several flow rates.

Flow rate	Clean stream		Concentrate stream		Influent
mL min^{-1}	mL	mS cm^{-1}	mL	mS cm^{-1}	mL
25[a]	397±20	0.61±0.01	520±19	17.84±0.14	1265±43
50[a]	306±11	0.53±0.01	555±24	15.04±024	1310±147
75[a]	257±24	0.52±0.01	660±91	13.65±0.11	1618±129
100[a]	213±22	0.68±0.03	829±85	15.19±0.19	1828±172
90[b]	198±15	0.56±0.02	1008±145	11.78±0.35	1860±517

[a] model urine; [b] real urine

The measurements show that the produced volume of concentrate increased with an increasing flow rate, whereas with an increasing flow rate the produced volume of clean stream decreased. In general, the conductivity of the clean stream was considerably lower ($\leq$ 0.68 mS cm^{-1}) compared to the model solution (9.85 mS cm^{-1}). The conductivity of the concentrate stream was increased ($\geq$ 13.65 mS cm^{-1}) compared to the model solution (9.85 mS cm^{-1}). Figure 3.4 presents the recoveries of the ions from the model urine solution.

The results indicate that a higher flow rate led to a higher recovery (%). The difference in recovery (%) between 75 and 100 mL min^{-1} was not significant and was found to be within the standard deviation. On average 99.3% of each analyte can be recovered using this MCDI stack. Figure 3.5 presents the concentration efficiencies (%) of the ions from the model urine solution.

In general it was observed that a lower flow rate led to a higher concentration efficiency (%). This can be explained by the smaller volume of concentrate stream
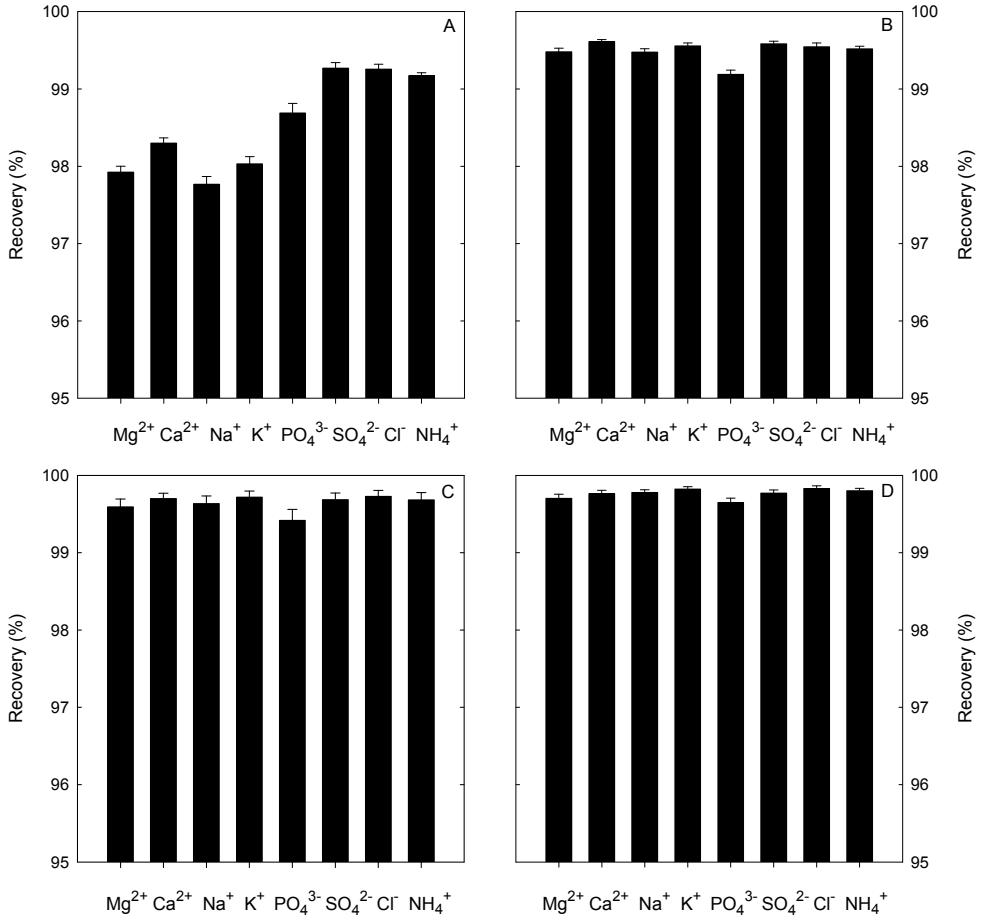
Figure 3.4: Recoveries (%) obtained during experiments using model urine at several flow rates: (A) 25 mL min^{-1}; (B) 50 mL min^{-1}; (C) 75 mL min^{-1}; (D) 100 mL min^{-1}.
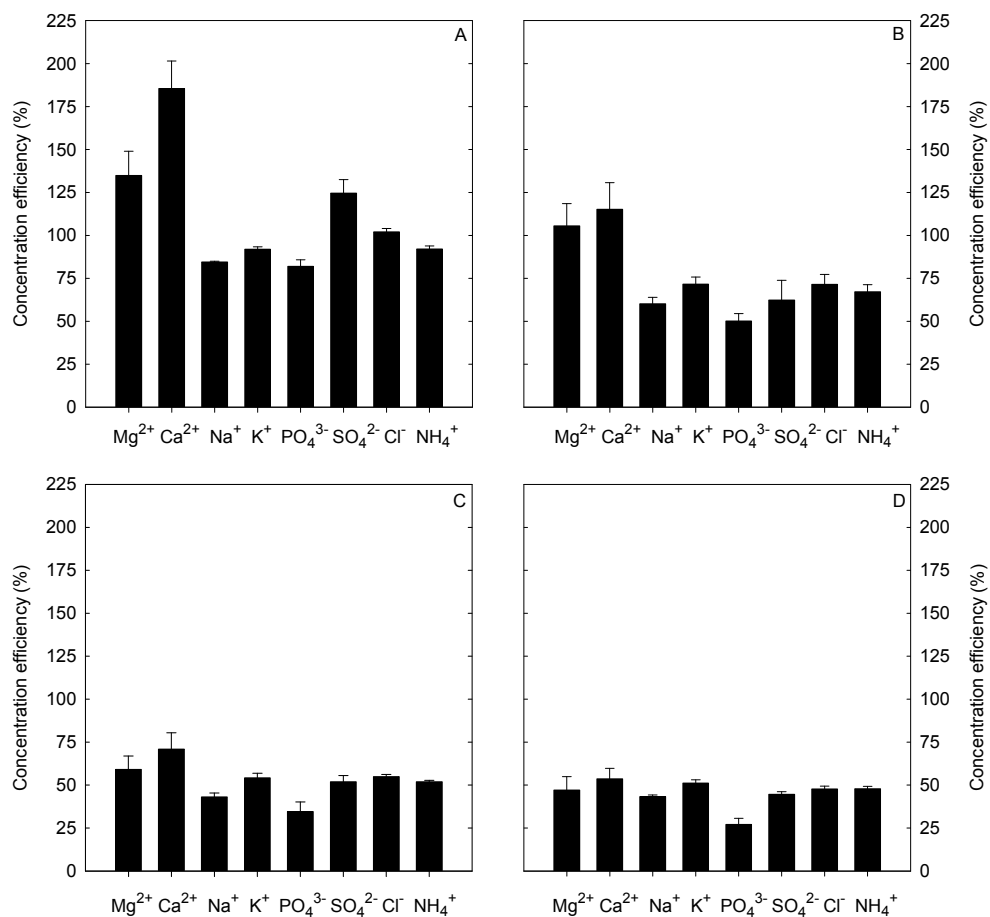
Figure 3.5: Concentration efficiency (%) obtained during experiments using model urine at several flow rates: (A) 25 mL min^{-1}; (B) 50 mL min^{-1}; (C) 75 mL min^{-1}; (D) 100 mL min^{-1}.

generated (Table 3.3) at a lower flow rate. The results indicate that polyvalent cations can be better concentrated than monovalent cations. Higher concentration efficiencies for polyvalent cations can be explained by the larger size and charge of these ions, which make them more susceptible to the applied electric field at the electrodes [22]. Ca^{2+} had a higher concentration efficiency than Mg^{2+}, due to its smaller hydration radius [22, 64]. According to their hydration radii NH_4^+ was better concentrated than K^+ and Na^+ [64]. The relative low concentration efficiencies of PO_4^{3-} compared to SO_4^{2-} can be explained by the low pH of the medium. At a pH of 3, phosphate is present as dihydrogen orthophosphate ($H_2PO_4^-$), which is less susceptible to the electric field. Furthermore, hydroxyapatite precipitation was found in the collected concentrate streams (flow rate of 25 mL min^{-1}). The latter indicates that the Ca^{2+} and PO_4^{3-} concentration efficiencies (%) were sufficient to induce precipitation.

MCDI is able to achieve high recoveries of ions (on average 98.5%) and high concentration efficiencies of $\geq 75\%$ at 25 mL min^{-1}. Similar to electrodialysis, MCDI can concentrate ions in 42% of the original volume. The reported concentrate volumes (in relation to the influent) are lower for vapor compressed distillation ($\leq 5\%$), evaporation (5%), and freeze-thaw (25%), while these techniques have equal or lower recoveries [56]. However, further improvements in concentration efficiencies could be made by using a "stop-flow" operation and "reversed voltage" to force ions away from the electrodes [7]. When those enhancements are applied, the special focus should be the prevention of scaling inside the MCDI stack.

3.3.2 Concentration of nutrients from a real urine solution

In order to confirm the results of the model urine solution, a real urine solution was processed with the same experimental setup. Recovery (%) and concentration efficiency (%) of the different analytes were used again for the assessment. 90 mL min^{-1} was chosen as the flow rate in order to achieve high recoveries. 198 $\pm$ 15 mL of clean stream was produced on average in each cycle with a conductivity of 0.56 $\pm$ 0.02 mS cm^{-1}. 1008 $\pm$ 145 mL of concentrate stream was produced on average in each cycle with a conductivity of 11.78 $\pm$ 0.35 mS cm^{-1}. The characteristics of the produced clean and concentrate streams are also shown in Table 3.3.

In total 1.122 L (0.56 mS cm^{-1}) of clean stream, 4.606 L (11.09 mS cm^{-1}) of concentrate stream and 3.288 L (8.49 mS cm^{-1}) of reject stream were produced during the 5 cycles. The calculated recoveries (%) and concentration efficiencies (%)

for ions and nutrients (excluding T_N and COD) are shown in Figure 3.6.
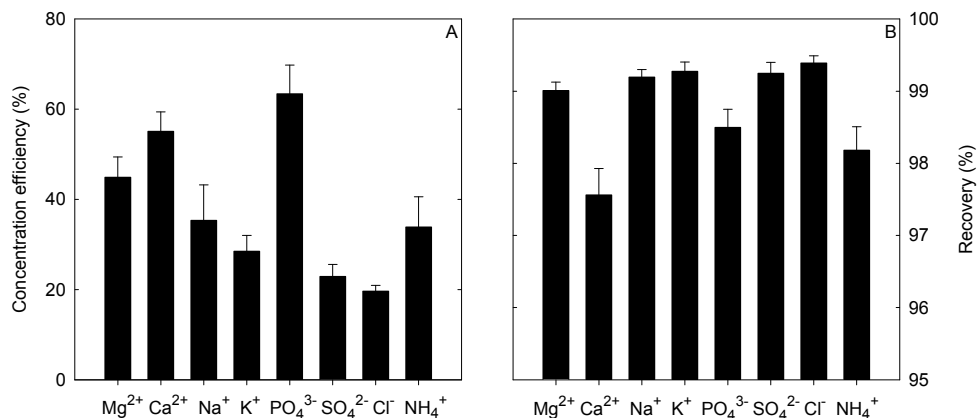
Figure 3.6: (A) Concentration efficiency (%) and (B) recovery (%) obtained in experiments using real urine at a flow rate of 90 mL min^{-1}.

99.3% of the potassium, 98.5% of the phosphate and 98.2% of the ammonium-nitrogen were recovered from urine at a flow rate of 90 mL min^{-1}. The concentration efficiencies (%) of Mg^{2+}, Ca^{2+}, Na^+, and NH_4^+-N were found to be similar to the concentration efficiencies for respective ions of the model solution (at 100 mL min^{-1}). The concentration efficiencies (%) of SO_4^{2-}, Cl^-, and K^+ were found to be lower than the concentration efficiencies for respective ions of the model solution (at 100 mL min^{-1}). This difference could be a result of the different inflow concentrations and a higher complexity of the real urine. The concentration efficiency (%) of PO_4^{3-} was found to be higher than the respective concentration efficiency of the model solution (at 100 mL min^{-1}).

The concentration of T_N in the clean stream was 1771 ± 4.2 mg L^{-1}, whereas the concentration in the concentrate stream was 1873 ± 6.8 mg L^{-1}. A recovery of 84.2% and concentration efficiency of 1.8% were calculated. This low recovery (%) and concentration efficiency (%) can be explained by the partition of urea in the various streams. Urea, a charge neutral compound, is not affected by the separation processes of MCDI. Therefore, the changes of the T_N concentration are a result of the changes in the NH_4^+-N concentration and charged organic nitrogen compounds

(e.g. amino acids). When a cell potential was applied, NH_4^+ and charged nitrogen compounds were stored in the formed electric double layer. When the cell potentials were equalized, the stored NH_4^+ and charged nitrogen compounds were released. The possibility to separate urea from ions was also confirmed using a model solution (results not shown). Thus MCDI technology can be used to separate urea from ions. Therefore, a concentrated NH_4^+ solution can be produced using the following approach. Stabilized urine is treated by MCDI. The concentrate stream will contain ions and charged organic compounds. The clean stream will contain non-charged organic compounds and urea. Urea can be hydrolyzed to ammonia/ammonium by addition of urea-amidohydrolase [58]. Acidification will then transform ammonia into ammonium. In a second MCDI treatment step ammonium will be separated from the non-charged organic compounds. Using this approach a concentrated NH_4^+ liquid could be collected.

Fate of the organic compounds

A recovery of 89.1% and a concentration efficiency of 0.8% were calculated for COD. The COD in the clean stream was 995 ± 31.1 mg L^{-1}, whereas the COD in the concentrate stream was 1608 ± 61.3 mg L^{-1}. These results can be explained by charged functional groups (e.g. COO^-) found within organic compounds (e.g. organic acids). The MCDI stack is able to store these organic compounds in the formed electric double layer on the electrodes. The chemical analysis of the effluents showed that a small fraction of the COD is retained within the MCDI stack. The real urine solution contained 14.61 g of COD before MCDI treatment. The clean stream contained 1.08 g of COD, the concentrate stream contained 7.42 g of COD and the reject stream contained 4.67 g of COD. Therefore, 1.44 g of COD was accumulated inside the MCDI stack, most likely on the carbon electrodes or the ion exchange membranes.

3.3.3 Energy demand of the desalination step

The energy consuming step in every conventional MCDI process is the desalination step. The energy demand was calculated according to Equations 3.3 and 3.4. The results are shown in Table 3.4.

The average energy needed in the desalination steps decreases with an increasing

Table 3.4: Average inflow during the desalination step (mL), average energy (kJ) needed in the desalination step and energy demand (MJ m^{-3}) based on the applied current in the MCDI setup

Flow rate mL min^{-1}	Average volume desalination step mL	Average Energy$_i$ kJ	Energy demand kJ L^{-1}
25[a]	484±14.2	8.11±0.36	16.77±0.36
50[a]	383±11.0	5.94±0.49	15.52±0.11
75[a]	349±22.9	5.13±0.36	14.68±0.09
100[a]	311±20	4.42±0.32	14.21±0.12
90[b]	313±53.2	4.62±0.83	14.72±0.28

[a] model urine; [b] real urine

flow rate. The main reason for this decrease is the earlier occurrence of the breakthrough (effluent exceeded 1 mS cm^{-1}) and therefore a smaller volume (L) of urine was processed in the desalination step (as presented in Table 3.4). The calculated energy demand ranged from 14.21 to 16.77 kJ L^{-1} for model urine and 14.72 kJ L^{-1} for real urine. The operational time of the desalination step was the influencing factor for the energy demand. At higher flow rates less time was needed to process one liter of influent. Thus, lower energy demands were found at higher flow rates.

The energy demand (for the desalination step) of the MCDI lies between 14.21 and 16.77 MJ m^{-3} (model urine) and 14.72 MJ m^{-3} (real urine). Therefore, MCDI would use less energy than electrodialysis (107 MJ m^{-3}) [56]. In addition an MCDI system also needs energy for pumping, controlling and possibly a pretreatment step (e.g. filtration for particle removal). Despite these concerns, the energy demand shows that MCDI technology could be an alternative to electrodialysis to concentrate nutrients from urine. Furthermore, possible benefits of energy recovery from the discharging step were not considered in this research, but this energy recovery can further decrease the energy demand [1].

3.4 Conclusion

This study demonstrates the capability of MCDI to concentrate nutrients from complex liquid streams, such as urine. Concentration of nutrients is of special interest

in situations where urine is diluted with flushing water. From a concentrated urine various products (i.e. hydroxyapatite, struvite) can be extracted more efficiently than from a diluted stream due to a higher concentration of nutrients in the produced concentrate stream. The energy demand of an MCDI system is low enough to become an interesting alternative to electrodialysis. Furthermore, the results of this study show that MCDI can be an interesting option for the treatment of liquid streams beyond the boundaries of its former purpose as a pure desalination technology.

Acknowledgements

4

Effects of NH$_4^+$ concentration and charge exchange on NH$_4^+$ recovery by an MFC

Abstract

Ammonium recovery using a two chamber microbial fuel cell (MFC) was investigated at high ammonium concentrations. Increasing the ammonium concentration (from 0.07 g to 4 g ammonium-nitrogen L^{-1}) by addition of ammonium chloride did not affect the performance of the MFC. The obtained current densities by DC-voltammetry were higher than 6 A m^{-2} for both operated MFCs. During continuous operation at an external resistance (250 Ω) a current density of 0.9 A m^{-2} was achieved. Effective ammonium recovery can be achieved by migrational ion flux through the cation exchange membrane to the cathode chamber, driven by the electron production from the degradation of organic substrate. The charge transport was proportional to the concentration of ions. Nonetheless, a concentration gradient will influence the charge transport. Furthermore, a charge exchange process can influence the charge transport and therefore the recovery of specific ions.

4.1 Introduction

Bioelectrochemical systems and particularly microbial fuel cells (MFCs) have been studied intensively for many applications [27, 53, 66]. In general, MFCs use microorganisms to catalyze reactions at the anode and thereby produce energy. Various applications have been considered for MFCs, including wastewater treatment [39], energy production [73], and recovery of metals [92].

It has been shown that cations (i.e. NH_4^+, Na^+, K^+, Mg^{2+} and Ca^{2+}) are even transported against a concentration gradient through the cation exchange membrane into the cathode chamber and will lead to an increase of the cathode pH [78]. It was also shown that ammonium ("ammonium" refers in a general sense to NH_3 and NH_4^+, whereas the chemical formulae are used to refer to its specific forms) is removed from the cathode chamber by volatilization of NH_3 [39]. These findings offer the possibility to concentrate and recover NH_3 from an ammonium rich wastewater (e.g. urine). However, in most MFC applications, only low strength anolytes (synthetic and real wastewaters) have been used for the assessment of the processes [39, 83, 91].

Ammonium is used by bacteria, fungi, and plants as an important nitrogen source and it is known for its cytotoxic effects [59]. As an example, a high ammonium concentration can affect anaerobic digestion [104, 116] by affecting methanogenesis. Despite these findings, it was recently suggested that bacteria could be generally resistant against high ammonium concentrations [59].

In this work, the effect of an increased ammonium concentration on the cell potential and current density of an MFC was investigated. Furthermore, the transport of cations to the cathodes was measured to determine the possibility of ammonium recovery using MFCs.

4.2 Materials and Methods

To make an adequate assessment on MFCs as a tool to recover ammonium, continuously fed MFCs were operated at high ammonium concentrations up to 4 $g_N L^{-1}$. The used MFCs were of a two chamber design, using a reliable catholyte: ferricyanide [91], to be able to focus solely on anode performances. The ammonium concentration and external resistance were alternated. For the assessment of ammonium recovery, the charge transport (Q_{ion}) was determined in relation to charge production(Q_e).

4.2.1 Microbial fuel cell design and setup

The setup consisted of two identical MFCs (MFC 1 & MFC 2) with the anode chambers hydraulically connected in series, whereas the cathode chambers were hydraulically separated. The cell design for the experiments was similar to previously studied MFCs [91]. Mechanical roughened graphite plates (22 cm^2) were used in the anode chambers and flat graphite plates (Mueller & Roesser GmbH & Co., Troisdorf, Germany) were used in the cathode chambers. The anode chamber and cathode chamber were separated with a Ralex cation exchange membrane, type CMH (Ralex, Mega, Straz pod Ralskem, Czech Republic). The anode compartment (including chambers, tubing, and buffer tank) had a combined liquid volume of 200 mL, and the cathode compartments (including chambers, tubing, and flask tank) had a liquid volume of 1 L each. Anode and cathode media were recirculated at 80 mL min^{-1} through the MFC using a peristaltic pump (Masterflex, Cole-Parmer, Vernon Hills, USA).

4.2.2 Microbial fuel cell operation

The MFCs were inoculated using effluent of another active MFC [83]. The anode potential for each MFC was measured using an Ag/AgCl reference electrode (ProSense QiS, Oosterhout, The Netherlands), connected to the anode chambers via a Haber-Luggin capillary. The anode pH was actively controlled at pH 7 using a controller (Liquisys M CPM 253, Endress + Hauser B.V., Naarden, The Netherlands), an RC 8 Stepdose pump$^{\copyright}$ (KNF, Trenton, USA) and a 1 M NaOH solution. The MFCs were operated at a continuous temperature of 30 ˚C using a water bath (DC 10/K10, Thermo-Haake, Thermo Temperature Control BV, Eindhoven, The Netherlands). The individual cell potentials, anode potentials and pH were recorded in a 5 s interval using an Ecograph T data logger (RSG 30, Endress & Hauser B.V., Naarden, The Netherlands). Anode and cathode were connected via an external circuit containing several external resistances (Table 4.1). During the initial period, a high external resistance (1 kΩ) was used to study only the effects of an increasing ammonium concentration on the cell potential and the current density. In later stages of the experiment, the ammonium concentration was kept constant, whereas the external resistance was lowered to study the increasing cation transport. Fresh anolyte was constantly supplied to the anodes (1 mL min^{-1}) using a peristaltic pump. The anolyte contained 1.36 g L^{-1} NaCH$_3$COO $\cdot$ 3 H$_2$O, 0.74 g L^{-1} KCl, 0.58 g L^{-1} NaCl, 0.68 g

Table 4.1: NH_4-N concentration and applied external resistances during the experimental period.

Day	NH_4-N ($g\,L^{-1}$)	External resistance (Ω)
1 - 6	0.07	1000
7 - 12	0.5	1000
13 - 19	1.0	1000
20 - 26	1.5	1000
27 - 33	2.0	1000
34 - 40	3.0	1000
41 - 47	4.0	1000
48 - 54	4.0[a]	1000
55 - 61	4.0[a,b]	1000
62 - 65	4.0[a,b]	500
66 - 68	4.0[a,b]	250

[a]alternative anolyte solution
[b]reduced volume of catholyte solution

L^{-1} KH_2PO_4, 0.87 g L^{-1} K_2HPO_4, 0.28 g L^{-1} NH_4Cl, 0.1 g L^{-1} $MgSO_4 \cdot 7\,H_2O$, 0.1 g L^{-1} $CaCl_2 \cdot 2\,H_2O$ and 0.1 mL L^{-1} of a trace element mixture [83]. The ammonium concentration of the anolyte was increased stepwise (0.07, 0.5, 1.0, 1.5, 2.0, 3.0, and 4.0 g_N L^{-1}) by addition of NH_4Cl. Further details on the MFC operation are shown in Table 4.1. All chemicals were purchased at Boom B.V. (Meppel, The Netherlands) in analytical grade. From day 48 onwards an alternative anolyte solution with an increased KCl concentration was used for determining transport numbers of specific cations. The anolyte contained 1.36 g L^{-1} $NaCH_3COO \cdot 3\,H_2O$, 5.4 g L KCl^{-1}, 0.58 g L^{-1} NaCl, 0.68 g L^{-1} KH_2PO_4, 0.87 g L^{-1} K_2HPO_4, 0.1 g L^{-1} $MgSO_4 \cdot 7\,H_2O$, 15.11 g L^{-1} NH_4Cl, 0.1 g L^{-1} $CaCl_2 \cdot 2\,H_2O$ and 0.1 mL L^{-1} of a trace element mixture. The cathode compartment contained a buffered ferricyanide catholyte as the electron acceptor.

During the first period (until day 48), the catholyte (1 L) contained 50 mmol $K_3Fe(CN)_6$ (FCN), 1.36 g L^{-1} $NaCH_3COO \cdot 3\,H_2O$, 0.74 g L^{-1} KCl, 0.58 g L^{-1} NaCl, 0.68 g L^{-1} KH_2PO_4, 0.87 g L^{-1} K_2HPO_4, 0.1 g L^{-1} $MgSO_4 \cdot 7\,H_2O$, 0.1 g

L^{-1} $CaCl_2 \cdot 2\,H_2O$, 0.1 mL L^{-1} of a trace element mixture and NH_4Cl of identical concentration to the anolyte.

4.2.3 Electrochemical characterization

Polarization curves were measured to determine current densities (A m^{-2}) of the MFCs before increasing the ammonium concentration. The polarization curves were prepared via DC-voltammetry using the chronoamperometry method on an Iviumstat.XR (Ivium Technologies, Eindhoven, The Netherlands). The cell potentials were decreased stepwise and kept constant for 900 seconds to stabilize the direct current. The sampling interval was 5 s. The MFCs were measured from 700 to 350 mV (cell voltage) in steps of 50 mV. The average current measured over 60 s at the end of each potential step was chosen for evaluation. The corresponding average anode potential measured over 60 s was taken from the data logger (Ecograph T). At least 3 repetitions using chronoamperometry were performed per polarization curve.

4.2.4 Calculation

The current density (A m^{-2}) was obtained according $i = E_{\text{Cell}}\,(R{\cdot}A)^{-1}$, where i (A m^{-2}) is the current density, E_{Cell} (V) is the cell voltage, R (Ω) is the resistance and A (m^2) is the area of the anode. The power density (W m^{-2}) is calculated from the current density according to P= i$\cdot$ E_{Cell}. The amount of produced charge (Q_e), expressed in coulombs (C), was calculated according to:

$$Q_e = \int_0^t I\,dt \qquad (4.1)$$

Where I is the current produced by the MFC over a certain period of time. The amount of charge transported to the cathode (Q_{ion}), expressed as coulombs (C), of specific ions through the cation exchange membrane was determined according to:

$$Q_{\text{ion}} = (C_{\text{ion}} - C_{\text{ion},0}) \cdot V \cdot z_{\text{ion}} \cdot F \qquad (4.2)$$

Where C_{ion} (mol L^{-1}) is the concentration inside the cathode compartment of a specific ion at the end of the experiment, $C_{\text{ion},0}$ (mol L^{-1}) is the concentration inside

the cathode compartment at the start of the experiment, V (L) is the volume of the cathode compartment, z_{ion} (-) is the charge of the ion and F is the Faraday constant (F 96,485 C mol^{-1}) [84]. The Concentration Factor for ammonium was determined according to:

$$\text{Concentration Factor}(\%) = \frac{(C_1 - C_0)}{C_0} \cdot 100\% \qquad (4.3)$$

Where C_0 (g L^{-1}) is the concentration at the start of a specific experiment and C_1 (g L^{-1}) is the concentration at the end of a specific experiment.

4.2.5 Chemical analysis

During the experiments, daily samples were taken from the anode compartment and cathode compartment. They were analyzed for the concentration of cations, anions, and NH$_4^+$-N. The cation concentrations were determined using an ICP-OES, type Perkin-Elmer Optima 3000 DV (Waltham, Massachusetts, USA). The measured cation concentrations were used to determine the cation transport. The anion concentrations were determined using an ion chromatography system, type Metrohm IC Compact 761 (Schiedam, The Netherlands). NH$_4^+$-N was analyzed using test kit LCK 303 (Dr. Lange, HACH, Loveland, Colorado, USA) in a spectrophotometer HACH XION 500 (HACH, Loveland, Colorado, USA). The samples for NH$_4^+$-N were distillated prior to analysis to avoid interference of FCN. All samples were analyzed in duplicate. Samples for determination of anion and cation concentrations were filtered using 0.45 μm filters (PTFE syringe filters, VWR, Amsterdam, The Netherlands) prior to analysis.

4.3 Results and discussion

4.3.1 Overall performance of the MFCs

The average cell potential and current density of MFC 1 and MFC 2 are shown in Figure 4.1. Linear regression analysis of the measured cell voltage over the applied NH$_4^+$-N range showed only a marginal increase of the cell potential from MFC 1 and MFC 2. For MFC 1, a slope of 0.017 and a minor correlation (R^2) of 0.86 were found. For MFC 2, a slope of 0.017 and a minor correlation (R^2) of 0.76 were found. These results indicate that there were no toxic effects of ammonium in the tested range.

The average current density for MFC 1 was found to be 0.320 ± 0.017 A m^{-2} (0.226 ± 0.025 W m^{-2}) and for MFC 2 was found to be 0.317 ± 0.022 A m^{-2} (0.222 ± 0.031 W m^{-2}). These results indicate no adverse effects of an increased ammonium concentration.
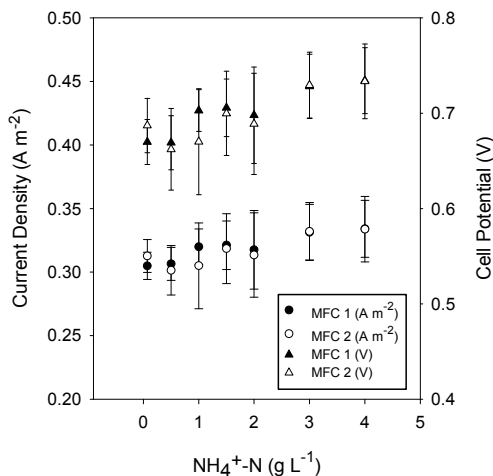
Figure 4.1: Cell potential averages (V) and current densities (A m^{-2}) of MFC 1 and MFC 2 at the various applied ammonium nitrogen influent concentrations.

For further investigation of the anode performance, polarization curves at the various ammonium nitrogen concentrations were recorded. Figure 4.2 displays the polarization curves for both MFCs.

The increasing ammonium concentration does not seem to affect the development of the biofilm on the anode as obtained current densities increase despite increasing the ammonium concentrations. A unimodal character was observed in Figure 4.2A-D. At high anode potentials ($>$-0.300 V), the MFCs show a maximum in current density, followed by a decrease, which reflects the maximum activity of the anode biofilm [91]. Our hypothesis is that this maximum of the current density and the subsequent decrease were caused by the early development stage (i.e. biomass limitations) of the anode biofilm. This would result in a unimodal character of these polarization curves. Figure 4.2E-H show a higher maximum current density at higher anode potentials for both MFCs, which indicates a more developed (mature) biofilm on the anode. High current densities (6 A m^{-2}) were obtained for both MFCs at potentials of -0.200
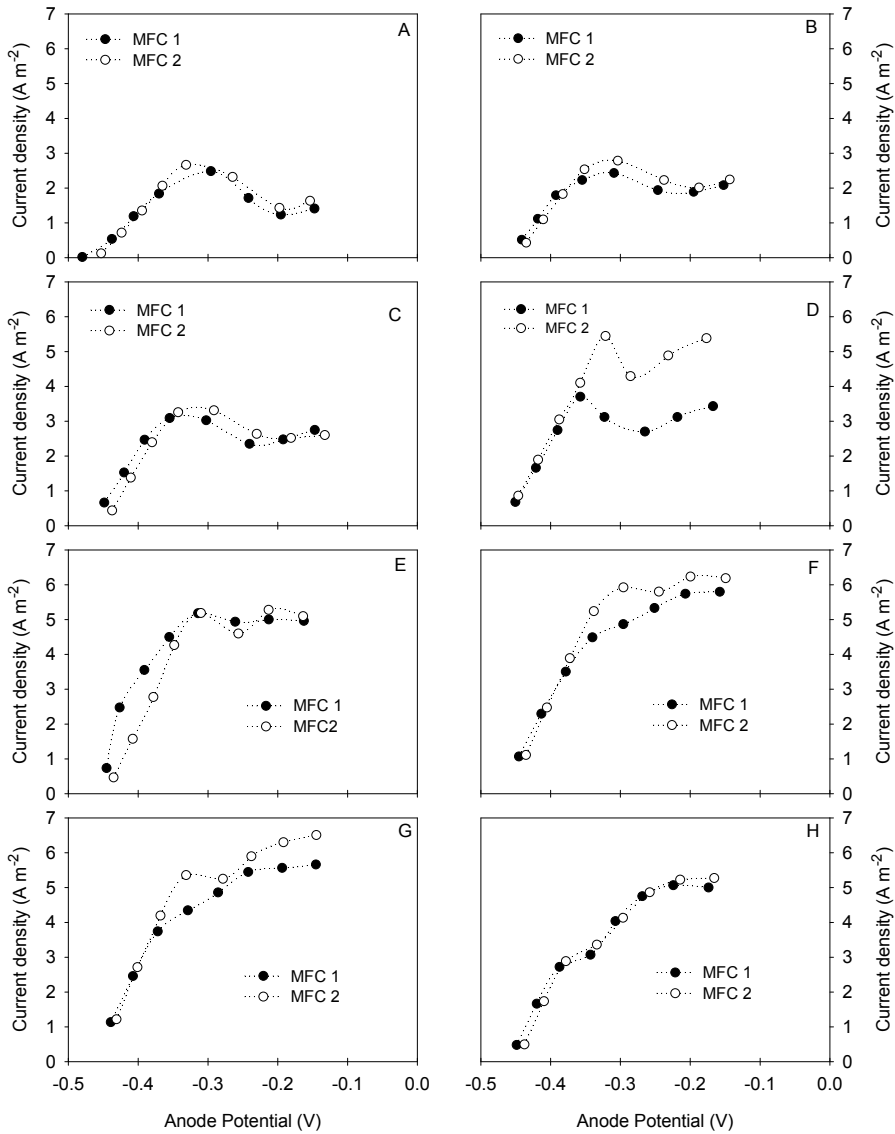
Figure 4.2: Polarization curves of MFC 1 and MFC 2 at various ammonium nitrogen influent concentrations. (A) 70 mg$_N$ L^{-1}, (B) 500 mg$_N$ L^{-1}, (C) 1 g$_N$ L^{-1}, (D) 1.5 g$_N$ L^{-1}, (E) 2 g$_N$ L^{-1}, (F) 3 g$_N$ L^{-1}, (G) 4 g$_N$ L^{-1}, and (H) 4 g$_N$ L^{-1} using the alternative anolyte solution with an increased KCl concentration.

V (vs. Ag/AgCl) at an ammonium concentration higher than 3 g$_N$ L^{-1}. Current densities obtained in these experiments were higher than current densities reported in earlier experiments with identical cell designs [91]. This can be the result of the continuous feeding of the MFCs with fresh anolyte and the higher conductivity of the anolyte.

Four aspects could explain the observation that NH$_4^+$-N is not toxic for the anode biomass: (1) The pH of the experiments remained lower than 7.1, at which little NH$_3$ occurs and all ammonium is present as NH$_4^+$ [42]; (2) The concentration of ammonium was increased gradually, which gave the bacteria a chance to adapt to the new conditions [104]; (3) Microorganisms at the bioanode are growing in a biofilm [68], which might protect them from toxic effects of ammonium; (4) A general tolerance or resistance of bacteria against high ammonium concentrations as recently suggested [59].

No ammonium toxicity was observed in these experiments, which can be explained by the neutral anode pH. Therefore, the anodic pH influences the ammonia toxicity. In the final application (wastewater treatment), the pH and therefore the presence of NH$_4^+$ can be influenced by controlling the supply of new anolyte. Protons are constantly produced by the bio-catalyzed anode reaction:

$$CH_3COO^- + 4\,H_2O \longrightarrow 2\,HCO_3^- + 8\,e^- + 9\,H^+ \tag{4.4}$$
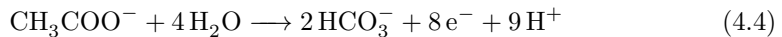
This anode reaction 4.4 will lead to an acidification of the anode.

4.3.2 Transport numbers

Literature showed that ammonium is transported to the cathode compartment [80] and can be removed by volatilization [39]. According to the Nernst-Plank flux equation the total ion flux through a membrane can be described by three processes: convection, diffusion and migration. When using an anion or cation exchange membrane only two of these processes can occur: migration and diffusion [80]. Whereas diffusion is caused by a concentration gradient, the migration is caused by the charge production.

The results of the ammonium measurements (day 1 - 41) of the samples taken from the cathode compartment (containing 50 mmol FCN), revealed a higher NH$_4^+$-N-transport than expected. As an example (day 34 - 40), the ammonium concentration

increased by 8.893 mmol d^{-1} (858 C d^{-1}) (average of MFC 1 and MFC 2), which cannot be explained by the charge production (Q_e) of 70 C d^{-1}, during the same period (average of MFC 1 and MFC 2). The ammonia concentrations in the anode and cathode compartments are identical at the start of the experiment, which excludes diffusion flux as the main cause for this high ammonium transport. Furthermore, the produced charge (Q_e) was too low to explain this transport, which excludes migrational flux as the main cause for this high ammonium transport. Also both compartments were buffered at pH 7 (using a 10 mmol phosphate buffer). Therefore, all ammonium remained in the NH_4^+ form, which excludes an unbalanced concentration caused by pH changes and formation of NH_3. The reason for this high NH_4^+ transport was found in a charge exchange process. The cathode compartment had a 180 mmol L^{-1} K$^+$ concentration, whereas the anode compartment only had a 30 mmol L^{-1} K$^+$ concentration. Therefore, a diffusional transport of K$^+$ from the cathode compartment to the anode compartment was induced. Samples taken from the cathode during this experimental time (day 34 - 40) confirmed the charge exchange process. The charge transport for K$^+$ was found to be -8.913 mmol d^{-1} (-860 C d^{-1}), indicating diffusion of K$^+$ from the cathode compartment to the anode compartment. This K$^+$ diffusion resulted in an unbalance of the anion to cation ratio within the cathode compartment. Therefore, the most prevalent cation (NH_4^+) in the anode compartment was transported to the cathode to maintain overall charge neutrality. Figure 4.3 shows the K$^+$ and NH_4^+ concentration (mol L^{-1}) at the cathode during day 27 - 46 (as a combined average of the MFCs) and the schematic representation of the charge exchange. From Figure 4.3a can be seen that at different anodic NH_4^+-N concentrations (indicated via the dashed vertical lines) the process of charge exchange took place. This process of charge exchange was also confirmed in experiments without biological activity (data not shown).

This observed effect of charge exchange should be considered especially when determining removal rates or charge transport, when using high strength catholytes (i.e. 50 mmol $K_3Fe(CN)_6$) in combination with cation exchange membranes.

To determine migrational transport numbers for ammonium, further experiments were needed. Between day 48 and 68 charge transport (Q_{ion}) was determined in relation to charge production (Q_e). The anolyte and catholyte were altered to be balanced in their cation concentration. Details on the alternate anolyte are given in the experimental section 4.2.2 (page 52). The catholyte was a buffered ferricyanide
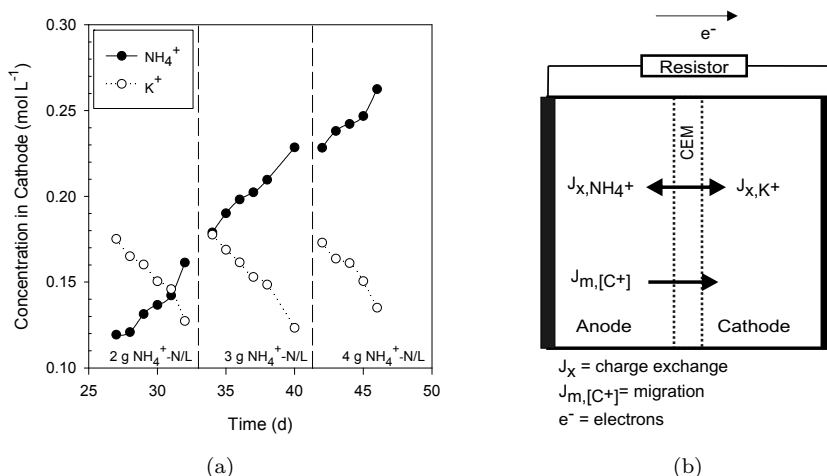
Figure 4.3: a) Measured NH$_4^+$ and K$^+$ concentrations (averages of MFC 1 and MFC 2) at the cathode (day 26 - 46) and b) schematic representation of the charge exchange.
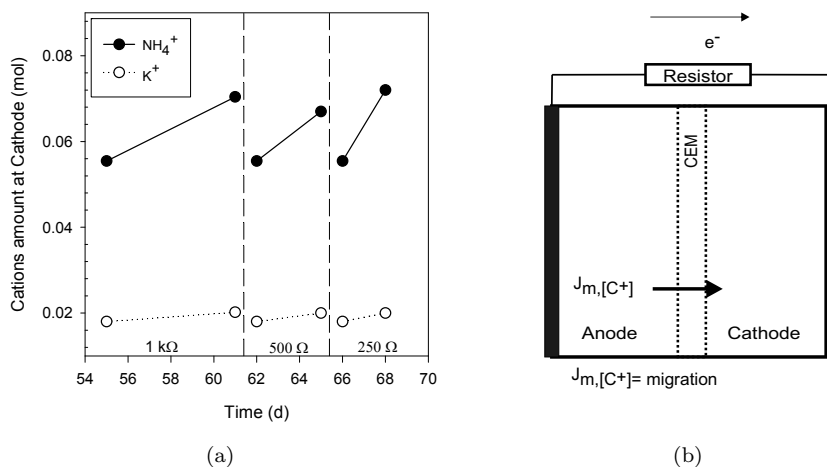
Figure 4.4: A)Measured NH$_4^+$ and K$^+$ amounts (averages of MFC 1 and MFC 2) at the cathode (day 55 - 68) and b) schematic representation of the migration flux.

solution with the same concentrations of cations as the anolyte. The concentration of the ferricyanide was effectively lowered (24 mmol L^{-1}) and the volume of the catholyte was reduced (day 55) to make it possible to measure changes in the ammonium concentration in shorter time periods. The operational time for each experiment was also shortened to compensate for the lower ferricyanide concentration. Additionally, the external resistance was lowered stepwise to the increase current density and the produced charge (Qe). Figure 4.4 shows the absolute amounts (mol) of NH_4^+ and K^+ measured at the cathode (as a combined average of the MFCs) at several applied external resistances (indicated by the dashed vertical lines) and the schematic representation of the migration flux. Furthermore, Figure 4.4 shows that the diffusion of K^+ from cathode to anode was prevented.

These results (Figure 4.3 and 4.4) show that the charge exchange should be taken into account when determining transport numbers for ammonium. This can be done by calculation of the contribution of charge exchange or experimentally by balancing the anodic and cathodic media composition.

Table 4.2 shows the obtained concentration factor for NH_4^+-N, current densities and power densities from the different external resistances (1 kΩ, 500 Ω and 250 Ω) which were used.   As expected the current density and power density increased

Table 4.2: Concentration factor for ammonium, current density and power density obtained with the alternative anolyte solution using a lower concentrated catholyte solution (day 55 - 68).

External resistance (Ω)	Current density (A m^{-2})		Power density (W m^{-2})		Concentration factor (%)	
	MFC 1	MFC 2	MFC 1	MFC 2	MFC 1	MFC 2
1000	0.313	0.319	0.216	0.224	7	6
500	0.608	0.619	0.407	0.422	5	5
250	0.877	0.917	0.625	0.675	7	7

with respect to the decreasing external resistance according to Ohm's law. Figure 4.5 shows the charge produced and the charge transported for both MFCs.

Ions were transported according to the following order $NH_4^+ \geq Na^+ > K^+ > Ca^{2+}$
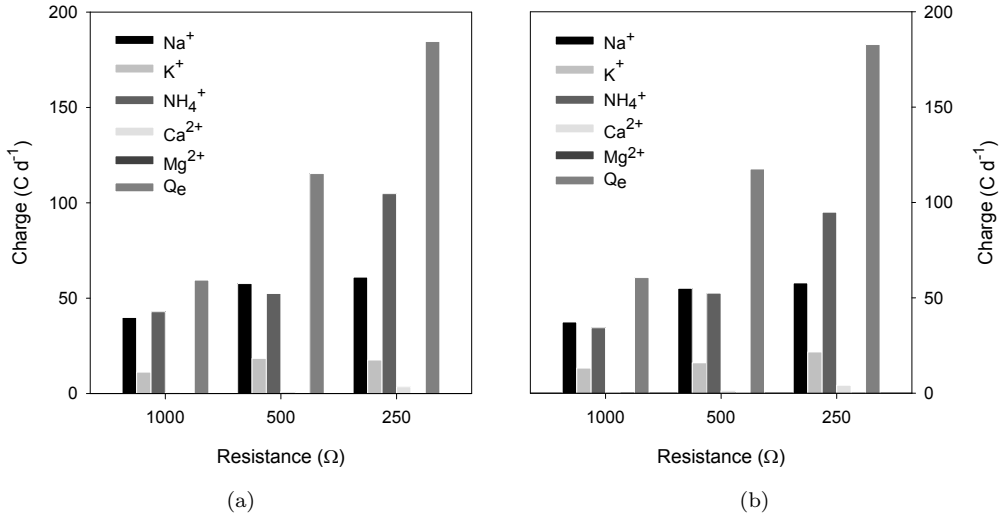
Figure 4.5: Charge produced (Q_e) and charged transported (Q_{ion}) of MFC 1 (a) and MFC 2 (b).

$\gg Mg^{2+}$, which corresponds to the concentration of the ions in the anode compartment. However, the transport of Na^+ was affected by the unbalance in concentration between the anode compartment and the cathode compartment, resulting from the pH control at the anode using 1 M NaOH. Thus, diffusion flux for Na^+ was still possible, which can explain the high transport of Na^+.

4.3.3 Ammonia recovery

Table 4.2 reports the achieved concentration factors for NH_4^+-N. The results show that similar concentration factors were obtained in the experiments. However, the necessary operational time (at 500 Ω and 250 Ω) to achieve these concentration factors decreased due to a higher current density. The concentration process of ammonium is related to the electron transport and the earlier described charge exchange had no direct influence on this concentration process (Figure 4.4 and 4.5). In combination with the previously reported localized pH increase at the cathode [80] and the volatilization of NH_3 [39] this would offer a pathway to recover NH_3 from high strength ammonium wastewater (e.g. urine). This recovery can be achieved via

diffusional flux and migrational flux of ammonium. Whereas diffusional flux only allows for ammonium transport until an equilibrium between the anode and cathode compartment is reached, migrational flux allows for increasing the ammonium concentration against a concentration gradient. The volatile NH_3 could be stripped from the cathode and adsorbed into an acid solution. Urine contains approximately 10 g COD L^{-1} and approximately 8.1 g_N L^{-1} (after hydrolysis) [56], which should provide enough energy (Q_e) to recover a substantial amount of ammonium from urine. Nonetheless, migrational flux of ions (other than NH_4^+), which occurs at the same time, will affect the recovery of ammonium.

4.4 Conclusions

In these experiments, no (cyto-)toxic effects of ammonium at concentrations up to 4 g_N L^{-1} were observed. Also the increasing salinity of the media did not affect the performance of the MFCs. These experiments prove that ammonium can be recovered using an MFC, while energy is produced at the same time. The main processes for ammonium transport are migrational flux and diffusional flux. Ammonium was transported against a concentration gradient by migrational flux. Higher transport rates can be achieved by further optimization of the current density.

Acknowledgements

5

Ammonium recovery and energy production from urine by an MFC

Abstract

Nitrogen recovery through NH_3 stripping is energy intensive and requires large amounts
of chemicals. Therefore, a microbial fuel cell was developed to simultaneously produce
energy and recover ammonium. The applied microbial fuel cell used a gas diffusion
cathode. The ammonium transport to the cathode occurred due to migration of ammonium and diffusion of ammonia. In the cathode chamber ionic ammonium was
converted to volatile ammonia due to the high pH. Ammonia was recovered from the
liquid-gas boundary via volatilization and subsequent adsorption into an acid solution. An ammonium recovery rate of 3.29 g_N d^{-1} m^{-2} (vs. membrane surface area)
was achieved at a current density of 0.50 A m^{-2} (vs. membrane surface area). The
energy balance showed a surplus of energy (3.46 kJ g^{-1}_N), which means more energy
was produced than needed for the ammonium recovery. Hence, ammonium recovery
and simultaneous energy production from urine was proven to be possible by this
novel approach.

5.1 Introduction

5.1.1 Nitrogen

Ammonium is an essential nutrient and an important nitrogen source for plants. Here "ammonium" refers to the sum of volatile NH_3 and ionic NH_4^+; the specific chemical formulae are used to distinguish between NH_3 and NH_4^+. Ammonium-based fertilizers are applied on a large scale to increase crop yields and to ensure a high food production. The production of ammonium fertilizer is dependent on the Haber-Bosch process, wherein N_2 is fixated as NH_3. After consumption of the produced food, nitrogen compounds (i.e. ammonia, nitrite, nitrate, etc.) end up in wastewater. These nitrogen compounds are removed as N_2 in wastewater treatment plants (WWTPs) by nitrification/denitrication or the Anammox process. The Haber-Bosch process and nitrogen removal are energy intensive and therefore costly. Energy can be saved by a direct NH_3 recovery from wastewater. The main obstacles for ammonia recovery from wastewater are the low nitrogen concentration and large volumes of wastewater to be processed, which result in a high energy demand [55].

Focusing on the composition of wastewater, 75% of the nitrogen load to a conventional WWTP originate from urine [48]. However, urine only contributes 1% to the volume of the wastewater. On average urine contains 1 g L^{-1} phosphorus, 9 g L^{-1} nitrogen and 10 g L^{-1} COD [56]. Due to these high concentrations, urine can be considered as a valuable resource for nitrogen, phosphorus and for energy recovery. Urine can be easily separated and kept concentrated by the use of separation toilets and water-free urinals.

In fresh urine most of the nitrogen is found in the form of urea $((NH_2)_2CO)$. Urea is hydrolyzed by the bacterial enzyme urease to NH_3 and carbamate, whereas carbamate hydrolyzes further to NH_3 and bicarbonate [58]. Urease is produced by bacteria which can be also found in the sanitary installation and storage tank. As a result of the decomposition of urea, the pH of the urine increases and triggers the precipitation of salts (i.e. $MgNH_4PO_4 \cdot 6H_2O$, $Ca_{10}(PO_4)_6OH_2$, $CaCO_3$, etc.) [97]. Ammonium concentrations up to 8.1 g_N L^{-1} can be found in urine [56].

5.1.2 Microbial fuel cell

Bio-electrochemical systems are an emerging technology with a wide range of applications [27]. In Microbial Fuel Cells (MFCs) - a specific type of bio-electrochemical systems - bacteria catalyze the oxidation of organic substrate (e.g. acetate) at the anode according to:

$$CH_3COO^- + 4\,H_2O \longrightarrow 2\,HCO_3^- + 8\,e^- + 9\,H^+ \tag{5.1}$$
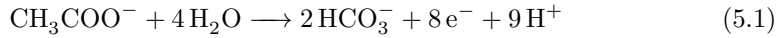
The electrons are used to reduce an electron acceptor (i.e. O_2) at the cathode. Given the neutral to alkaline environment (pH $\geq$7) of the cathode, the reduction of oxygen results in the production of hydroxide according to:

$$O_2 + 4\,e^- + 2\,H_2O \longrightarrow 4\,OH^- \tag{5.2}$$
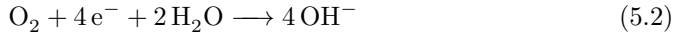
Anode and cathode are often separated by an ion exchange membrane [53]. Ion exchange membranes and the cathode-electrode can be combined to form a so called membrane electrode assembly (MEA) [47, 69, 70]. In a MEA, the membrane separates the anode from the cathode and serves as an ion conductor, while the electrode can be directly exposed to the gas phase (air-cathode).

5.1.3 Ammonium recovery by an MFC

The principle of ammonium recovery by an MFC was reported in Chapter 4 ([45]) using a sacrificial $K_3Fe(CN)_6$-cathode and synthetic wastewater. Recently, ammonium has been reported as a proton shuttle (between anode and cathode) and ammonium recovery was demonstrated by stripping from a synthetic wastewater[13]. The feasibility of using highly diluted (0.035 vol/vol) urine solutions as fuel in MFCs has been reported in literature [33]. The aim of this study is to investigate ammonium recovery from real undiluted urine using a more sustainable air-cathode under high NH_3 concentrations and a high pH. Therefore, ammonium recovery and energy production were studied not only from synthetic urine but also from real urine. The obtained results were compared to the previous work in Chapter 4 ([45]). Furthermore, the energy demand for this ammonium recovery (kJ g_N^{-1}) was calculated and compared to the energy demand of conventional NH_3-stripping processes. The new MFC facilitated ammonium recovery concept is shown in Figure 5.1a.
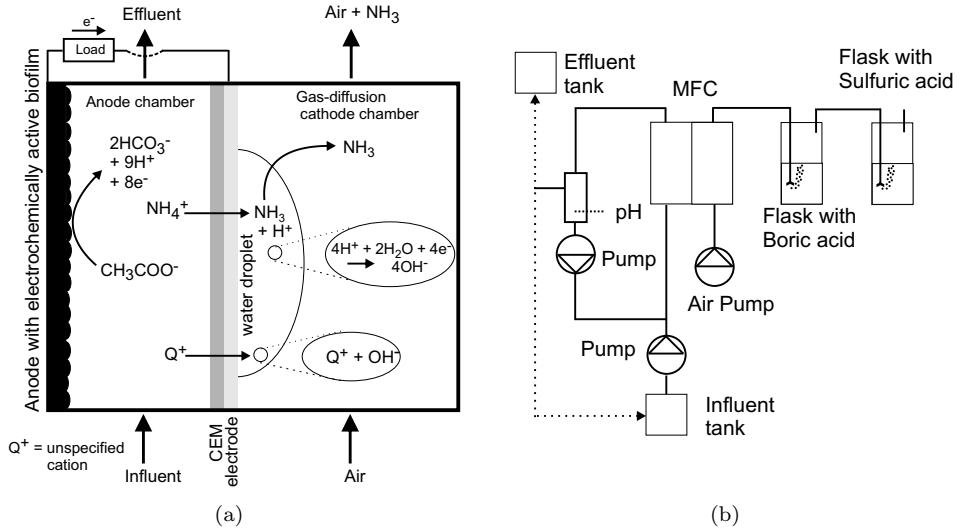
Figure 5.1: (a) Schematic representation of the processes involved in the ammonium recovery using an MFC; (b) Schematic representation of the experimental setup for ammonium recovery using an MFC.

At the anode, electrons are produced (equation 5.1) and transported via an external load (resistor) to the cathode, where oxygen is reduced (equation 5.2). The electron transport induces a charge transport (i.e. anion or cation transport) across the membrane to maintain the charge neutrality of the system. In case of the applied Cation Exchange Membrane (CEM), cation transport (i.e. H_3O^+, Na^+, K^+, Mg^{2+}, Ca^{2+}, NH_4^+) occurs from the anode chamber through the CEM to the cathode chamber (migrational flux) and leads in time to a concentration gradient between the cathode and anode chamber of the MFC. The pH in the cathode chamber increases during operation due to the production of hydroxide (OH^-) according to equation 5.2 and a migrational transport of cations other than H_3O^+ and NH_4^+. During continuous MFC operation an equilibrium will be reached, where forward (anode to cathode) migrational flux and backward (cathode to anode) diffusion flux of cations will be equal and a maximum concentration of cations and OH^- in the cathode chamber is reached. At this point, the cathode pH remains stable, because the constant production of OH^- leads to a diffusion flux of OH^- from cathode to anode [78, 84].

The high pH in the cathode chamber results in formation of volatile NH_3. NH_3 is

stripped [13] from the liquid-gas boundary at the MEA by the air stream supplied to the air-cathode. Subsequently, NH_3 can be recovered from the gas stream leaving the cathode by adsorption in an acid as NH_4^+. Therefore, this innovative concept couples energy production from urine by a MFC with NH_3 stripping.

5.2 Materials and Methods

5.2.1 MFC design and experimental setup

The applied MFC was of a two chamber design similar to recently published work [36]. The MFC was made from two identical Plexiglas plates (21 cm×21 cm), each plate contained one flow through chamber (10cm × 10 cm × 0.2 cm) with a 9 channel inlet and 9 channel outlet for flow distribution. In the anode chamber (volume 20 mL), a graphite felt (100 cm^2 thickness 3 mm, National Electrical Carbon BV, Hoorn, The Netherlands) was used as the anode. The anode chamber and the cathode chamber (volume 20 mL) were separated using a MEA. The MEA (100 cm^2) was produced by hot pressing (5 minutes, 140˚C, 534 bar) a platinum coated (20 g m^{-2}) titanium fine mesh (Dexmet, Magneto Special Anodes B.V., Schiedam, The Netherlands) into a Nafion N117 (Dupont, Geneva, Switzerland) CEM using a Labopress P 400 S (Vogt Maschinenbau GmbH, Berlin, Germany). Anode (graphite felt) and cathode (Pt coated Ti felt) were each contacted via 4 Pt/Ir (80/20) wires (0.025 cm diameter, Advent Research Materials, Oxford, UK) to the outside of the MFC. Anode medium was recirculated at 80 mL min^{-1} through the MFC using a peristaltic pump (Masterflex, Cole-Parmer, Vernon Hills, USA). New influent was supplied at a flow rate of 1 mL min^{-1} by another peristaltic pump. The total volume of the anode was 250 mL, including tubes (PTFE-based), anode chamber, mixing flow cell (Schott Duran®, VWR, The Netherlands). The MFC was operated at room temperature (20 ± 2˚C). Air was supplied to the MEA in the cathode chamber at a flow rate of 10 mL min^{-1} using a compressor (Kaeser Sigma SM 9, USA), a multistage pressure regulator (VWR, The Netherlands) and a PTFE needle valve (VWR, The Netherlands) for flow control. The gas stream from the cathode was channelled through two 500 mL gas washing bottles with filter disks (Schott Duran®, VWR, The Netherlands) placed in series. The first bottle was filled with boric acid (20 g L^{-1}) to collect the volatile NH_3 as NH_4^+ (adsorption bottle). The boric acid was renewed periodically. The gas

stream from the adsorption bottle was channelled to a second bottle filled with a 0.4M H_2SO_4 solution to prevent contamination of boric acid with ammonia from the laboratory environment. Figure 5.1b presents the scheme of the experimental setup.

5.2.2 MFC operation

The MFC was inoculated using effluent of another active MFC operated at 30 ˚C on synthetic media with acetate [45]. The anode potential of the MFC was measured via a Haber-Luggin capillary relative to an Ag/AgCl reference electrode (+0.200 V vs. NHE, ProSense QiS, Oosterhout, The Netherlands). The anode pH was measured using an Orbisint CPS11D pH electrode connected to a Liquisys M CPM 253 transmitter (Endress + Hauser B.V., Naarden, The Netherlands). The cell voltage, anode potential and the pH in the anode chamber were recorded in a 5 s interval using an Ecograph T data logger (RSG 30, Endress + Hauser B.V., Naarden, The Netherlands). The anode and the cathode were connected through an external resistor.

The experiment consisted of two parts. In part one, synthetic urine was used to study the effects of the anode ammonium concentration and electron transport rate (current density) on ammonium transport. In part two, the feasibility of this ammonium recovery and energy production by an MFC was studied under realistic conditions using real urine.

The effects of an increasing anode ammonium concentration on the ammonium recovery was studied at a high external resistance of 1 kΩ. The effects of the electron transport rate on the ammonium recovery was studied at a constant anode ammonium concentration and a decreasing external resistance. Further details about part one of this experiment are given in Table 5.1.   The synthetic urine contained 1.36 g L^{-1} $NaCH_3COO \cdot 3\,H_2O$, 0.74 g L^{-1} KCl, 0.58 g L^{-1} NaCl, 0.68 g L^{-1} KH_2PO_4, 0.87 g L^{-1} K_2HPO_4, 0.28 g L^{-1} NH_4Cl, 0.1 g L^{-1} $MgSO_4 \cdot 7\,H_2O$, 0.1 g L^{-1} $CaCl_2 \cdot 2\,H_2O$ and 0.1 mL L^{-1} of a trace element mixture [83]. The ammonium concentration was increased by addition of NH_4Cl. All chemicals were purchased at VWR (Amsterdam, The Netherlands) in analytical grade. The synthetic urine had a measured COD of 600 mg L^{-1}.

On day 77 the influent was changed to real urine and one day later the effluent of the MFC was connected to the influent tank to recycle the same batch of urine over a longer period of time. The ammonium concentrations in the urine batch were expected to decline at a moderate rate, based on the expected produced currents and

Table 5.1: Ammonium concentration, applied external resistances during the experiment, conductivity of the influent and pH of the influent.

Time	Anode ammonium concentration	External resistance	Conductivity influent	pH influent
(d)	$(g_N\ L^{-1})$	(Ω)	$(mS\ cm^{-1})$	(-)
1 - 6	0.07[a]	1000	5.4	7.0
7 - 14	0.07	1000	5.4	7.0
15 - 20	0.5	1000	9.1	7.0
21 - 27	1.0	1000	13.3	7.0
28 - 34	2.0	1000	21.5	6.9
35 - 41	3.0	1000	29.2	6.9
42 - 48	4.0	1000	37.2	6.8
49 - 55	4.0	500	37.2	6.8
56 - 62	4.0	250	37.2	6.8
63 - 76	4.0	100	37.2	6.8
77 - 119	4.05[b]	500	35.0	8.85
120 - 135	3.96[b]	250	35.0	8.85
136 - 149	4.05[c]	250	35.0	8.85
150 - 160	4.01[c]	100	35.0	8.85

[a]inoculation; [b]1[st]batch real urine; [c]2[nd]batch real urine

previous experiments [45]. Therefore, the same batch of urine can be recycled for longer periods without the risk of depleting the urine batch of COD or ammonium. Two batches of urine (each 9 L) were used during part two of the experiment. This urine (from 60 persons: 6 female and 54 male) was collected at Landustrie B.V. (Sneek, The Netherlands) by DeSaH B.V. (Sneek, The Netherlands) using separation toilets (Villeroy & Boch Gustavsberg AB, Gustavsberg, Sweden) and Urimat® eco, water free urinals, (Biocompact Environmental Technology B.V., Rotterdam, The Netherlands). The urine was pretreated by centrifugation at 8000 rpm for 5 minutes (Avanti J-26XP, Beckman Coulter, USA) to remove particulate matter, suspended particles and crystals (i.e. struvite).

Table 5.2 presents key parameters measured in the real urine after centrifugation.

Table 5.2: Key parameters measured in the real urine after centrifugation.

Parameter	Value	Unit
Na^+	1.85	g L^{-1}
K^+	1.49	g L^{-1}
Mg^{2+}	$\leq$5.0	mg L^{-1}
Ca^{2+}	7.1	mg L^{-1}
NH_4^+/NH_3-N	4.05	g L^{-1}
Cl^-	3.29	g L^{-1}
PO_4^{3-}-P	0.21	g L^{-1}
SO_4^{2-}-S	0.21	g L^{-1}
COD	3.9	g L^{-1}
pH	8.85	-
Conductivity	35.0	mS cm^{-1}

5.2.3 Chemical analysis

The urine was analyzed for the concentrations of relevant cations, anions and COD after centrifugation. An ICP-OES, type Perkin Elmer Optima 5300 DV (Waltham, Massachusetts, USA) was used to determine cation concentrations. An ion chromatography system, type Metrohm IC Compact 761 (Schiedam, The Netherlands) was used to determine anion concentrations. The COD was analyzed using test kit LCK 514 and the ammonium content was analyzed using test kit LCK 303 (Dr. Lange, HACH, Loveland, Colorado, USA) and a spectrophotometer HACH XION 500 (HACH, Loveland, Colorado, USA). Ammonium concentrations from the absorption bottle were measured throughout the experimental time to determine ammonium transport numbers. Samples of the influent and anode media were filtered (0.45 μm, PTFE syringe filters, VWR, Amsterdam, The Netherlands) prior to analysis. All samples were analyzed in duplicate. The conductivity was determined using a conductivity electrode QC281x and a controller P 862 (ProSense BV - QiS, Oosterhout, The Netherlands).

5.2.4 Calculations

The current density was calculated according to $i = E_{Cell} \cdot R^{-1} \cdot A^{-1}$, where i (A m^{-2}) is the current density, E_{Cell} (V) is the cell voltage, R (Ω) is the external resistance and A (m^2) is the surface area of the membrane (equal to the projected anode surface area). The power density (W m^{-2}) is calculated according to $P = i \cdot E_{Cell}$. From the recorded (pH and anode potential) and calculated (current density and power density) parameters average values and standard deviation were calculated based on the results obtained during a specific set of operation conditions (applied concentration or resistance) over a certain period of time (as indicated in Table 5.1). The amount of produced charge (Q_e), expressed in coulombs (C), was calculated according to:

$$Q_e = \int_0^t I \, dt \qquad (5.3)$$

Where I is the current (A) produced by the MFC over a certain sampling period. The transport of ammonium from anode to cathode was determined indirectly by measuring the ammonium concentration in the gas washing bottle filled with boric acid. The ammonium transport (Q_{NH_4}) is presented as charge transport, which is expressed in coulombs (C) and was calculated according to:

$$Q_{NH_4} = (c_{NH_4} - c_{NH_{4,0}}) \cdot V \cdot z_{NH_4} \cdot F \qquad (5.4)$$

Where, c_{NH_4} (mol L^{-1}) is the concentration of ammonium at the end of a certain sampling period, $c_{NH_{4,0}}$ (mol L^{-1}) is the concentration of ammonium at the start of a certain sampling period, V (L) is the volume of the boric acid used in the adsorption bottle, z_{NH_4} (-) is the charge of the NH_4^+ and F is the Faraday constant (96485 C mol^{-1}). The Coulombic efficiency (η_{CE}) was calculated according to:

$$\eta_{CE} = \frac{Q_e}{F \cdot b \left(\frac{1}{M_{O_2}} \right) \cdot \Delta COD \cdot V} \qquad (5.5)$$

Where Q_e is the amount of produced coulombs during a specific time period (equation 5.3), b is the amount of electrons (4) exchanged per mole of O_2, F is the Faraday constant, M_{O_2} is the molar mass of oxygen, ΔCOD is the change in the measured COD during a specific time period and V is the volume of the urine (9 L).

The NH_3 content (%) present in the solution at a specific pH was calculated according equation 5.6 based on a pK_A of 9.24 (at 25˚C) [90].

$$NH_3 \text{ content} = 100 \cdot \left[1 + \frac{10^{-pH}}{10^{-pK_A}} \right] \tag{5.6}$$

The ammonium recovery rate (g_N d^{-1} m^{-2}), which is based on the daily measured ammonium transport and the membrane surface area was calculated according to:

$$\text{Recovery rate} = \frac{\Delta \left(m_i \right)}{A_M} \tag{5.7}$$

Where $\Delta \left(m_i \right)$ is the transported amount of NH_4^+ or NH_3 amount (g_N d^{-1}) and A_M is the membrane area (m^2).

5.3 Results and discussion

5.3.1 Ammonium recovery from synthetic urine

In part one of the experiment, first the effect of an increasing anode ammonium concentration and second the effect of an increasing current density on the ammonium transport were investigated. Figure 5.2a shows the average anode potential and the average current density reached at a constant external resistance (1 kΩ) at increasing anode ammonium concentrations.

The current density stabilizes above an ammonium concentration of 1 g_N L^{-1} and shows a peak at an ammonium concentration of 2 g_N L^{-1}. At 2 g_N L^{-1} an average current density of 59 mA m^{-2} and an average power density of 34.22 mW m^{-2} were obtained. The measured average anode potential shows only a marginal increase with an increasing anode ammonium concentration. The results show that no adverse effects were found in the tested ammonium concentration range. This observation is in agreement with earlier published work [45]. However, these results are in contrast to the reported ammonium toxicity in a single chamber MFC [61].

For all applied anode ammonium concentrations, the relation between ammonium transport and produced charge is shown in Figure 5.2b. A direct linear relation ($R^2 = 0.995$) was found between ammonium transport and produced charge in these experiments. Independent of the ammonium concentration, 30% (slope = 0.30) of the produced charge was used for ammonium transport to the cathode.

(a) (b)
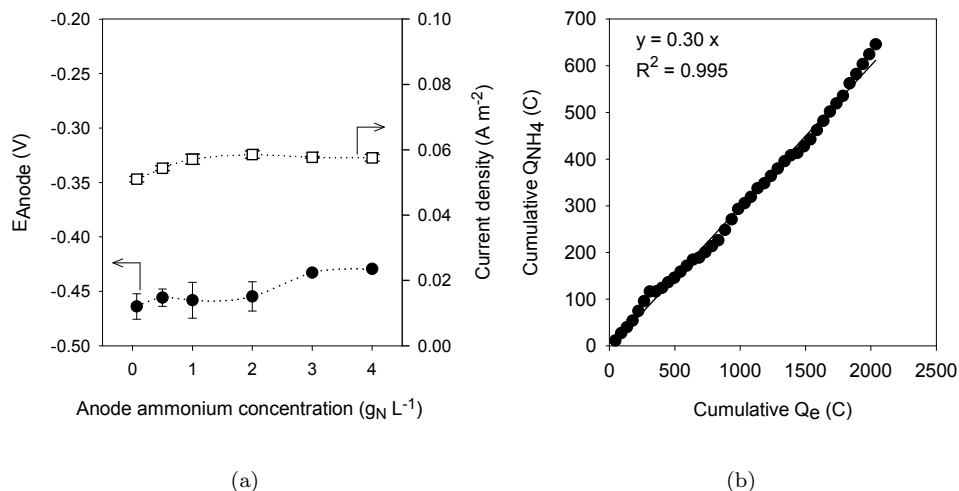
Figure 5.2: (a) Average anode potential and average current density with standard deviation obtained at 1 kΩ and at increasing ammonium concentrations (day 7 - 48 synthetic urine); (b) Ammonium transport against produced charge from day 7 until day 48.

Figure 5.3a shows the measured average anode potential, current density and average power density obtained at higher current densities and at a constant anode ammonium concentration (4 g_N L^{-1}).

At an increasing current density (from 0.1 to 0.47 A m^{-2}), a slight increase of the anode potential was observed (from -0.42 to -0.39 V). A power density of 222 mW m^{-2} was measured at a current density of 0.47 A m^{-2} under the given operational conditions. The obtained current densities in this work were found to be lower than the current density obtained in previous work [45]. This difference can be explained by the respective cathode systems used in the experiments. The air-cathode is affected by the conditions (e.g. pH, low buffer concentration, oxygen supply) found in the MFC [117], whereas the $K_3Fe(CN)_6$-cathode is not limited by these conditions.

The relation between ammonium transport and produced charge at these current densities is shown in Figure 5.3b. A direct linear relation ($R^2 = 0.998$) was found between ammonium transport and produced charge in these experiments at the different current densities. The ammonium transport increased together with the produced

(a)   (b)
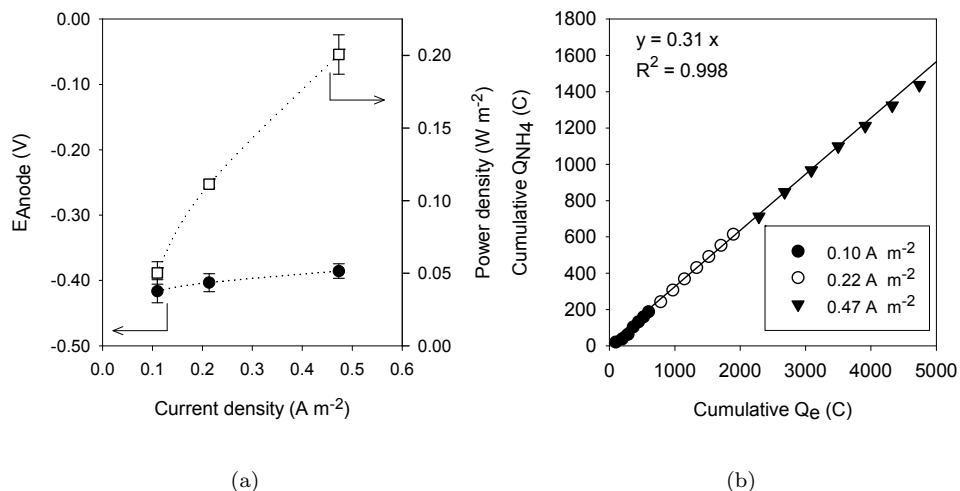
Figure 5.3: (a) Average anode potential and average power density with standard deviations obtained at higher current densities and a constant anode ammonium concentration of 4 g_N L^{-1} (day 49 - 69 synthetic urine); (b) Relation of ammonium transport and produced charge from day 49 until day 69.

charge. Independent of the current density, 31% (slope 0.31) of the produced charge from synthetic urine was used to transport ammonium. The ammonium transport using a $K_3Fe(CN)_6$-cathode was reported to be 50% of the produced charge [45]. This difference could be caused by the difference in MFC designs. The advantage of the air-cathode is the removal of NH_3 from the cathode by the supplied air [39]. In a $K_3Fe(CN)_6$-cathode, ammonium is concentrated in the cathode and needs to be separated from $K_3Fe(CN)_6$ in an additional step (i.e NH_3 stripping). Since the pH of the $K_3Fe(CN)_6$-cathode does not increase during operation, chemicals need to be added prior to NH_3 stripping.

The ammonium transport was found to be independent of the anode ammonium concentration and increases with current density. This successfully demonstrates the principal of ammonium recovery and energy production from synthetic urine by an MFC using an air-cathode system.

5.3.2 Ammonium recovery from real urine

In part two of the experiment, ammonium recovery from real urine was investigated. Figure 5.4a shows the measured average anode potential, current density and power density obtained during experiments with real urine.

(a)   (b)
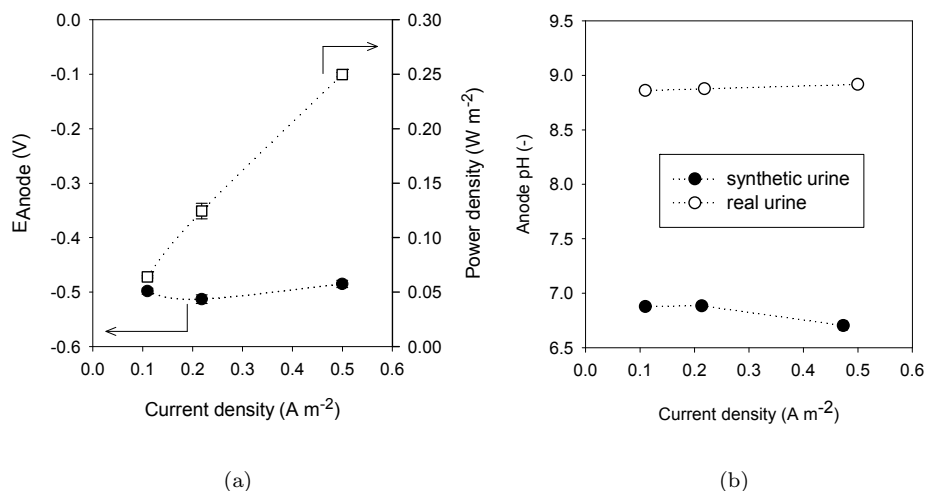
Figure 5.4: (a) Average anode potential and average power density with standard deviation obtained at higher current densities during operation on real urine; (b) Average anode pH with standard deviation during operation on synthetic urine and real urine.

A stable anode potential was observed at increasing current densities. A power density of 250 mW m^{-2} was measured at a current density of 0.50 A m^{-2} under the given operational conditions. Although a more complex substrate was used, comparable current densities and power densities were obtained during the operation on real urine and synthetic urine. This shows that the biomass was able to use real urine as a substrate. The anode potentials were lower during the operation on real urine compared to operation on synthetic urine. This decrease in anode potential can be explained by the change in the anode pH. Figure 5.4b shows the average recorded anode pH during the experiments. The anode pH during operation on synthetic urine was 6.8±0.1 and the anode pH during operation on real urine was

8.85±0.1. The anode pH remained stable at 8.85 during the operation on urine, because of the high concentration of the buffer. The two buffers which are present were ammonium-ammonia ($pK_A = 9.24$) with a concentration of 0.29 mol L^{-1} and bicarbonate-carbonate ($pK_A = 10.33$) with a concentration of 0.25 mol L^{-1}.

The anode potential [53] decreases with a decreasing proton concentration (due to the high pH) at the anode according to:

$$E_{Anode} = E^0_{Anode} - \frac{RT}{nF} ln \left(\frac{[CH_3COO^-]}{[HCO_3^{2-}]^2 [H^+]^9} \right) \qquad (5.8)$$

Where E^0_{Anode}(V) is the standard potential of the anode reaction, R is the universal gas constant (8.314 J mol^{-1} K^{-1}), T the temperature (K), n the number of electrons transferred per reaction (mol), F the Faraday constant (96485 C mol^{-1}), $[x_i]$ the concentration (mol L^{-1}) of the reactants (x_i).

High ammonium concentrations have been reported to inhibit microbial processes and to influence the performance of anaerobic digestion [10, 104]. Generally, the NH_3 form has been reported to be more toxic than the NH_4^+ form [43]. The anolyte ammonium concentration was measured after 2 days of operation and from this result the NH_3 concentration was determined according to equation 5.6. The NH_3 concentration in the anode was 1.15 g_N L^{-1} as a result of the anode pH. However, no toxic effects on the biological processes in the MFC were found, since the anode potential remained stable at increasing current densities and power densities. These results are in contrast to reports of ammonium toxicity in a single chamber MFC [61], which showed that already a low NH_3 concentration can be toxic. However, the operational conditions (start up, cell type) and the inoculums (possible adaptation to a high ammonium concentration) were different in the respective works. No published information was found on MFC operation at high ammonium concentrations at alkaline pH conditions (pH $\geq$ 8.5) for comparison.

Although similar current densities were obtained with synthetic urine and real urine, the daily ammonium transport was significantly higher in experiments with real urine (Table 5.3). Also the relation between ammonium transport and produced charge was different during the operation on real urine (Figure 5.5).

A slope of 1.32, 0.81 and 0.53 was found at a current density of 0.11, 0.22 and 0.50 A m^{-2}, respectively. A slope higher than 1.00 shows that more coulombs of ammonium were transported than coulombs of electrons were transported. Therefore,

Table 5.3: Average ammonium transport (C d^{-1}) and the average produced charge (C d^{-1}) during operation on synthetic urine (4 g$_N$ L^{-1}) and real urine at the respective current densities.

synthetic urine			real urine		
i	Q$_{NH_4}$	Q$_e$	i	Q$_{NH_4}$	Q$_e$
A m^{-2}	C d^{-1}	C d^{-1}	A m^{-2}	C d^{-1}	C d^{-1}
0.10	27±5	85±5	0.11	123±10	94±5
0.22	61±2	185±3	0.22	160±10	192±6
0.47	117±13	406±8	0.50	227±26	431±4

the ammonium transport can not solely originate from migrational transport. Since convection transport of ammonium is impossible through a CEM, the ammonium transport is limited to migration and diffusion. The explanation for this difference in ammonium transport is diffusion of NH_3. NH_3 diffusion through perfluorosulfonic ion exchange membranes ("Nafion") has been reported in literature [28, 94, 105]. At a pH $\leq$ 7 (operation on synthetic urine) less than 0.7% of the ammonium is present as NH_3. Whereas at a pH of 8.85 (operation on urine) 28.5% of the ammonium is present as NH_3 (see equation 5.6).

The NH_3 diffusion ($n_{NH_3,dif}$) can be determined by calculation, because the total ammonium transport ($n_{NH_4,total}$) is equal to the sum of NH_3 diffusion and NH_4^+ migration ($n_{NH_4^+,mig}$).

$$n_{NH_4,total} = n_{NH_3,dif} + n_{NH_4^+,mig} \tag{5.9}$$

$n_{NH_4^+,mig}$ can be substituted with "$\alpha \cdot n_e$" given that the NH_4^+ migration is equal to a fraction (α) of the transported electrons (n_e).

$$n_{NH_4,total} = n_{NH_3,dif} + \alpha \cdot n_e \tag{5.10}$$

Where n$_{NH_4,total}$ (mmol d^{-1}) is the measured total ammonium transport, n$_{NH_3,dif}$ (mmol d^{-1}) is the NH_3 diffusion and α is a factor and n_e (mmol d^{-1}) is the amount of transported electrons (measured current). n$_{NH_3,dif}$ and α were determined using the amount of transported electrons and total ammonium transport obtained during the experiments at various current densities. n$_{NH_3,dif}$ was 0.995±0.06 mmol d^{-1} (equal
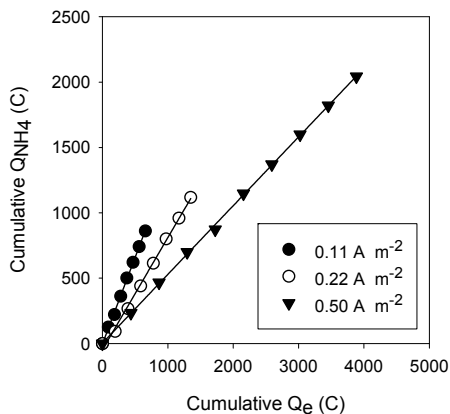
Figure 5.5: Ammonium transport against produced charge at various current densities during operation on real urine.

to 96±6 C d^{-1}) and α was 0.31±0.01. Hence, the diffusion of NH$_3$ from the anode to cathode chamber affects the total ammonium transport. As shown in section 5.3.1, similar α values (i.e. 0.30 and 0.31) were obtained during experiments using synthetic urine.

To determine NH$_3$ diffusion experimentally, synthetic urine (ammonium concentration (4 g$_N$ L^{-1}) without NaCH$_3$COO $\cdot$ 3 H$_2$O) was prepared according to details given in section 5.2.2 and adjusted to the desired pH using 1M NaOH. The setup was identical to the MFC setup, while anode and cathode were not connected by an external circuit. No ammonium transport was measured during 7 days of operation at an anode pH of 7. A diffusional ammonium transport of 1.03±0.05 mmol d^{-1} (equal to 100±5 C d^{-1}) was measured during 7 days of operation at an anode pH of 8.8.

The NH$_3$ diffusion accounts for 42.2% of the ammonium transport measured at the highest current density, whereas at lower current densities NH$_3$ diffusion is the dominant ammonium transport mechanism.

5.3.3 Ammonium recovery rates

The ammonium recovery rates were determined according to equation 5.7. The highest ammonium recovery rate was 3.29 g_N $d^{-1}m^{-2}$ at a current density of 0.50 A m^{-2}. This recovery rate can be divided into NH_3 diffusion (concentration gradient and pH dependent) and NH_4^+ migration (current density and concentration dependent). Figure 5.6 shows the ammonium recovery rates with the respective NH_3 transport and NH_4^+ transport obtained during the experiments on real urine. Higher ammonium recovery rates can be reached by increasing the current density or increasing the NH_3 diffusion.
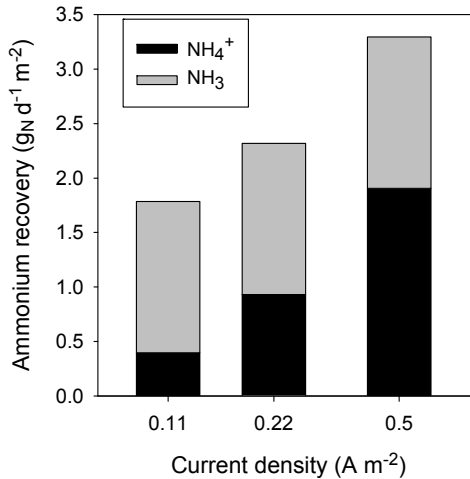
Figure 5.6: Recovery rates calculated at achieved current densities divided in NH_3 transport and NH_4^+ transport.

5.3.4 Energy analysis for ammonium recovery by an MFC

The energy analysis for ammonium recovery by MFC was performed at the highest current density (highest ammonium recovery) for an MFC, operated on real urine, with a membrane surface area of 1 m^2 and compared to conventional NH_3 stripping. The energy demand of the ammonium recovery by MFC was calculated based on aeration, the energy demand for ammonium recovery (adsorption in H_2SO_4) and the energy production of the MFC. The energy demand for aeration ($E_{(aeration)}$ (kJ g^{-1}))

of the scaled-up MFC was calculated according to:

$$E_{(aeration)} = \frac{\Delta P \cdot Q \cdot 86400}{\eta \cdot A_M \cdot recovery\,rate} \tag{5.11}$$

Where ΔP is the measured pressure drop in the gas diffusion cathode ($2.0 \cdot 10^4$ N m^{-2}) in a single cell, Q is the air flow ($1.67 \cdot 10^{-7}$ m^3 s^{-1}), η is the pump efficiency (conservatively chosen 0.8), A_M is the membrane surface area (0.01 m^2), 86400 (s d^{-1}) is the amount of seconds per day and *recovery rate* (g$_N$ d^{-1}m^{-2}) is the ammonium recovery rate (equation 5.7). The ΔP measured in a single cell is representative for a scaled-up MFC, which is a stack of identical cells with a similar geometry to the here applied prototype. An energy demand for aeration of 10.93 kJ g$_N^{-1}$ was calculated. Details on the energy demand of conventional NH$_3$ stripping, including chemical usage (CaO and H$_2$SO$_4$) and aeration were obtained from literature [55]. The comparison between ammonium recovery by an MFC and conventional NH$_3$ stripping is shown in Table 5.4. These results highlight the advantages of the MFC facilitated ammonium

Table 5.4: Detailed energy analysis for conventional NH$_3$ stripping and ammonium recovery by an MFC.

	NH$_4$ recovery by an MFC	Conventional NH$_3$ Stripping
Aeration (kJ g$_N^{-1}$)	10.93	26.3 [a]
Energy production (kJ g$_N^{-1}$)	-6.69	0
CaO (kJ g$_N^{-1}$)	n.r. [b]	13.9 [a]
H$_2$SO$_4$ (kJ g$_N^{-1}$)	-7.7 [a]	-7.7 [a]
Net energy yield (kJ g$_N^{-1}$)	-3.46	32.5 [a]

[a][55], [b] not required

recovery over the conventional NH$_3$ stripping. The ammonium recovery by an MFC requires less energy for aeration. The MFC produces energy and no CaO (or NaOH) addition is necessary for the NH$_3$ stripping. Therefore, a net energy yield of -3.46 kJ g$_N^{-1}$ was calculated for ammonium recovery by an MFC, whereas the conventional NH$_3$ stripping needs 32.5 kJ g$_N^{-1}$ [55].

5.3.5 Perspectives for the ammonium recovery by an MFC

One drawback of the ammonium recovery by an MFC is that only 31% of the produced electrons ($\alpha \leq 0.31$) were used for transport of ammonium. This limits the total amount of ammonium which can be transported by migration. The measured COD of the urine (3.9 g L^{-1}) shows that a maximum of 0.49 moles of electrons (per liter urine) can be produced and therefore only 0.15 moles of NH_4^+ (50%) can be recovered. The COD in the urine batches was monitored during the experiments, after the COD decreased to 1.5 g/L the urine batch was changed. A Coulombic efficiency of 10% was calculated during the operation on real urine at the highest current density, which shows that further improvements are needed. An electricity production coupled to ammonium, as shown recently [29], was not possible in this tested prototype MFC, because the anode was anaerobe and no nitrite was measured during the experiments. The total ion transport through the membrane can be influenced by the ion concentration at the anode and cathode [78]. A lower NH_4^+ concentration at the cathode compared to the anode leads to NH_4^+ diffusion. At the same time the ammonium transport is influenced by the NH_3 diffusion through the membrane. Therefore, ammonium needs to be removed from the cathode at a high rate to increase the total ammonium transport.

To become a competitive ammonium recovery technology, the ammonium recovery rate (g_N $d^{-1}m^{-2}$) must be increased. Since a higher current density leads to a higher rate of NH_4^+ transport, this can be achieved by increasing the current densities of the MFC. Recent literature reports current densities up to 5.5 A m^{-2} for a scaled-up MFC [93] and 22.8 A m^{-2} for a Microbial Electrolysis Cell [36] on a similar cell design. Although these current densities were reached using synthetic media, it shows that high current densities can be reached in bio-electrochemical systems.

The potential ammonium recovery efficiency (η_{NH_4}) was calculated on basis of the measured Coulombic efficiency (η_{CE}), the measured ratio of charge transport (Q_{NH_4}) to produced charge (Q_e) during experiments on real urine and the realistic concentration of ammonium ($C_{NH_4-N} = 8.1 g_N$ L^{-1}) and COD (10 g L^{-1}) found in urine [56] for a scaled-up MFC according to:

$$\eta_{NH_4} = \frac{b \cdot \left[\frac{COD}{M_{O_2}}\right] \cdot \eta_{CE} \cdot \left[\frac{Q_{NH_4}}{Q_e}\right]}{\left[\frac{C_{NH_4-N}}{M_N}\right]} \tag{5.12}$$

Where b is the amount of electrons (4) exchanged per mole of O_2, M_{O_2} is the molar mass of O_2, M_N is the standard atomic weight of nitrogen, η_{CE} is the Coulombic efficiency (0.1) and Q_{NH_4}/Q_e is the ratio of the total ammonium transport to the produced charge (0.53). A potential ammonium recovery efficiency of 11.4% was found. The low Coulombic Efficiency and the relatively low total ammonium transport to produced charge ratio are the limiting factors for the recovery of ammonium by an MFC. The Coulombic efficiency can be increased by limiting unwanted biomass growth (i.e. methanogens), due to an optimized operational control (i.e. lower retention time of anolyte) of the MFC [27]. Further investigation on ammonium recovery and Coulombic efficiency will be performed on a scaled-up version of this promising new technology.

The precipitation of crystals (e.g. struvite) inside MFCs is an important issue to consider when using highly concentrated streams (like urine) as a fuel. As a pretreatment step, partial removal of phosphorus can be necessary to avoid precipitation inside the MFC. In this work, the precipitated crystals were removed from the hydrolyzed urine to avoid scaling inside the MFC. No further precipitation inside the MFC was observed during the experiments.

5.4 Conclusions

This work demonstrates successfully the principal of simultaneous ammonium recovery and energy production from real urine using an MFC. The electrons needed for the transport of NH_4^+ from anode to cathode are produced by microorganisms on the anode. Additional NH_3 diffusion enhances the total ammonium transport to the cathode. NH_3 stripping from the liquid-gas boundary at the cathode occurs due to the localized high pH and the aeration of the gas diffusion cathode. The energy analysis shows that this technology can be a sustainable ammonium recovery technology. Further improvements to the ammonium transport rates are necessary, in order to become a competitive ammonium recovery technology.

Acknowledgements

6

Urine treatment concept

Abstract

In this study nutrient recovery from urine was investigated based on experiments and theoretical calculations. A process combination of phosphorus recovery via struvite precipitation and ammonium recovery using a Microbial Fuel Cell (MFC) was evaluated. The results show a high market potential for the proposed nutrient recovery concept. Phosphorus recovery by struvite precipitation does not only recover a valuable product, it also reduces the risk of scaling inside the MFC. The electricity production combined with the energy efficient ammonium recovery in the MFC are the biggest advantages of the proposed technology, as theoretical calculations show that enough electric energy is produced to operate the treatment process independently. The products of the proposed process are struvite, ammonia (or an ammonium sulfate solution) and electricity. Since urine contributes the biggest part of the nutrient load (i.e. 80% N and 50% P) to conventional wastewater treatment plants, a wide scale application of the proposed concept could significantly reduce this nutrient load and produce valuable fertilizers and energy.

Authors P. Kuntke, H. Bruning, G. Zeeman and C.J.N. Buisman

6.1 Introduction

6.1.1 Urine as a resource

Urine contains valuable resources, such as nitrogen and phosphorus, in high concentrations. Urine contributes about 80% of the nitrogen load and 50% of the phosphorus load to conventional wastewater, while it only contributes 1 % of the total volume to this wastewater [15, 40, 48, 56]. In conventional wastewater treatment plants (WWTPs) these resources are lost due to mixing with other waste streams and subsequent conversion or discharge. When urine is collected separately phosphorus and nitrogen can be recovered more effectively [55, 56, 108, 75, 46]. Phosphorus in urine is mostly found in a phosphate form ($\geq$90% [15, 48]). Nitrogen in urine is mostly found as urea ($\geq$84% [15, 48]). Urea can be hydrolyzed by the bacterial enzyme urease to NH_3 and carbamate, the latter is hydrolyzed further to NH_3 and bicarbonate [58]. Urease is produced by many bacteria, which can also be found in sanitary installations (toilets, pipework and plumbing) and the storage tank.

6.1.2 Recovery process

The presented recovery process includes a phosphorus recovery via struvite (often called MAP $MgNH_4PO_4 \cdot 6\,H_2O$) precipitation and nitrogen removal via NH_3 stripping with simultaneous energy production. This process differs from the process of Zang et al. [115], which also combines MAP precipitation and an MFC. Zang et al. [115] proposed an ammonium recovery via MAP precipitation which requires the addition of a surplus of phosphate [56, 115]. The process presented in this work recovers ammonium directly from an MFC system via NH_3-stripping [45, 46]. The schematic of the proposed process is shown in Figure 6.1.
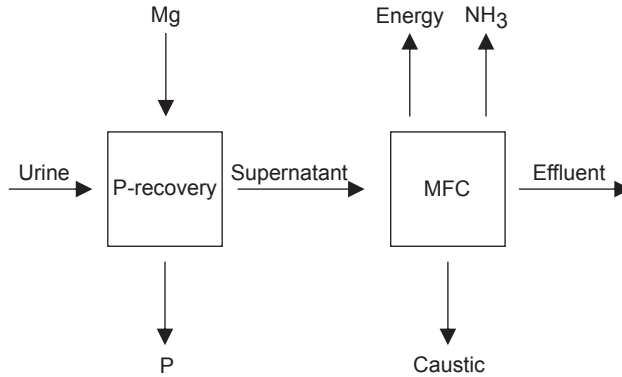
Figure 6.1: Schematic representation of the proposed treatment processes for the recovery of nutrients by struvite precipitation and ammonium recovery with simultaneous energy production (Mg = Magnesium salt, P = Phosphorus, Caustic = NaOH/KOH solution, Energy = electricity, NH_3 = Ammonia).

6.1.3 Phosphate recovery by precipitation

A quantitative recovery of phosphates from urine can be achieved by precipitation of phosphate salts (e.g. hydroxyapatite and MAP) [56]. Due to the occurrence of bi-carbonate and carbonate ions after urea hydrolysis [58], phosphate recovery via hydroxyapatite (HAP - $Ca_5(OH)(PO_4)_3$) precipitation requires an additional CO_2 stripping step (including pH adjustments) to avoid calcite ($CaCO_3$) formation. MAP precipitation has been proven effective in urine [111, 97, 75] as the pH of hydrolyzed urine (pH 8.85-9.25) is well suited for this. An additional advantage of MAP is the fact that it contains Mg^{2+}, NH_4^+ and PO_4^{3-} in equal molar amounts, which makes it a potentially effective fertilizer [23] and economically attractive [60, 112]. MAP has a high estimated market value (€763 per ton) [16]. A suitable magnesium salt has to be added to the urine [111, 75, 56], since the amount of magnesium ions in urine is too low for a complete P-recovery[1]. Experiments on struvite precipitation by Wilsenach et al. [111] showed that a PO_4^{3-}-P : Mg^{2+} ratio of 1 : 1 resulted in a high

---

[1]The molar ratio PO_4^{3-}-P : Mg^{2+} is 1 : 0.15 based on work in Chapter 2 and 1 : 0.17 based on Diem and Lentner [15].

phosphate removal of 99% independent of the magnesium source ($MgCl_2$ or MgO).

6.1.4 Ammonium recovery by an MFC

Bio-electrochemical systems are an emerging technology with a wide range of applications [27]. In Microbial Fuel Cells (MFCs), a specific type of bio-electrochemical systems, bacteria catalyze the oxidation of organic substrate (e.g. acetate) at the anode according to:

$$CH_3COO^- + 4\,H_2O \longrightarrow 2\,HCO_3^- + 8\,e^- + 9\,H^+ \tag{6.1}$$
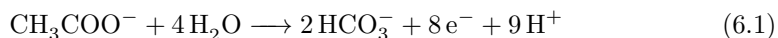
Due to the absence of an electron acceptor (i.e. O_2) in the anode chamber, the electrons are transported over an external electrical circuit to the cathode. At the cathode, the electrons are used to reduce oxygen. Given a neutral to alkaline environment (pH ≥ 7) in the cathode chamber, the reduction of oxygen results in the production of hydroxide according to:

$$O_2 + 4\,e^- + 2\,H_2O \longrightarrow 4\,OH^- \tag{6.2}$$
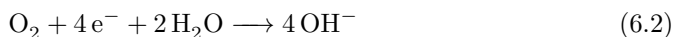
The anode chamber and cathode chamber are often separated by an ion exchange membrane [53]. The ammonium recovery as demonstrated in Chapter 5 is based on the migration and diffusion transport of the ammonium from anode to cathode through the cation exchange membrane and followed by the volatilization of NH_3 [46]. The transformation of ionic NH_4^+ to volatile NH_3 is the result of the high pH at the cathode ($NH_4^+(aq) + OH^-(aq) \longrightarrow NH_3(g) + H_2O$).

6.1.5 Scope

In this study nutrient recovery from urine was investigated based on experiments and theoretical calculations. A process combination of phosphorus recovery via struvite and ammonium recovery using an MFC was evaluated. This study is divided into two parts. The first part investigates the ammonium recovery by an MFC and phosphorus recovery by struvite precipitation. The focus lies on phosphate removal during the struvite precipitation and ammonium transport and energy production by the MFC. The second part will use the obtained results and literature data to extrapolate the benefits from the two processes in an up-scaled situation where one cubic meter

of urine per day is treated. Possible products, the energy demand of the process combination and bottlenecks are evaluated and presented to show the feasibility of this treatment concept.

6.2 Materials and Methods

6.2.1 Batch struvite precipitation

Batch precipitation experiments were performed using urine collected via a separation toilet (Villeroy & Boch Gustavsberg AB, Gustavsberg, Sweden) and water free urinals, Urimat® eco (Biocompact Environmental Technology B.V., Rotterdam, The Netherlands) at DeSaH BV (Sneek, The Netherlands). The pH of the urine was adjusted using a 1M NaOH or a 1M HCl solution. The batch experiments were performed at room temperature over a 24 hour period of time with constant agitation (100 rpm - Shaking Water Baths SW 22, JULABO Inc., USA) of the samples (each volume was 200 mL) in 500 mL bottles (HDPE bottles, Nalgene® VWR, The Netherlands). $MgCl_2 \cdot 6\,H_2O$ was chosen as the magnesium ion source for the precipitation experiments and was added in equal molar concentration to the phosphate concentration. Subsamples (2 mL) were taken before addition of $MgCl_2 \cdot 6\,H_2O$ and after one, two, four and 24 hours of treatment. These samples were filtered through a 0.2 μm filter to remove crystals. The collected filtrate was directly prepared for analysis of the phosphorus concentration in an ICP-OES (further details on page 93). The preparation step included the addition of 68% HNO_3 (145 μL per 10 mL sample, VWR, The Netherlands) to the diluted ICP samples (dilution factors 10x, 100x). The dilution and the acid addition prevented further crystallisation.

6.2.2 MFC operation and design

The MFC setup used for the experiment was identical to the setup applied in Kuntke et al. [46]. The MFC was made from two identical Plexiglas plates (21 cm×21 cm). Each plate contained one flow through chamber (10 cm × 10 cm × 0.2 cm) with a 9 channel inlet and 9 channel outlet for flow distribution. In the anode chamber (volume 20 mL), a graphite felt (100 cm^2, thickness 3 mm, National Electrical Carbon BV, Hoorn, The Netherlands) was used as the anode. The anode chamber and the cathode chamber (volume 20 mL) were separated using a membrane electrode assem-

bly (MEA). The MEA (100 cm^2) was produced by hot pressing (5 minutes, 140°C, 534 bar) a platinum coated (20 g m^{-2}) titanium fine mesh (Dexmet, Magneto Special Anodes B.V., Schiedam, The Netherlands) into a Nafion N117 (Dupont, Geneva, Switzerland) CEM using a Labopress P 400 S (Vogt Maschinenbau GmbH, Berlin, Germany). The anode (graphite felt) and the cathode (Pt coated Ti felt) were each contacted via 4 Pt/Ir (80/20) wires (0.025 cm diameter, Advent Research Materials, Oxford, UK) to the outside of the MFC. Anode medium was recirculated at 80 mL min^{-1} through the MFC using a peristaltic pump (Masterflex, Cole-Parmer, Vernon Hills, USA). New influent was supplied at a flow rate of 1 mL min^{-1} by another peristaltic pump. The total volume of the anode was 250 mL, including tubes (PTFE based), anode chamber, mixing flow cell (Schott Duran$^®$, VWR, The Netherlands). The MFC was operated at room temperature (20 $\pm$ 2°C). Air was supplied to the MEA in the cathode chamber at a flow rate of 10 mL min^{-1} using a compressor (Kaeser Sigma SM 9, USA), a multistage pressure regulator (VWR, The Netherlands) and a PTFE needle valve (VWR, The Netherlands) for flow control. The gas stream from the cathode was channelled through two 500 mL gas washing bottles with filter disks (Schott Duran$^®$, VWR, The Netherlands) placed in series. The first bottle was filled with boric acid (20 g L^{-1}) to collect the volatile NH$_3$ as NH$_4^+$ (adsorption bottle). The boric acid was renewed periodically. The gas stream from the adsorption bottle was channelled to a second bottle filled with a 0.4 M H$_2$SO$_4$ solution to prevent contamination of boric acid with ammonia from the laboratory environment.

6.2.3 Chemical analysis

Liquid samples (i.e. urine, supernatant) were analyzed for the concentration of relevant cations, anions and COD. An ICP-OES, type Perkin Elmer Optima 5300 DV (Waltham, Massachusetts, USA) was used to determine cation concentrations. An ion chromatography system, type Metrohm IC Compact 761 (Schiedam, The Netherlands) was used to determine anion concentrations. The COD was analyzed using test kit LCK 514 (Dr. Lange, HACH, Loveland, Colorado, USA) and the ammonium content was analyzed using test kit LCK 303 (Dr. Lange, HACH, Loveland, Colorado, USA) and a spectrophotometer HACH XION 500 (HACH, Loveland, Colorado, USA). Ammonium concentrations from the absorption bottle were measured throughout the experimental time to determine ammonium transport numbers. Samples of the influ-

ent and anode media were filtered (0.45 µm, PTFE syringe filters, VWR, Amsterdam, The Netherlands) prior to analysis. All samples were analyzed in duplicate. Precipitated crystals were analyzed using an ATR-FTIR spectrometer, type Shimadzu 4800 (Shimadzu Benelux, s-Hertogenbosch, Netherlands).

6.2.4 Calculation and simulation

MFC related parameters (current density and power density) and ammonium recovery parameters (recovery rate and energy demand) were determined as described in Chapter 5. A model urine with consistent composition (electron neutrality and adjusted pH) was derived using the OLI Analyzer 3.1.2 software (OLI Systems Inc., New Jersey, USA) based on the measured ion concentrations. Furthermore, the OLI Analyzer was applied to determine possible precipitation products and their respective scaling tendencies. The scaling tendency describes the thermodynamic driving force to form a specific solid, at a value of 1.0 this solid should form [89].

6.3 Results and discussion

6.3.1 Urine for the experiments

The average composition of the collected urine is presented in Table 6.1.

Table 6.1: Average composition of the urine used for the MFC and MAP experiments.

Parameter	Value	Unit
Na^+	1.85	$g\ L^{-1}$
K^+	1.49	$g\ L^{-1}$
Mg^{2+}	≤ 5.0	$mg\ L^{-1}$
Ca^{2+}	7.1	$mg\ L^{-1}$
NH_4^+/NH_3-N	4.05	$g\ L^{-1}$
Cl^-	3.29	$g\ L^{-1}$
PO_4^{3-}-P	0.21	$g\ L^{-1}$
SO_4^{2-}-S	0.21	$g\ L^{-1}$
COD	3.9	$g\ L^{-1}$
pH	8.85	-
Conductivity	35.0	$mS\ cm^{-1}$

The collected urine had an almost identical composition to the urine collected at the same location for an earlier study [46].

6.3.2 Phosphate recovery by MAP precipitation

Figure 6.2 shows the calculated scaling tendencies of important salts in hydrolyzed urine as a function of the pH (8.5 - 12.5) and the percentage of experimentally recovered PO_4^{3-}-P through MAP precipitation at various applied pH values from urine.

(a)   (b)
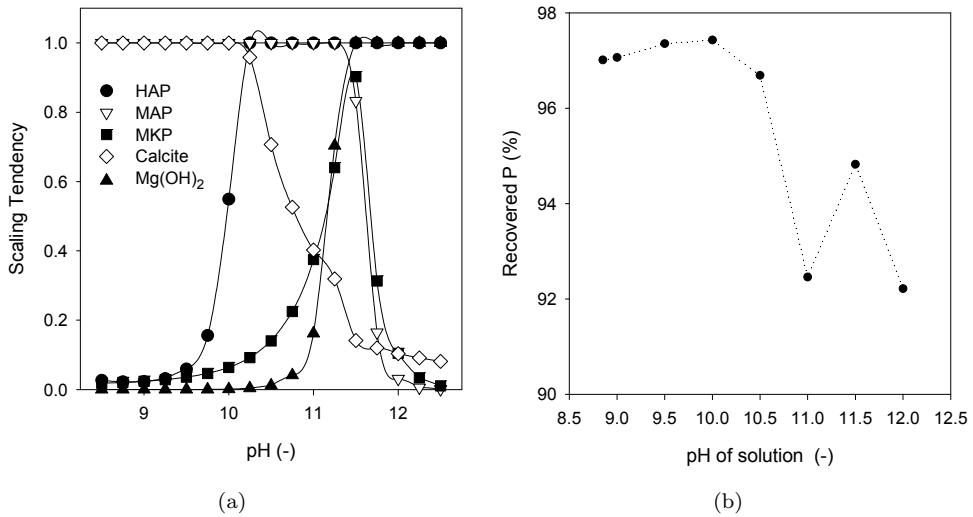
Figure 6.2: (a) Scaling tendencies of several salts in urine calculated using OLI Analyzer 3.1.2 software (OLI Systems, Inc.) based on measured ion concentrations (Table 6.1) with NaOH and HCl as titrans; (b) PO_4^{3-}-P recovery by Struvite precipitation determined at several pH values using $MgCl_2 \cdot 6\,H_2O$ from urine collected at DeSaH B.V.

Figure 6.2a shows that until a pH of 10 only the scaling tendency for MAP and calcite ($CaCO_3$) are equal to one. At higher pH values a shift from calcite to hydroxyapatite (HAP - $Ca_5(OH)(PO_4)_3$) at a pH $\geq$10, and MAP to MKP (potassium struvite, $MgKPO_4 \cdot 6\,H_2O$) at a pH $\geq$11.5 will occur. At a pH higher than 12, the scaling tendency for $Mg(OH)_2$ is equal to one. Figure 6.2b shows that a pH of 8.85 already yields a high phosphorus recovery of 97% in the performed batch experiments. A lower P-recovery (95%) at pH values higher than 11 was observed, which could

indicate the formation of unwanted $Mg(OH)_2$. Furthermore, a relative short time frame is needed (one hour) to reach high P-recovery. To summarize; phosphate can be efficiently removed as struvite at a molar ratio of PO_4^{3-}-P : Mg^{2+} of 1 : 1 and at a pH of 9 in a relative short time frame of one hour, which corresponds to findings of Wilsenach et al. [111]. Figure 6.3 shows the IR analysis of the samples of the crystals after 24h of experiment.
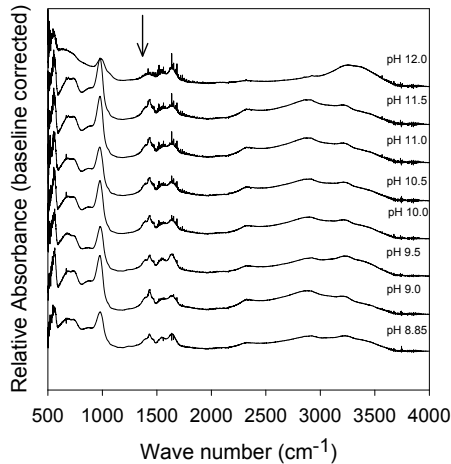
Figure 6.3: IR analysis of samples from struvite precipitation at various applied pH values from real urine.

The arrow indicates the ammonium-ions and water molecules bending vibration region (1400 - 1500 cm^{-1}) [87, 88]. In samples at pH 11.5 and higher, the peaks in these regions are less intensive indicating a change in the crystal samples from MAP to MKP.

6.3.3 Ammonium recovery by an MFC

The proposed concept is shown in Figure 6.4a, which is based on results of the research presented in Chapter 5. Figure 6.4b shows a polarization curve obtained during experiments using real urine. Each measuring point represents the average value determined over a period of at least 6 days. The highest current density and power density reached in this system are 2.6 A m^{-2} and 0.67 W m^{-2}, respectively.

(a)   (b)
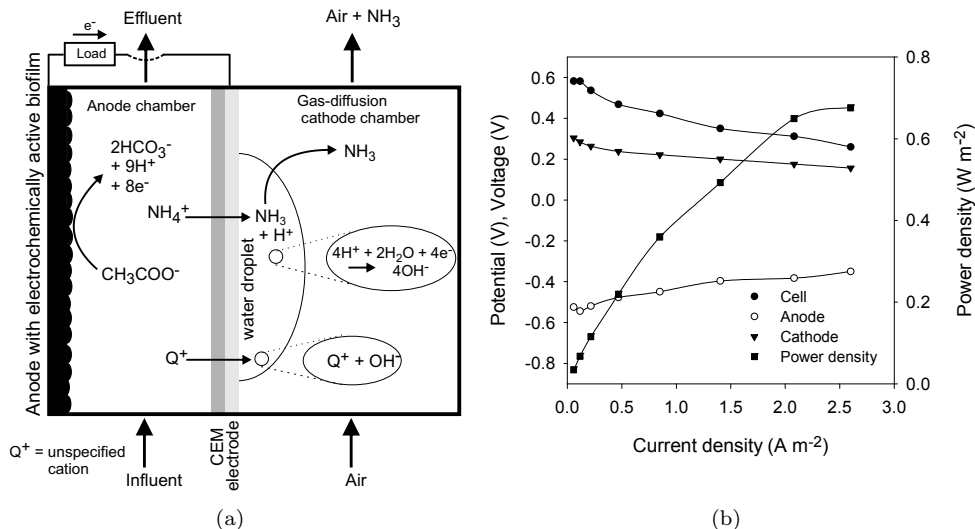
Figure 6.4: (a) Concept of an MFC-based ammonium recovery and energy production showing the involved processes. (b) Polarization curve obtained during experiments with undiluted urine. Each data point represents the average measured value over a time frame of at least 6 days.

The highest ammonium recovery achieved inside this system was 9.57 g_N d^{-1} m^{-2} at a current density of 2.6 A m^{-2}. The energy analysis for ammonium recovery using this MFC was performed as described in Equation 5.11 of Chapter 5 [46]. An energy production of 6.1 kJ g_N^{-1} and a net energy yield of -10.0 kJ g_N^{-1} for the recovery of ammonium by the MFC were determined, highlighting the possibility to simultaneously produce energy and recover ammonia. Next to the energy efficiency, the advantage of this approach is that a recovery of ammonia by stripping at the cathode does not require additional chemicals to increase the pH. For comparison, the N-recovery concept as proposed by Zang et al. [115] requires large quantities of phosphate for the recovery of ammonium as struvite [56][2].

The ammonium recovery can be further optimised by increasing the ammonium transport through the ion exchange membrane. Possibilities to increase this transport are increasing the diffusion flux and/or migration flux through the membrane (see Chapter 5). The diffusion flux of ammonium can be enhanced by effectively lowering

---

[2]molar ratio NH_4^+-N:PO_4^{3-}-P of 1:25.4 according to Table 6.1

the NH_4^+ and NH_3 concentration in the cathode chamber by increasing the NH_3-stripping rate. The second option is to increase the current density as it determines the migration flux. The results indicate that the cathode is limiting the performance of the MFC. The theoretical cathode potential for the reduction of oxygen E_{pH7} is +0.6 V vs Ag/AgCl [3]. As can be seen from Figure 6.4b, the cathode potential deviates from this theoretical cathode potential. Better catalysts for oxygen reduction in MFCs and improved aeration are crucial points. Recent literature suggests that higher current densities (up to 16.4 A m^{-2}) can be reached in MFCs [20]. However, the results of Fan and Liu [20] rely on the use of synthetic wastewater (containing 100 mM Phosphate buffer and 100 mM Acetate) and the application of a stacked MFC design (with a double cloth electrode assembly).

The Coulombic Efficiency (CE) of the employed MFC is another important point for future research. The CE describes the relation between recovered electrons (current) and the removed substrate (COD) [53]. Although high CEs of 83.5% and higher have been reported for synthetic wastewaters and defined media [20, 27], the reported CEs for urine processing MFCs are considerably lower [46, 115]. A key aspect is to limit the growth of other microorganisms which are competing for the COD inside the MFC [27].

6.3.4 Potential products of a scaled up recovery system

Model urine

A model urine was defined for the second part of this study in order to calculate the amount of products which can be recovered. This model urine composition is based on the average measured concentration as presented in Chapter 2 (Table 6.2), which was collected directly in bottles without any dilution.   Since urea $((NH_2)_2CO)$ is the major N-containing compound in fresh urine [15, 40, 98], the total amount of urea inside this average urine was estimated to be 90% of the total nitrogen which is equal to a urea concentration of 15.77 g L^{-1} or 0.2625 mol L^{-1} [4].

---

[3]typical cathode potential for oxygen reduction 0.805 V vs Standard Hydrogen Electrode (SHE) [77] and Ag/AgCl 0.205 V vs SHE

[4]Determined according to:

$$\text{Urea} = \frac{(T_N - NH_4^+\text{-N}) \cdot 0.9}{M_N \cdot 2} \cdot M_{Urea} \tag{6.3}$$

with $M_N = 14.0067$ g moL^{-1} $M_{Urea} = 60.06$ g moL^{-1}

Table 6.2: Average concentrations as presented in Table 2.1 Chapter 2.

Parameter	Concentration
COD (g L^{-1})	9.0
T$_N$ (g L^{-1})	8.6
Cl$^-$ (g L^{-1})	3.8
PO$_4^{3-}$ (g L^{-1})	2.00
SO$_4^{2-}$ (g L^{-1})	1.18
Na$^+$ (g L^{-1})	2.41
K$^+$ (g L^{-1})	1.89
Mg^{2+} (g L^{-1})	0.078
Ca^{2+} (g L^{-1})	0.106
NH$_4^+$/NH$_3$-N (g L^{-1})	0.431

A complete decomposition of urea[5] yields a NH$_4^+$ concentration of 4.73 g L^{-1}, a NH$_3$ concentration of 4.46 g L^{-1} and a HCO$_3^-$ concentration of 16.02 g L^{-1}. The pH of the model urine was set to the pK_a-value of the ammonium ($pK_a = 9.3$). The assumed volume stream to be treated is one cubic meter per day, which corresponds to the volume of daily excreted urine by approximately 667 persons (1.5 L p^{-1} d^{-1}).

On the basis of this set of parameters a model urine was derived using the OLI Analyzer 3.1.2 software (OLI Systems, Inc.)[6]. The composition of the hydrolyzed urine is given in table 6.3. The COD and its composition was not considered in the model at this point. The COD of urine, which was found to be mostly aliphatic (Chapter 2), is assumed to be biodegradable to a large extent ($\geq 85\%$). Similar high biodegradability has been reported by Udert et al. [95].

Phosphate-recovery

A suitable magnesium ion source has to be added to the urine, since the amount of magnesium ions in urine is too low (Table 6.3) for a complete P-recovery[7]. Various types of magnesium salts are available (e.g. Mg(OH)$_2$, MgO, MgCl$_2 \cdot 6$H$_2$O, etc.) as

---

[5]Overall reaction of the urea decomposition: $(NH_2)_2CO + 2H_2O \longrightarrow NH_3 + NH_4^+ + HCO_3^-$ [97]

[6]OLI Function: Add Water analysis, Reconciliation pH 9.3; NaOH and HCl as titrants; Ammonium as dominant ion to adjust for electron neutrality.

[7]Molar ratio PO$_4^{3-}$-P:Mg^{2+} is 1 : 0.15 or 1 : 0.17 according to Table 6.3 and Diem and Lentner [15], respectively.

Table 6.3: Model urine derived from OLI Analyzer 3.1.2 software (OLI Systems, Inc.).

Parameter	Concentration	Difference
	$(g\ L^{-1})$	%
Cl^-	3.80	-0.05
PO_4^{3-}	1.999	-0.05
SO_4^{2-}	1.179	-0.05
HCO_3^-	16.012	-0.05
Na^+	2.409	-0.05
K^+	1.889	-0.05
Mg^{2+}	0.078	-0.05
Ca^{2+}	0.106	-0.05
NH_4^+	5.275	7.81
NH_3	4.460	-0.05
NaOH	1.240	100.00
H_2O	$9.77 \cdot 10^2$	-2.27

potential magnesium sources. Economically interesting for the MAP production is magnesium oxide (MgO, 55% Mg^{2+}), €475-525 per ton [106] [8], due to its low price and high quantity of Mg^{2+}.

A quantitative recovery ($\geq$ 98%) of phosphate is possible at the pH of the hydrolyzed urine, as shown in Figures 6.2b and 6.5. The main product of the precipitation is MAP, but calcite ($CaCO_3$) precipitation occurs as a by-product. From one cubic meter of urine 5.11 kg MAP (20.85 mol) can be recovered. The calculated amount of MgO is 0.78 kg per m^3 of urine treated resulting in estimated costs of €0.37 - 0.41 per m^3 of urine. A market value of €3.90 was estimated for the daily produced MAP (5.11 kg) as slow release fertilizer [16].

Due to the large surplus of NH_4^+-N in the hydrolyzed urine, a quantitative recovery of potassium (K) as MKP is not feasible [111]. An increase of the pH to 11.5 would yield MKP (Figure 6.5a), but also results in the formation of $Mg(OH)_2$ as a byproduct (Figure 6.5b). The $Mg(OH)_2$ formation combined with the necessary addition of caustic for the pH increase to $\geq$11.5 makes K recovery by MKP production economically less attractive.

---

[8]Quotation from M.A.F. Magnesite `http://www.magnesiumoxide.com`, May 2012
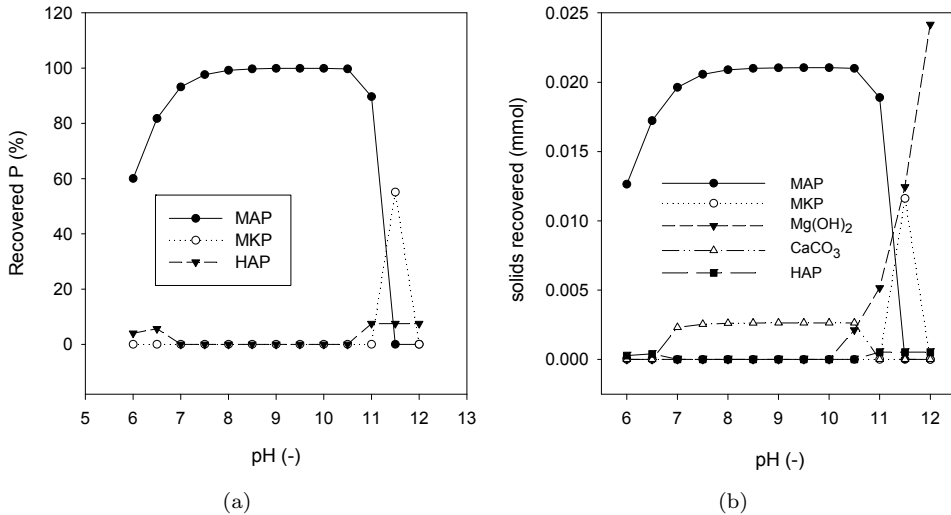
Figure 6.5: (a) Recovered P-salts presented in % of total recovered P and (b) recovered P-salt from one liter of urine presented in mmol in dependence of the pH using MgO as magnesium source. All results were determined using the OLI Analyzer 3.1.2 software (OLI Systems, Inc.)

One issue concerning the MAP production is the fact that it usually yields very fine crystals, which can wash out of the reactor and cause scaling in succeeding treatment steps [111]. Therefore, crystal growth has to be enhanced to allow for better separation or the formed struvite crystals have to be retained by other means (e.g. a filter).

Maurer et al. [55] reported in the Life-Cycle-Assessment that MAP precipitation requires 3.7 MJ kg_P^{-1} of energy (electricity) and 13.4 MJ kg_{Mg}^{-1} for chemicals usage (MgO). Based on these requirements, the production of 5.11 kg MAP will require a total of 8.14 MJ energy[9]. The urine after MAP precipitation (supernatant) still contains a considerable amount of COD and ammonium. This makes this stream interesting for further treatment in a MFC system for the recovery of ammonium and production of electricity [46].

---

[9]MgO: 13.4 (MJ kg_{Mg}^{-1}) · 0.55 (kg_{Mg} kg_{MgO}^{-1}) · 0.78 (kg_{MgO}) = 5.76 MJ

Energy: 3.7 (MJ kg_P^{-1}) · 20.85 ($mol_{P\text{-recovered}}$) · 30.97 g mol^{-1} / 1000 (g kg^{-1}) = 2.39 MJ

Ammonia-recovery and energy production

Based on the results of Chapter 2, a high biodegradability of the organic compounds[10] is expected. The maximum amount of available electrons from the COD can be determined according to $e_{max}^-(mol) = 4 \cdot \frac{COD(\frac{g}{L})}{32(\frac{g}{mol})} \cdot V_{urine}(L)$. Given a COD of 9 g L^{-1} [11] a theoretical maximum of 1,125 moles of electrons or 108,546 kC [12] are available per cubic meter of urine. The amount of dominant positively charged ions after struvite recovery [13] is equal to 68,098 kC. This means that in theory enough electrons are available to transport all dominant charged cations by migrational transport and therefore all ammonium can theoretically be recovered (7.26 g$_N$L^{-1}). The current (I) produced from the maximum amount of available electrons can be determined by Equation 6.4 and assuming a hydraulic retention time (HRT) of 24 hours:

$$I = \frac{e_{max}^- \cdot F}{HRT} \cdot \eta_{CE} \tag{6.4}$$

Where e_{max}^- are available electrons (1,125 mol), F is the Faraday constant (96485 C mol^{-1}), HRT is the hydraulic retention time (86,400 s) and η_{CE} is the coulombic efficiency (0.85). A current (I) of 1,067 A was determined.

The theoretical cell voltage can be determined on basis of Equation 6.5:

$$E_{Cell} = E_{Cathode} - \eta_{Cathode} - E_{Anode} - \eta_{Anode} - I \cdot R_{\Omega} \tag{6.5}$$

Where $E_{Cathode}$ is the cathode potential (V), $\eta_{Cathode}$ is the overpotential at the cathode (V), η_{Anode} is the anode potential (V), E_{Anode} is the overpotential at the anode (V), I is the current (A) and R_{Ω} is the total ohmic resistance of the anode and cathode (Ω).

As $\eta_{Cathode}$, η_{Anode} and $I \cdot R_{\Omega}$ are influencing the cell voltage, they can be summarized as the Voltage efficiency [26]. Therefore, Equation 6.5 can be simplified to Equation 6.6:

$$E_{Cell} = (E_{Cathode} - E_{Anode}) \cdot \eta_{Voltage} \tag{6.6}$$

---

[10] aromatic compounds $\leq 5\%$

[11] see Table 6.2 on page 99

[12] electrical charge (C): $Q_e = e_{max}^- \cdot F$

[13] e.g. K$^+$, Na$^+$, NH$_4^+$; assuming that all NH$_3$ is present as NH$_4^+$, due to the acidification of the anode as a result of the proton production Equation 6.1

Where η_{Voltage} is the voltage efficiency which was assumed to be 70% (0.7). Furthermore, E_{Cathode} is the cathode potential (0.805 V vs SHE) and E_{Anode} is the anode potential (-0.296 V vs SHE) under typical conditions found in MFCs [53]. This leads to a cell potential (E_{Cell}) of 0.771 V for the MFC according to Equation 6.6.

Therefore, 19.76 kWh [14] can be produced from one cubic meter of urine, which corresponds to an energy production equivalent of 71.16 MJ. For the design of the MFC (to treat 1 m^3 urine), an anode surface area of 67 m^2 was estimated on basis of a current density of 16 A m^{-2} [15]. A stacked design (monopolar or bipolar [16]) is envisioned, which consists of electrode pairs with a total surface area of anode and cathode equal to the projected membrane surface area. Assuming an average thickness of 1.5 cm per cell pair, the MFC has an estimated size of 1.05 m^3. Although the feasibility of a stacked MFC design has been presented by Shin et al. [81], intensive research will be necessary to realize an MFC of these dimensions.

An energy demand of -17.21 kJ g$_N^{-1}$ for the ammonium recovery was determined according to Chapter 5 [46] [17]. Which shows that the energy production by the MFC yields more energy than is required for the recovery of the ammonium, which is conform with the results presented in Chapter 5.

Energy demand

The energy demand for the treatment of one cubic meter of urine per day is shown in detail in Table 6.4. The calculations are based on the reported energy demands for struvite recovery [55], ammonium recovery by an MFC [18] and the calculated energy requirements for the recycle pump for the anode media and feeding pump to the MFC.

The pump energy demand (kJ m^{-3}) for recycling of the anode liquid in the MFC was calculated on basis of Equation 6.7 adapted from Jeremiasse [35].

$$E_{\text{Pump}} = \frac{Q_{recycle} \cdot \Delta P \cdot N \cdot HRT}{V \cdot \eta_{\text{Pump}}} \tag{6.7}$$

---

[14]$P = I \cdot E_{\text{Cell}} \cdot 24$

[15]Membrane surface area (m^2) = $\frac{1,067A}{16A\ m^{-2}} = 66.75$m^2

[16]to be addressed in future research

[17]Power density: 12.24 W m^{-2}, Recovery rate: 109 g$_N$ m^{-2} d^{-1}, Aeration: 0.36 kJ g$_N^{-1}$, Energy production: -9.84 kJ g$_N^{-1}$, H$_2$SO$_4$: -7.7 kJ g$_N^{-1}$

[18]as presented in this chapter and in Chapter 5

Where $Q_{recycle}$ is the volumetric recycle rate (m^3 s^{-1}), ΔP is the pressure drop over the anode chamber (N m^{-2}), η_{Pump} is the pump efficiency (0.8), N is the number of electrode pairs (67), HRT the hydraulic retention time in seconds (86,400 s) and V is the volume of urine treated per day (1 m^3 d^{-1}). Based on the work of Jeremiasse [35], a volumetric recycle rate of $3.33 \cdot 10^{-4}$ m^3 s^{-1}, which is equal to 28.8 m^3 d^{-1}, with a corresponding ΔP of $3.3 \cdot 10^3$ N m^{-2} (Pa) were used for the calculation. The pump energy demand for the feed pump was determined by equation 6.7, while substituting the $Q_{recycle}$ with Q_{feed}. Q_{feed} is the feed flow of $1.161 \cdot 10^{-05}$ m^3 s^{-1} (1 m^3 d^{-1}) to the MFC. All other parameters where kept as mentioned above, assuming a pressure difference of at least $\Delta P \cdot N$ ($3.3 \cdot 10^3$ N m^{-2} $\cdot$ 67 = $2.21 \cdot 10^5$ Pa).

Table 6.4: Energy demand for the treatment of one cubic meter of urine per day.

Treatment step	Energy requirement	Quantity	Energy demand MJ m^{-3}
MAP			
MgO	13.40 kJ g$_{Mg}^{-1}$	429.0 g$_{Mg}$ m^{-3}	5.75
Energy use	3.70 kJ g$_P^{-1}$	645.71 g$_P$ m^{-3}	2.39
Subtotal			8.14
MFC			
Recirc. pump	7.96 MJ m^{-3}		7.96
Feed pump	276.38 kJ m^{-3}		0.28
Aeration	0.33 kJ g$_N^{-1}$	7260.0 g$_N$ m^{-3}	2.40
Energy prod.	-9.84 kJ g$_N^{-1}$	7260.0 g$_N$ m^{-3}	-71.44
H$_2$SO$_4$ use	-7.70 kJ g$_N^{-1}$	7260.0 g$_N$ m^{-3}	-55.90
Subtotal			-116.71
Total			-108.57

Financial aspects

Table 6.5 shows the quantity of produced and consumed products and their value or costs derived from market prices and predicted daily production from one cubic

meter of urine. Overall, a yearly net income of € 5,900 is foreseen based on these assumptions. Additional benefits may be derived from reductions of wastewater discharge taxes, as urine is treated and COD, N and P are removed from the wastewater stream.

Table 6.5: Value and quantity of produced and consumed products from the daily treatment of one cubic meter urine.

Product	Costs price		Quantity [a]	Revenues (€ d^{-1})	Revenues (k€ yr^{-1})	Ref.
MAP	0.76	€ kg$_{MAP}^{-1}$	5.10 kg	3.9	1.4	[16]
MgO	0.5	€ kg$_{Mg}^{-1}$	-0.78 kg	-0.4	-0.1	[16]
electricity[b]	0.3	€ (kWh)$^{-1}$	16.80 kWh	5.0	1.8	[86]
NH$_3$	1.3	€ kg$_N^{-1}$	7.30 kg	9.4	3.4	[106]
H$_2$SO$_4$	0.297	€ kg$_{H_2SO_4}^{-1}$	-18.20 kg	-5.4	-2.0	[16]
Caustic[c]	0.43	€ kg$_{Caustic}^{-1}$	8.30 kg	3.6	1.3	[16]
Total				16.2	5.9	

[a] -x consumed +x produced per m^3, [b] corrected for the energy demand of the pumps (2), [c] NaOH/KOH

The costs of the here proposed treatment concept is highly dependent on the costs of the MFC, since this is by far the largest investment due to its complexity, the individual material costs and size. Table 6.6 shows the estimated costs for the MFC system as presented in this chapter. These estimations show that the costs for the cathode and the cation exchange membrane are the biggest contributors determining the total costs of the MFC. The use of other CEMs from different producers and other cathode materials might reduce the costs of the MFC significantly. Therefore, further research into alternative designs and materials will be necessary to further reduce the costs of the MFC.

Table 6.6: Estimated material costs for the MFC stack[$].

Part	Costs	Costs of the Reactor
	$(\text{\texteuro} \ \text{m}_{\text{reactor}}^{-2})$	$(67\text{m}^2) \ \text{\texteuro}$
Current collector [a]	5	335
Anode [b]	42	2,814
Cathode [c]	470	31,490
Ion Exchange Membrane [d]	255	17,085
Stack housing [e]	2,500	2,500
Others [f]	5,000	5,000
Total	8,272	59,224

[$] does not include labour and maintenance costs [a] Pt/Ir (80:20) wire, estimation based on [35], [b] Graphite felt - Morgan AM&T UK , [c] PTFE/Ni-mesh/MnO$_2$/C Gas diffusion Cathode - Electric Fuel Israel, [d] Fumasep FKE-PK - Fumatech Germany, [e] HDPE, estimation based on [35], [f] estimated costs for controls, pumps and the electrical circuit

6.4 Conclusions

The results presented in this study show that a process combination of MAP precipitation and an MFC for ammonium recovery and energy production can produce valuable fertilizers and electrical energy. This combination of these processes is especially interesting as more than 95% of the phosphate is removed during struvite precipitation, resulting in an effluent that is suitable for ammonia recovery by an MFC without risk of scaling. The laboratory scale MFC technology needs to be significantly scaled up and issues concerning the cathode performance have to be overcome. The electricity production combined with the energy efficient ammonium recovery in the MFC are the biggest advantages of the proposed technology, as estimates show that enough electricity is produced to operate the treatment process independently. The products of the proposed process are struvite, ammonia (i.e. ammonium sulfate solution) and electricity. Additional benefits may be derived from the reduction of wastewater taxes, as resources are recovered leading to a lower nutrient

load to conventional WWTPs. Since urine contributes the biggest part of the nutrient load (i.e. 80% N and 50% P) to conventional WWTPs, a wide scale application of the proposed technology could significantly reduce this nutrient load and produce valuable fertilizers and energy.

Acknowledgements

7

General discussion and outlook

7.1 Introduction

Nutrients are the base of fertilizers, which are applied in agriculture to ensure sufficient food supply for a growing world population. In 2012, 10 Mt of Nitrogen (N) based fertilizers and 1.5 Mt of phophorus (P) based fertilizers were used in the EU alone [18]. Unsustainable Nitrogen fertilizer production and limited resources of phosphor-rock are the incentives for the recovery of nutrients from wastewater.

Urine contributes only a small volume (about 1%) to domestic wastewater, but most of the nutrients found in domestic wastewater originate from it (about 80% of the N and 50% of the P). Domestic wastewater contains 20 to 70 mg_N L^{-1} and 1 to 4 mg_P L^{-1}, whereas urine contains 8.6 g_N L^{-1} and 0.7 g_P L^{-1}. Therefore, urine should be seen as a valuable source for nutrient recovery. The use of separation toilets and water-free urinals offers the possibility to collect a concentrated urine stream.

In this chapter, the work presented in this thesis is placed in perspective while limitations and possible future research directions are presented.

7.2 Prospects for nutrient recovery from urine

Urine as a resource

Considering the European situation with no known available deposits of rock-phosphate and the foreseeable depletion and scarcity of phosphorus in the future [65], a recovery of P from waste(water) streams and especially urine is an interesting approach. Next to scarcity of rock-phosphate, its pollution with cadmium, uranium and other heavy metals is a big concern [17, 14]. Therefore, wastewater could be a clean and sustainable P source. The advantages of urine as a source for P recovery are the relatively high concentration of phosphate and low concentrations of possible inorganic pollutants [15, 76]. Furthermore, work by Ronteltap et al. [76] on struvite precipitation showed that more than 98% of organic micro-pollutants (hormones and pharmaceuticals) remained in solution. Heavy metals can co-precipitate but were not detected in struvite produced from normal stored urine [76]. Furthermore, the high concentration of N in urine, which is predominantly found as ammonium nitrogen (NH_3 and NH_4^+) after urea hydrolysis [15, 48], allows the development of a more efficient recovery technology, as less volume needs to be treated compared to conventional wastewater.

The composition of urine is quite stable as shown in Chapter 2, which is in agree-

ment to earlier findings [15]. Arguably, the chosen sample set is not entirely representative for all inhabitants of Europe (or the world) as the age group of the Wetsus sample set was 18-65 years. Interestingly enough, the organic composition is relatively constant and only a dilution effect is shown. This shows that although different amounts of oxidizable organic material (hence differences in measured COD) were measured, the overall composition of the organic material is almost identical between samples. Bio-electrochemical systems (i.e. Microbial Fuel Cells) and other systems relying on microorganisms prefer an inflow stream of constant and stable composition so these microorganisms can adapt over time. Results of Chapter 2 show that urine can be such a stream. Especially interesting is the high occurrence of aliphatic compounds, which indicates a high biodegradability. A high biodegradability of the organic compounds in urine was reported in experiments by Udert et al. [95].

Urine treatment by MCDI

The treatment of diluted urine by electrosorption (i.e. Membrane Capacitive Deionization - MCDI) to concentrate the nutrients can be an interesting solution when flushing water is collected along with the urine. As described in Chapter 3, the MCDI technology allows for recovery of nutrients via concentration. The limitation for recovery is the solubility of the various salts (e.g. $Ca_5(PO_4)_3(OH)$, $MgNH_4PO_4 \cdot 6\,H_2O$, $CaCO_3$) in order to avoid precipitation (scaling) inside the MCDI unit. The separation and concentration steps are based on the temporary storage of charged ionic compounds in the double layer formed at the electrodes, while a potential is applied. Therefore, the major drawback of this technology is the energy consumption. An energy demand of at least 14.72 kJ per litre of diluted urine was determined in Chapter 3. Based on recently published work by Zhao et al. [118] this energy consumption can be as low as 7.64 kJ per litre[1] and additionally up to 40% of energy could be recovered from the discharge step in an ideal situation. However, it has to be mentioned that the operation parameters (i.e. flow rate, time steps, media composition, etc.) and design (e.g., dimensions) of the respective systems were not identical.

The possibility to separate and concentrate ammonium apart from other nutrients and COD needs to be investigated in future research. Theoretically ammonium could be separated following a strict regime for the treatment of the collected urine. This

---

[1]Based on the reported lower limit of energy consumption of 22 kT per removed ion. Energy (kJ) = 22 $kT \cdot 2.48$ kJ $mol_{ions}^{-1} \cdot 0.14$ mol_{ions} L^{-1} = 7.64 kJ L^{-1}

includes the following steps:

1. Stabilization to preserve the urea (H_2SO_4 addition to pH $\leq$ 5)

2. First MCDI treatment, separation of charged and uncharged compounds

3. Controlled hydrolysis of the urea to form NH_4^+

4. Second MCDI treatment, separation of NH_4^+ and uncharged compounds

Ammonia recovery by an MFC

Currently, the high energy and chemical demand of nitrogen recovery technology (e.g. adsorption, NH_3 stripping) makes a direct recovery economically uninteresting [55, 56]. An indirect nitrogen recovery over the atmosphere via the Sharon-Anammox process (N-removal) and the Haber-Bosch process (N-fixation) requires a relatively low amount of energy [55]. The bottlenecks for any nitrogen recovery technology are the relatively low energy demand for the Sharon-Anammox and Haber-Bosch process and the availability of vast amounts of N_2-gas from the atmosphere. Therefore, a nitrogen recovery technology needs to out compete the Haber-Bosch process or to find a niche market in order to be a successful alternative.

The possibility of using a Microbial Fuel Cell (MFC) for the recovery of ammonium from high strength ammonium wastewater (e.g. urine) was shown in Chapter 4. The effect of an increasing ammonium concentration (up to 4 g L^{-1}) on the MFCs was studied and it was shown that no negative effects could be found on the MFC performance or stability. In this work, ammonium was concentrated in the cathode compartment during the experiments, but ammonium removal from the cathode was not investigated.

Therefore, an adapted ammonium recovery by an air-cathode-system microbial fuel cell was developed and studied in further detail (Chapter 5). The process of ammonium recovery by NH_3-stripping from the cathode in combination with energy production shows great potential. The results show that more energy can be produced than is necessary for ammonium recovery. The recovery of ammonium is a result of the migrational and diffusional transport of ammonium from the anode through the cation ion exchange membrane to the cathode. The high pH at the cathode transforms ionic NH_4^+ to volatile NH_3. The latter is removed by the gas stream passing through the cathode chamber. Subsequently, NH_3 can be collected in an acid washer to produce

enriched ammonium liquids. The combination of energy and chemical efficient NH_3-stripping and the energy production by the MFC make this ammonium recovery technology a promising alternative to conventional treatment (e.g. Anammox and nitrification/denitrification) and recovery systems (e.g., NH_3-Stripping).

Numerous applications can be derived from this MFC-based ammonium recovery process, focusing on different types of wastewater (e.g. manure, conventional wastewater, etc.). The requirements are a liquid stream containing a low amount of solid particles and a balanced ratio of oxidizable organics to ammonium-nitrogen. Based on the work presented in Chapter 5, a molar ratio of 0.83 to 1 (COD to N) is necessary, but diffusional transport can lower the requirements for COD.

Urine treatment concept

One of the requirements for the safe application of an MFC on urine is the removal of Ca^{2+}, Mg^{2+} and PO_4^{3-} ions from urine to prevent crystallization of struvite (MAP - $MgNH_4PO_4 \cdot 6\,H_2O$), calcite and calcium phosphate inside the MFC. Therefore, a logical step is to combine the ammonium recovery by an MFC with a phosphate recovery step. The most attractive option for a phosphate recovery step is struvite precipitation, due to the composition of urine. In Chapter 6 this process combination was evaluated and it was shown that this combination is highly promising. The products of this process are struvite, an ammonium solution and electricity. At this moment, further research and development need to focus on up-scaling and integration of the technology. Additionally, the performance of the MFC needs to be improved with a focus on Coulombic Efficiency, cathode performance and ammonia stripping. From an economic point of view the MFC is too costly, as the estimated material costs for the MFC alone are about €60,000 (not including installation costs) for the treatment of 1 m^3 per day, while the predicted revenue per year from the products is about €5,900. Membrane and cathode electrode material are main cost factors with €470 and €255 per square meter reactor[2], respectively. The material costs per square meter reactor is about €880, while a prediction shows that bio-electrochemical systems (e.g. MFCs) can be produced for about €100 in the future [79, 82].

As Sleutels et al. [82] presented, MFCs can become a successful technology when wastewater treatment is combined with electricity production and the production

---

[2]Based to the necessary electrode surface area (m^2) including other materials see Chapter 6 for further details.

of valuable products. Therefore, ammonium recovery by an MFC seems to be a promising path. Additionally, benefits may be derived from savings or revenues due to wastewater taxes. For the Netherlands, wastewater taxes need to be paid on the basis of pollution equivalents ("vervuilingseenheden") [30]. A theoretical revenue of about €17,320 can be expected (see supporting information, page 117), which would significantly lower the return of investment time of this technology. The scale (centralized or decentralized system) of the application will, amongst others, depend on the logistics of chemicals and products. A centralized treatment system requires the transport of large amounts of water, as urine contains only 1.2 wt% of nutrients. Additionally, ammonia could be lost during storage and transport. In contrast, a decentralized system requires logistics of chemicals and products. Furthermore, the recovery system needs to be robust enough to work without constant need of service.

7.3 Comparison of technologies

Two technologies for urine treatment were used as a benchmark for the proposed treatment concept presented in Chapter 6; the SaNiPhos® [25, 8] and the 'Gele stroom' ('Yellow current') [24, 32]. In short; The SaNiPhos® uses a process combination of struvite precipitation and NH_3-stripping to produce struvite and ammonium-sulphate from urine collected at different locations [25] (see also page 11). The 'Gele stroom' produces struvite ($MgNH_4PO_4 \cdot 6\,H_2O$) from urine, which is thermally decomposed to NH_3 and $MgHPO_4$. The NH_3 is used as a fuel in a modified solid oxide fuel cell and part of the $MgHPO_4$ is reused for the struvite production [24] (see also page 10).

The technologies were compared based on their respective energy demands. The energy demands for the processes were calculated based on available literature data and reported energy demands for the respective recovery technologies according to Maurer et al. [55, 56] and the calculated energy production. Details of this calculation are presented in the supporting information (page 117).

The 'Gele stroom' process produces a surplus of energy of about 70 MJ and MAP - MFC process combination produces a surplus of energy of about 61 MJ, whereas the SaNiPhos® process requires 171 MJ of energy. As mentioned by Bisschops et al. [8], the energy demand of the SaNiPhos® process is expected to be lower in an up-scaled situation. However, no information was available to assess the actual energy demand

of a scaled up installation. For the 'Gele stroom' process, it has to be mentioned that the energy demand for the transport of $MgNH_4PO_4 \cdot 6\,H_2O$ and $MgHPO_4$ is not included and will increase the energy demand of this process. Table 7.1 summarizes the maximum amount of products which can be recovered using the respective treatment processes for the treatment of one cubic meter of urine. Only the SaNiPhos® process is currently operational on a full scale, whereas both of the other technologies are still under development. Yet, the centralized installation of the SaNiPhos® process requires the transport of large amounts of water (urine contains only 1.2 wt% of nutrients).

Table 7.1: Product summary based on the treatment of one cubic meter of urine.

Treatment Process	Energy production	N recovered	P recovered
MAP+MFC	61 MJ	267 mol [a]	21 mol [b]
'Gele stroom'	70 MJ	-	21 mol [c]
SaNiPhos®	-171 MJ	267 mol [a]	21 mol [b]

[a] $(NH_4)_2SO_4$ (aq) , [b] $MgNH_4PO_4 \cdot 6\,H_2O$, [c] $MgHPO_4$

7.4 Concluding remarks for future research

- Ammonium recovery by an air-cathode MFC is the most promising technology for urine treatment investigated in this thesis. This technology can be applied to various wastewater streams containing ammonium-nitrogen.

- Further research on the use of MFCs to recover nutrients from urine is necessary to overcome its current limitations. This includes material development, limitations of the current catalyst for oxygen reduction and ammonium removal from the cathode compartment to enhance diffusional transport of ammonium from anode to cathode.

- Alternatives to the MFC approach (such as Microbial Electrolysis Cells for hydrogen production) should be considered and addressed in future research.

- A process combination of struvite precipitation and ammonium recovery by an MFC shows a high potential as a nutrient recovery concept. Up to 98% of

the nitrogen and phosphorus can be recovered from urine in this process. The electricity production combined with the energy efficient ammonium recovery in the MFC is the biggest advantage of this proposed technology.

- Ammonium recovery by an MFC is a breakthrough in urine treatment.

Acknowledgements

Supporting Information

Calculation of the pollution equivalent

The pollution equivalent (P.E.) is calculated according to equation 7.1:

$$\text{P.E.} = \frac{Q \cdot (\text{COD} + 4.57 \cdot T_N)}{1000} \cdot \frac{365}{54.8} \tag{7.1}$$

Where Q is the volume (0.0015 m^3 d^{-1}), COD is the chemical oxygen demand (9000 mg L^{-1}), T$_N$ is the total nitrogen (8600 mg L^{-1}), 1000 is the factor for the gram to kilogram conversion, 365 is the number of days per year (d yr^{-1}) and 54.8 is the required oxygen amount of oxygen per year (kg yr^{-1}). Urine has a P.E. of 0.48. Based on an average price of €53.8 per P.E. [12] the total revenue is €17,320 per year for the treatment of urine from 667 persons (1 m^3 d^{-1}).

Comparison of technologies

All assumptions are based on a treatment of one cubic meter of urine per day. The composition of model urine is based on Chapter 6.

Table 7.2: Average concentration as presented in Table 2.1 Chapter 2.

Parameter	Concentration
COD (g L^{-1})	9.0
T$_N$ (g L^{-1})	8.6
Cl$^-$ (g L^{-1})	3.8
PO$_4^{3-}$ (g L^{-1})	2.00
SO$_4^{2-}$ (g L^{-1})	1.18
Na$^+$ (g L^{-1})	2.41
K$^+$ (g L^{-1})	1.89
Mg^{2+} (g L^{-1})	0.078
Ca^{2+} (g L^{-1})	0.106
NH$_4^+$/NH$_3$-N (g L^{-1})	0.431

The energy production in the solid oxide fuel cell was determined on the basis of Equation 7.2 with the respective conditions for the NH$_3$ oxidation (NH$_3 \longrightarrow \frac{1}{2}N_2$ +

$3\,H^+ + 3\,e^-$):

$$I = \frac{e^-_{max} \cdot F}{HRT} \cdot \eta_{CE} \tag{7.2}$$

Where e^-_{max} are available electrons (mol), F is the Faraday constant (96485 C mol^{-1}), HRT is the hydraulic retention time (86,400 s) and η_{CE} is the coulombic efficiency (0.80). With $e^-_{max} = 3 \cdot \frac{C_{NH_3}}{M_{NH_3}}$, e^-_{max} was determined to be 1.6 mol L^{-1}. C_{NH_3} is the amount of ammonia and M_{NH_3} is the molar mass of ammonia (g mol^{-1}). Therefore, the current (I) was determined to be 1,43 A. The cell potential of the SOFC was determined based on literature [21] according to equation 7.3:

$$E_{Cell} = E^0_{Cell,1123K} \cdot \eta_{voltage} \tag{7.3}$$

Where $E^0_{Cell,1123K}$ is 1.33 V and $\eta_{voltage}$ is 0.8. Therefore, the overall 36.5 kWh are produced from the ammonium present in one cubic meter urine (534 moles), which corresponds to an energy production equivalent of 131.57 MJ.

The energy demand for the MAP precipitation was determined on the basis of the required P removal. The amount of P removed is to be equal to the total amount of N removed. One cubic meter urine contains 534 moles ammonium nitrogen, therefore 16.52 kg P needs to be removed. The results of the energy balance are shown in table 7.3.

For the SaNiPhos® process, the energy demand was calculated based on published results from Bisschops et al. [8]. The authors report an electrical energy demand of 58 MJ g$_N^{-1}$ based on a 38% efficiency for electricity production. Hence, independent of the source and efficiency for energy, 22.04 MJ g$_N^{-1}$ is required for the SaNiPhos® process. Therefore, the recovery of all ammonium-nitrogen (7.76 kg m^{-3}) requires 171 MJ.

Table 7.3: Energy balance 'Gele stroom' and MAP + MFC based on one cubic meter urine to be treated.

Treatment step	Gele Stroom		MAP + MFC	
	Required (MJ)	Produced (MJ)	Required (MJ)	Produced (MJ)
MAP				
Energy use	61.14 [a]		2.39 [d]	
SOFC				
Energy production		131.56		
MAP decomposition	(2.45) [b]			
MAP transport	not known			
MHP recycle	not known			
MFC				
Recirculation pump			7.96 [d]	
Feed pump			0.28 [d]	
Aeration			2.40 [d]	
Energy production				71.44 [d]
Net Energy production	70.43 [c]		60.80	

[a] Energy use based on removed phosphorus 3.70 kJ g_P^{-1} and 16.52 kg_P [b] Energy for thermally decomposed of MAP [5] 4.60 kJ mol_N^{-1} and 533.57 mol N not considered as SOFC produce an excess of heat during operation. [c] Does not include energy required for the transportion of MAP and MHP (MgHPO$_4$). [d] Based on results from Chapter 6

Summary

Humankind relies on the use of artificial fertilizers to ensure safety of the food supply. Especially large quantities of nitrogen and phosphorus based fertilizers are applied annually. They are produced by energy intensive processes. Next to the energy consumption, the availability and quality of phosphate-rock - the raw material for phosphate fertilizer production - are of a big concern. On the other side, household wastewater contains nitrogen and phosphorus compounds and could be used as a source for these valuable compounds. **Chapter 1** describes the current situation including dependence and importance of fertilizers as well as the current practise of removal and recovery of nitrogen and phosphate in wastewater treatment plants. Nitrogen and phosphate compounds are essential nutrients for life. Due to their application as fertilizers, these nutrients enter the waterbodies directly (run off from lands) or indirectly (over the animal-human food chain) which can cause eutrophication. Urine contributes a small volume fraction of household wastewater, but contains most of the nutrients. In households, nutrients are diluted due to the combined collection of different types of wastewater. This dilution is a big obstacle for nutrient recovery. Furthermore, in wastewater treatment plants nutrients are considered pollutants and therefore converted and removed from wastewater. Nitrogen compounds are mostly converted to inert nitrogen gas using either the nitrification-denitrification or the Anammox process. Phosphate can be removed by precipitation or via biological processes, often resulting in products with a low solubility or products which

are polluted with sewage sludge. These products need further processing before they can be used as fertilizers. Urine can be collected separately from other wastewater streams to avoid dilution to be able to recover the valuable fertilizers more efficiently. In the EU, urine could provide up to 18% of the phosphorus and 24% of the nitrogen used in agriculture as fertilizers. Furthermore, urine contains a considerable amount of oxidizable organic compounds, which could be used in a bio-electrochemical system to generate energy. However, existing technologies for recovery of nutrients are energy intensive.

In **Chapter 2**, the organic and inorganic fraction of 106 urine samples were characterized to investigate their compositions and study their variations. This characterization is useful for the development and optimization of a suitable nutrient recovery strategy using the potential energy contained in the organic compounds. Two sets of urine samples were collected. The first urine sample set was collected from colleagues at Wetsus (Leeuwarden, The Netherlands) and the second sample set was collected from patients at the hospital MCL (Medisch Centrum Leeuwarden, The Netherlands). The urine samples were analyzed for the most abundant cations, anions, the ammonium nitrogen, total nitrogen content, protein content and the chemical oxygen demand (COD). Furthermore, the urine samples were analyzed by ^{1}H-NMR on the basis of functional groups of organic compounds commonly found in urine. Theoretical COD values were calculated from the ^{1}H-NMR results and compared to the actual measured COD values in the respective urine samples. The results show that although a broad spectrum of urine samples was taken, the composition of the organic compounds was similar in these samples. However, relatively large fluctuations in the concentrations of total organic compounds present in the urine samples were observed. This difference in the measured COD of the urine samples was caused by dilution, due to the individual water consumption of the respective sample donors. Over 73% of the COD in non-hospital samples is aliphatic and can be considered biodegradable. A higher protein content - a result of the donor's medical conditions - was found in the hospital urine samples compared to the other samples. No direct correlation between the total nitrogen concentration and the measured COD was found.

In **Chapter 3**, the application of membrane capacitive deionization (MCDI) as a tool to concentrate and recover nutrients from urine was investigated. Concentration of nutrients is of special interest in situations where urine is diluted with

flushing water. From concentrated urine, various products (i.e. hydroxyapatite and struvite) can be extracted more efficiently, due to a higher concentration of nutrients in the produced concentrate stream. The concentration step is based on the temporary storage of charged ionic compounds in the double layer formed at the electrodes while a potential is applied. The results obtained with model urine show that the flow rate has an effect on the concentration efficiency and recovery of nutrients. Higher flow rates led to high recoveries, whereas lower flow rates led to higher concentration efficiencies. By the use of MCDI it was possible to recover 99.3% of the potassium, 98.5% of the phosphate and 98.2% of the ammonium-nitrogen from diluted real urine. The limitation for recovery is the solubility of the various salts (e.g. $Ca_5(PO_4)_3(OH)$, $MgNH_4PO_4 \cdot 6\,H_2O$, $CaCO_3$) in order to avoid precipitation (scaling) inside the MCDI unit. The relatively low energy requirements (14.21 to 16.77 kJ L^{-1}) could make MCDI a potentially attractive alternative to electrodialysis. Furthermore, MCDI allows for the separation of urea (main nitrogen containing compound) from ions.

The application of a bio-electrochemical system (BES) to produce energy from a carbon source and recover ammonium at the same time was investigated in **Chapters 4 and 5**. In Microbial Fuel Cells (a specific type of a BES), bacteria catalyze the oxidation of organic substrate (e.g. $CH_3COO^- + 4\,H_2O \longrightarrow 2\,HCO_3^- + 8\,e^- + 9\,H^+$) at the anode. Due to the absence of an electron acceptor (e.g. O_2, Fe^{3+}) in the anode chamber, the electrons are transported over an external electric circuit to the cathode. At the cathode, the electrons are used to reduce an electron acceptor (e.g. $O_2 + 2\,H_2O + 4\,e^- \longrightarrow 4\,OH^-$). The electron transport induces a charge transport (i.e. anion or cation transport) across the membrane that separates the anode and cathode chamber, to maintain the charge neutrality of the system. In case a Cation Exchange Membrane (CEM) is applied, cation transport (i.e. H_3O^+, Na^+, K^+, Mg^{2+}, Ca^{2+}, NH_4^+) occurs from the anode chamber through the CEM to the cathode chamber. In **Chapter 4**, ammonium recovery using two microbial fuel cells was investigated at high ammonium concentrations to demonstrate the feasibility of the aforementioned concept. Increasing the ammonium concentration (from 0.07 g to 4 g ammonium-nitrogen L^{-1}) by addition of ammonium chloride did not affect the performance of the MFC. The obtained current densities measured by DC-voltammetry were higher than 6 A m^{-2} for both operated MFCs. During continuous operation a current density of 0.9 A m^{-2} was achieved. Effective ammonium recovery was achieved

by a migrational ion flux through the cation exchange membrane to the cathode chamber. Furthermore, an influence of the $K_3Fe(CN)_6$-cathode on the ammonium transport was found. A high potassium concentration in the cathode chamber led to a potassium diffusion from the cathode chamber to the anode chamber. This potassium diffusion resulted in an unbalance of the anion to cation ratio within the cathode chamber. Therefore, the most prevalent cation (i.e. NH_4^+) in the anode chamber was transported to the cathode to maintain overall charge neutrality of the system.

In **Chapter 5**, a recovery concept based on the work of Chapter 4 was developed and investigated for both model and real urine. A microbial fuel cell was used to simultaneously produce energy and recover ammonium via ammonia-stripping in the cathode chamber. The microbial fuel cell was equipped with a gas diffusion cathode. The ammonium transport to the cathode occurred due to simultaneous migration of ammonium and the diffusion of ammonia. The pH on the cathode surface increased during operation due to the production of hydroxide (OH^-) according to $O_2 + 2\,H_2O + 4\,e^- \longrightarrow 4\,OH^-$ and a migrational transport of cations other than H_3O^+ and NH_4^+. During continuous MFC operation an equilibrium was reached, where forward (anode to cathode) migrational flux and backward (cathode to anode) diffusion flux of cations were equal and a maximum concentration of cations and hydroxide in the cathode chamber was reached. At this point the cathode pH remained stable, because the constant production of OH^- led to a diffusion flux of OH^- from cathode to anode. In the cathode chamber, ionic ammonium was converted to volatile ammonia due to the high pH. Ammonia was recovered from the liquid-gas boundary via volatilization and subsequent adsorption into an acid solution. An ammonium recovery rate of 3.29 g_N d^{-1} m^{-2} was achieved at a current density of 0.50 A m^{-2}. The energy balance showed a surplus of energy (3.46 kJ g_N^{-1}), which means more energy was produced than needed for the ammonium recovery. Hence, ammonium recovery and simultaneous energy production from urine by this novel approach was proven.

Chapter 6 presents an urine treatment concept in which a nutrient recovery from urine was investigated based on experiments and theoretical calculations. A process combination of phosphorus recovery via struvite precipitation and subsequent ammonium recovery using an MFC was evaluated. This chapter was divided into two parts. The first part investigated the ammonium recovery by an MFC and phosphorus recovery by struvite precipitation. The second part used the obtained results and

literature data to extrapolate the benefits from these two processes in an up-scaled situation in which one cubic meter of urine per day is treated. Possible products, the energy demand of the process combination and bottlenecks were evaluated and presented to show the feasibility of this treatment concept. The products of the proposed process are struvite ($MgNH_4PO_4 \cdot 6\,H_2O$), ammonia (or an ammonium sulfate solution) and electricity. The electricity production combined with the energy efficient ammonium recovery in the MFC were the biggest advantages of the proposed technology, as theoretical calculations show that enough electric energy is produced to operate the treatment process independently. Big risks for the deployment of the proposed technology are the high cost of the MFC technology (i.e. membrane and cathode material) in combination with the predicted income due to the relatively low value of the products.

Chapter 7 reflects on the presented work in this thesis. Especially the ammonium recovery by an MFC seems to be a promising alternative to conventional nitrogen recovery or removal processes with a wide field of applications in the future. The promising concept proposed in Chapter 6, which combines phosphate recovery by struvite precipitation and subsequent ammonium recovery by an MFC, was compared to state-of-the-art recovery concepts (SaNiPhos® from GMB and the 'Gele stroom' from DHV) for nutrient recovery from urine. All evaluated processes have good features, but only the concept proposed in Chapter 6 recovers nutrients (ammonia and phosphate) and produces energy at the same time. However, only the SaNiPhos® process is currently in operation on full scale, whereas both other technologies are still under development. In order to successfully launch the promising recovery process proposed in Chapter 6, further research and development is necessary. Looking at financial aspects, next to expected decreasing cost for material used in the MFC, benefits derived from wastewater taxes could reduce the pay-back time (return of investment) of this technology.

Samenvatting

De mensheid is afhankelijk van het gebruik van kunstmest om de veiligheid van zijn voedseltoevoer te garanderen. Jaarlijks worden bijzonder grote hoeveelheden op stikstof en fosfor gebaseerde kunstmesten toegepast. Deze worden in energie-intensieve processen geproduceerd. Naast deze energieconsumptie zijn de beschikbaarheid en kwaliteit van de fosfaaterts, welke de grondstof is voor fosforgebaseerde kunstmest, van grote zorg. Daarentegen bevat huishoudelijk afvalwater stoffen die stikstof en fosfor bevatten en zou daarom als bron gebruikt kunnen worden om deze waardevolle stoffen terug te winnen. Hoofdstuk 1 beschrijft de huidige situatie, inclusief onze afhankelijkheid en het belang van kunstmest, en daarnaast ook de huidige wijze waarop stikstof en fosfor in waterzuiveringsinstallaties wordt verwijderd en hoe deze teruggewonnen worden uit afvalwater. Stikstof en fosfor zijn essentiële voedingsstoffen voor al het leven op aarde. Doordat deze stoffen als kunstmest worden toegepast, stromen zij direct (door afwatering van akker- en weilanden) of indirect (via de dier-mens-voedselketen) de waterketen in, hetgeen tot eutroficering kan leiden. Urine draagt maar een kleine volumefractie bij aan het huishoudelijk afvalwater, maar het bevat de meeste voedingsstoffen. In huishoudens worden voedingsstoffen verdund door de gecombineerde afvoer van alle verschillende soorten afvalwater. Deze verdunning is een groot obstakel voor het terugwinnen van voedingsstoffen. Hier komt nog bij dat de voedingsstoffen in afvalwaterzuiveringen worden gezien als vervuiling en om deze reden worden omgezet in andere stoffen en worden verwijderd uit het

afvalwater. Stikstofhoudende stoffen worden vooral omgezet in inert stikstofgas in het nitrificatie-denitrificatie proces of in het Anamox proces. Fosfaat kan verwijderd worden door middel van precipitatie of via biologische processen, wat vaak resulteert in producten die een lage oplosbaarheid hebben of in producten die vervuild zijn met afvalwaterslib. Voordat deze producten gebruikt kunnen worden als kunstmest moeten deze verder behandeld worden. Urine kan apart opgevangen worden van andere afvalwaterstromen om zo verdunning te voorkomen en het op deze manier mogelijk te maken de waardevolle kunstmesten efficiënter terug te winnen. Urine zou de EU in tot 18% van de fosforbehoefte en tot 24% van de stikstofbehoefte kunnen voorzien die in de landbouw gebruikt worden als kunstmest. Daarbij komt dat urine ook een aanzienlijke hoeveelheid oxideerbare organische stoffen bevat welke gebruikt zou kunnen worden in bio-elektrochemische systemen om energie mee op te wekken. De bestaande technologiën vergen echter erg veel energie.

In hoofdstuk 2 zijn de organische en anorganische fracties van 106 urinemonsters gekarakteriseerd om hun samenstellingen en onderlinge variaties te onderzoeken. Deze karakterisatie is nuttig voor de ontwikkeling en optimalisatie van een geschikte strategie voor het terugwinnen van voedingsstoffen uit urine waarbij de potentiële energie die zich in de organische stoffen bevindt wordt gebruikt. Twee reeksen van urinemonsters zijn verzameld. De eerste reeks bestond uit urinemonsters van collega's binnen Wetsus (Leeuwarden, Nederland) en de tweede reeks bestond uit urinemonsters van patiënten van het MCL (Medisch Centrum Leeuwarden, Nederland). De urinemonsters werden geanalysserd op de meest voorkomende kationen, anionen, het ammoniumstikstof, het totale stikstofgehalte, het eiwitgehalte en het chemisch zuurstofverbruik (CZV). Verder werden de urinemonsters geanalyseerd met behulp van ^{1}H-NMR op de functionele groepen van de meest voorkomende organische stoffen in urine. Uit de resultaten van deze ^{1}H-NMR analyse werden theoretische waarden voor het CZV berekend en deze werden vergeleken met de daadwerkelijk gemeten CZV-waardes van de respectievelijke urinemonsters. De resultaten laten zien dat hoewel een breed spectrum aan urinemonsters was genomen, de samenstelling van de organische stoffen van deze monsters gelijk was. Er werden echter grote schommelingen gevonden in de concentraties van de organische stoffen die aanwezig zijn in de unrinemonsters. Dit verschil in de gemeten CZVs van de urinemonsters werd veroorzaakt door verdunning: de individuele waterconsumptie van de respectievelijke personen. Meer dan 73% van het CZV in de niet-ziekenhuismonsters is alifatisch en

kan als bio-afbreekbaar worden beschouwd. Vergeleken met de andere monsters werd een hoger eiwitgehalte (een resultaat van de ziektes van de personen) gevonden in de ziekenhuisurinemonsters. Er is geen directe correlatie gevonden tussen het totale stikstofgehalte en het gemeten CZV.

In hoofdstuk 3 is de toepassing van membraan capacitieve deonisatie (MCDI) om voedingsstoffen uit urine te concentreren en terug te winnen onderzocht. Het concentreren van voedingsstoffen is van speciaal belang in situaties waarin urine wordt verdund met spoelwater. Uit geconcentreerde urine kunnen namelijk verscheidene producten (bijvoorbeeld hydroxyapatiet en struviet) efficiënter worden onttrokken, doordat de concentraties van voedingsstoffen in de geproduceerde concentraatstroom hoger zijn. De concentratiestap is gebaseerd op de tijdelijke opslag van elektrisch geladen ionische stoffen in de electrochemische dubbellaag die gevormd wordt bij de elektodes terwijl een potentiaal over deze wordt toegepast. De resultaten die met een modelurine zijn behaald, laten zien dat de stromingssnelheid van de verdunde urine een effect heeft op de efficiëntie waarmee de urine geconcentreerd wordt en de voedingsstoffen worden herwonnen. Hogere stromingssnelheden leiden tot hogere herwinningen, terwijl lagere stromingssnelheden leiden tot hogere efficiënties van het concentreren van de stoffen. Met behulp van MCDI was het mogelijk om 99,3% van de kalium, 98,5% van de fosfor en 98,2% van de ammoniumstikstof uit verdunde (echte) urine terug te winnen. De limiterende factor voor de terugwinning is de oplosbaarheid van de verschillende zouten (bijvoorbeeld $Ca_5(PO_4)_3(OH)$, $MgNH_4PO_4 \cdot 6\,H_2O$, $CaCO_3$) om precipitatie van zouten in de MCDI installatie te voorkomen. De relatief lage energieconsumptie (14,21 tot 16,77 kJ L^{-1}) kan MCDI een potentieel aantrekkelijk alternatief maken voor elektrodialyse. Daarnaast maakt MCDI het mogelijk urea (de voornaamste stikstofbevattende stof) te scheiden van de ionen uit urine.

De toepassing van bio-elektrochemische systemen (BES) om energie uit een koolstofbron te produceren en tegelijkertijd ammonium terug te winnen is onderzocht in hoofdstukken 4 en 5. In biobrandstofcellen (een specifiek type BES) katalyseren bacteriën de oxidatie van een organisch substraat (bijvoorbeeld $CH_3COO^- + 4\,H_2O \longrightarrow 2\,HCO_3^- + 8\,e^- + 9\,H^+$) bij de anode. Door de afwezigheid van een elektronenacceptor (bijvoorbeeld O_2 or Fe^{3+}) in het anodecompartiment worden de elektronen door een extern elektrisch circuit naar de kathode getransporteerd. Bij de kathode worden de elektronen gebruikt om een elektronacceptor te reduceren (bij-

voorbeeld $O_2 + 2\,H_2O + 4\,e^- \longrightarrow 4\,OH^-$). Het transport van elektronen veroorzaakt een transport van lading (bijvoorbeeld anion- of kationtransport) door het membraan dat de anode- en kathodecompartimenten scheidt om de neutraliteit van lading van het systeem te behouden. In het geval dat een kationuitwisselingsmembraan (KUM) wordt toegepast, treedt kationtransport (bijvoorbeeld H_3O^+, Na^+, K^+, Mg^{2+}, Ca^{2+}, NH_4^+) op van het anodecompartiment door het KUM naar het kathodecompartiment. In hoofdstuk 4 is de ammoniumherwinning van twee biobrandstofcellen onderzocht bij hoge ammoniumconcentraties om de haalbaarheid van het eerder genoemde concept te demonstreren. De prestaties van de biobrandstofcellen werden niet negatief beïnvloed door het laten toenemen van de ammoniumconcentratie (van 0,07 g tot 4 g ammoniumstikstof L^{-1}) door toevoeging van ammoniumchloride. De behaalde stroomdichtheden gemeten door middel van gelijkstroomvoltametrie waren hoger dan 6 A m^{-2} voor beide biobrandstofcellen. Tijdens continue operatie werd een stroomdichtheid van 0,9 A m^{-2} behaald. Een effectieve ammoniumherwinning werd behaald door een migrationele flux van ionen door het kationuitwisselingsmembraan naar het kathodecompartiment. Verder werd een invloed van de $K_3Fe(CN)_6$-kathode op het ammoniumtransport gevonden. Een hoge kaliumconcentratie in het kathodecompartiment leidde tot diffusie van kalium van het kathodecompartiment naar het anodecompartiment. Deze kaliumdiffusie resulteerde in een inbalans in de anion-kationratio binnen het kathodecompartiment. Hierdoor werd het meest voorkomende kation in het anodecompartiment (bijvoorbeeld NH_4^+) getransporteerd naar de kathode om de algehele neutraliteit van lading van het systeem te behouden.

In hoofdstuk 5 is een herwinningsconcept dat gebaseerd is op het werk uit hoofdstuk 4 ontwikkeld en getest met zowel modelurine als echte urine. Een biobrandstofcel werd gebruikt om tegelijkertijd energie te produceren en ammonium te herwinnen via ammoniakstrippen in het kathodecompartiment. De biobrandstofcel was uitgerust met een gasdiffusiekathode. Het ammoniumtransport naar de kathode vond plaats door gelijktijdige migratie van ammonium en diffusie van ammoniak. De pH aan het kathode-oppervlak steeg tijdens operatie door de productie van hydroxylionen (OH^-) volgens $O_2 + 2\,H_2O + 4\,e^- \longrightarrow 4\,OH^-$ en een migratietransport van kationen anders dan H_3O^+ en NH_4^+. Tijdens continue operatie van de biobrandstofcel werd een evenwicht bereikt waarin de voorwaardse (anode naar kathode) migratieflux en de achterwaardse (kathode naar anode) diffusieflux van kationen gelijk waren en een maximale concentratie van kationen en hydroxyl werd bereikt in het kathodecom-

partiment. In dit stadium bleef de pH van de kathode stabiel, omdat de constante productie van OH^- leidde tot een diffusieflux van OH^- van de kathode naar de anode. In het kathodecompartiment werd ionisch ammonium omgezet naar vluchtig ammoniak door de hoge pH. Ammoniak werd teruggewonnen uit de vloeistof-gasgrenslaag via verdamping en daaropvolgende adsorptie in een zuuroplossing. Een ammonium-herwinningssnelheid van 3,29 g_N d^{-1} m^{-2} werd behaald bij een stroomdichtheid van 0,50 A m^{-2}. De energiebalans laat een overschot van energie zien (3,46 kJ g_N^{-1}), wat betekent dat meer energie werd geproduceerd dan dat er benodigd was voor de herwinning van ammonium. Hiermee is de terugwinning van ammonium met gelijktijdige energieproductie uit urine door deze nieuwe aanpak bewezen.

Hoofdstuk 6 presenteert een urinebehandelingsconcept waarin een voedingsstoffenherwinning uit urine onderzocht werd, gebaseerd op experimenten en theoretische berekeningen. Een combinatie van de processen van fosforherwinning via struvietprecipitatie en een opeenvolgende ammoniumherwinning met behulp van een biobrandstofcel werd geëvalueerd. Dit hoofdstuk is in twee gedeeltes verdeeld. Het eerste deel onderzocht ammoniumherwinning door een biobrandstofcel en fosforherwinning door struvietprecipitatie. Het tweede deel gebruikte de behaalde resultaten en gegevens uit de literatuur om de voordelen van deze twee processen te extrapoleren naar een opgeschaalde situatie waarin één kubieke meter urine per dag wordt behandeld. Mogelijke producten, de energiebehoefte van de combinatie van de processen en knelpunten werden geëvalueerd en gepresenteerd om de haalbaarheid van dit behandelingsconcept te laten zien. De producten van het voorgestelde proces zijn struviet ($MgNH_4PO_4 \cdot 6H_2O$), ammoniak (of een ammoniumsulfaatoplossing) en elektriciteit. De productie van elektriciteit gecombineerd met de energie-efficiënte ammoniumherwinning in de biobrandstofcel waren de grootste voordelen van de voorgestelde technologie, omdat theoretische berekeningen laten zien dat genoeg elektrische energie wordt geproduceerd om het behandelingsproces onafhankelijk te laten opereren. De grootste risico's voor de inzetbaarheid van de voorgestelde technologie zijn de hoge kosten van de biobrandstofceltechnologie (bijvoorbeeld het membraan- en het kathodemateriaal) in combinatie met het voorspelde inkomen door de relatief lage waarde van de producten.

Hoofdstuk 7 beschouwt het in deze thesis gepresenteerde werk. Vooral de ammoniumherwinning door een biobrandstofcel lijkt een veelbelovend alternatief te zijn voor conventionele stikstofherwinnings- of stikstofverwijderingsprocessen met een groot

scala aan toepassingen in de toekomst. Het veelbelovende concept dat voorgesteld werd in hoofdstuk 6, waarin fosforherwinning door struvietprecipitatie gecombineerd wordt met een daarop volgende ammoniumherwinning door een biobrandstofcel, werd vergeleken met de huidige state-of-the-art concepten (SaNiPhos® van GMB en de 'Gele stroom' van DHV) voor de herwinning van voedingsstoffen uit urine. Alle geëvalueerde processen hebben goede eigenschappen, maar alleen het concept dat in hoofdstuk 6 is voorgesteld herwint voedingsstoffen (ammoniak en fosfaat) en produceert tegelijkertijd energie. Alleen het SaNiPhos® proces wordt echter op dit moment op volledige schaal toegepast, terwijl beide andere technologiën nog ontwikkeld worden. Om het veelbelovende herwinningsproces dat in hoofdstuk 6 is voorgesteld succesvol te lanceren is verder onderzoek en verdere ontwikkeling nodig. Met het oog op financiële aspecten, naast de verwachte toename in kosten voor het materiaal dat in de biobrandstofcel gebruikt wordt, zouden inkomsten van waterzuiveringsbelastingen gebruikt kunnen worden om de terugbetaaltijd (return of investment) van deze technologie te reduceren.

Bibliography

[1] M. A. Anderson, A. L. Cudero, and J. Palma. Capacitive deionization as an electrochemical means of saving energy and delivering clean water. comparison to present desalination practices: Will it compete? *Electrochimica Acta*, 55 (12):3845–3856, 2010.

[2] The World Bank. World population, world development indicators & global development finance, 2012. URL `http://www.worldbank.org/`. Accessed on: 18 July 2012.

[3] J.L. Barnard. Elimination of eutrophication through resource recovery. In K. Ashley, D. Mavinic, and F. Koch, editors, *International Conference on Nutrient Recovery from Wastewater Streams*, pages 1–22, Vancouver BC, Canada, 2009. IWA Publishing.

[4] J. Behrendt, E. Arevalo, H. Gulyas, J. Niederste-Hollenberg, A. Niemiec, J. Zhou, and R. Otterpohl. Production of value added products from separately collected urine. *Water Science and Technology*, 46(6-7):341–346, 2002.

[5] M. I. H. Bhuiyan, D. S. Mavinic, and F. A. Koch. Thermal decomposition of struvite and its phase transition. *Chemosphere*, 70(8):1347–1356, 2008.

[6] P. M. Biesheuvel. Thermodynamic cycle analysis for capacitive deionization. *Journal of Colloid and Interface Science*, 332(1):258–264, 2009.

[7] P. M. Biesheuvel and A. van der Wal. Membrane capacitive deionization. *Journal of Membrane Science*, 346(2):256–262, 2010.

[8] I. Bisschops, M. van Eekert, F. van Rossum, M. Wilschut, and H. van der Spoel. Betuwse kunstmest: Winning van stikstof en fosfaat uit urine. Technical Report 2010-30, STOWA, 2010.

[9] M. M. Bradford. A rapid and sensitive method for the quantitation of microgram quantities of protein utilizing the principle of protein dye binding. *Analytical Biochemistry*, 72(1-2):248–254, 1976.

[10] R. Braun, P. Huber, and J. Meyrath. Ammonia toxicity in liquid piggery manure digestion. *Biotechnology Letters*, 3(4):159–164, 1981.

[11] Bruker. *Bruker Almanac 2008 Tables*. Bruker Biospin GmbH, Rheinstetten, Germany, 2008.

[12] Afvalwater Services b.v. Tarieven zuiverings- en verontreinigingsheffing in 2012, 2012. URL `http://www.afvalwaterservices.nl/withframes/pictures/pdf2012.pdf`. Accessed on: 19 December 2012.

[13] R. Cord-Ruwisch and K.Y. Law, Y.and Cheng. Ammonium as a sustainable proton shuttle in bioelectrochemical systems. *Bioresource Technology*, 102(20): 9691–9696, 2011.

[14] D. Cordell, T. T. Schmid-Neset, S. White, and J.-O. Drangert. Preferred future phosphorus scenarios: a framework for meeting long-term phosphorus needs for global food demand. In K. Ashley, D. Mavinic, and F. Koch, editors, *International Conference on Nutrient Recovery from Wastewater Streams*, pages 23–44, Vancouver BC, Canada, 2009. IWA Publishing.

[15] K. Diem and C. Lentner. *Documenta Geigy: Scientific tables*. Georg Thieme Verlag Stuttgart, 7 edition, 1975.

[16] T. Dockhorn. About the economy of phosphorus recovery. In K. Ashley, D. Mavinic, and F. Koch, editors, *International Conference on Nutrient Recovery from Wastewater Streams*, pages 145–158, Vancouver BC, Canada, 2009. IWA Publishing.

[17] J. Driver, D. Lijmbach, and I. Steen. Why recover phosphorus for recycling, and how? *Environmental Technology*, 20(7):651–662, 1999.

[18] Fertilizers Europe. Fertilizers europe - 2011 annual overview, 2012. URL `http://www.fertilizerseurope.com/site/fileadmin/issuu/Overview2011.pdf`. Accessed on: 20 July 2012.

[19] Eurostat. European demography 110/2011, 2011. URL `http://epp.eurostat.ec.europa.eu/cache/ITY_PUBLIC/3-28072011-AP/EN/3-28072011-AP-EN.PDF`. Accessed on: 10 September 2011.

[20] Sun-Kee Fan, Y.and Han and H. Liu. Improved performance of cea microbial fuel cells with increased reactor size. *Energy & Environmental Science*, 5(8):8273–8280, 2012.

[21] A. Fuerte, R. X. Valenzuela, M. J. Escudero, and L. Daza. Ammonia as efficient fuel for sofc. *Journal of Power Sources*, 192(1):170–174, 2009.

[22] Y. Gao, L. K. Pan, H. B. Li, Y. P. Zhang, Z. J. Zhang, Y. W. Chen, and Z. Sun. Electrosorption behavior of cations with carbon nanotubes and carbon nanofibres composite film electrodes. *Thin Solid Films*, 517(5):1616–1619, 2009.

[23] K. Gell, F.J. de Ruijter, P. Kuntke, M.S. de Graaff, and A.L. Smit. Safety and effectiveness of struvite from black water and urine as a phosphorus fertilizer. *Journal of Agricultural Science*, 3(2):67–80, 2011.

[24] A. Giessen. Volkskrant: 'gele stroom' uit urine krijgt internationale octrooirechten, 2012. URL `http://www.dhv.nl/Newsroom/In-de-media/2012/2012-03-13-Volkskrant--Gele-stroom-uit-urine-krijg`. Accessed on: 1st December 2012.

[25] GMB. Saniphos, http://www.saniphos.nl/, 2012. URL `http://www.gmb.eu/images1/gmb/data/SaNiPhos/Beschrijving_Saniphos-installatie.pdf`. Accessed on: 20 June 2012.

[26] B. Hamelers, T. H. J. A. Sleutels, A. W. Jeremiasse, J.W. Post, D. P. B. T. B Strik, and R. A. Rozendal. Technological factors affecting bes performance and bottlenecks towards scale up. In K. Rabaey, L. Angenent, U. Schröder, and J. Keller, editors, *Bioelectrochemical Systems - From Extracellular Electron*

Transfer to Biotechnological Application, pages 203–223. IWA, London, UK, 2010.

[27] H.V.M. Hamelers, A. Ter Heijne, T.H.J.A. Sleutels, A.W. Jeremiasse, D.P.B.T.B. Strik, and C.J.N. Buisman. New applications and performance of bioelectrochemical systems. *Applied Microbiology and Biotechnology*, 85(6): 1673–1685, 2010.

[28] Yuankang He and E. L. Cussler. Ammonia permeabilities of perfluorosulfonic membranes in various ionic forms. *Journal of Membrane Science*, 68(1-2):43–52, 1992.

[29] Zhen He, Jinjun Kan, Yanbing Wang, Yuelong Huang, Florian Mansfeld, and Kenneth H. Nealson. Electricity production coupled to ammonium in a microbial fuel cell. *Environmental Science & Technology*, 43(9):3391–3397, 2009.

[30] Hefpunt. Zuiveringsheffing/verontreinigingsheffing, 2012. URL `http://www.hefpunt.nl/verordeningen`. Accessed on: 18 July 2012.

[31] D. Hellstrom, E. Johannson, and K. Grennberg. Storage of human urine: acidification as a method to inhibit decomposition of urea. *Ecological Engineering*, 12(3-4):253–269, 1999.

[32] K. Hemmes, P. Luimes, A. Giesen, A. Hammenga, P. V. Aravind, and H. Spanjers. Ammonium and phosphate recovery from wastewater to produce energy in a fuel cell. *Water Practice and Technology*, 6(4), 2011.

[33] I. Ieropoulos, J. Greenman, and C. Melhuish. Urine utilisation by microbial fuel cells; energy fuel for the future. *Physical Chemistry Chemical Physics*, 14 (1):94–98, 2012.

[34] M. Ikematsu, K. Kaneda, M. Iseki, and M. Yasuda. Electrochemical treatment of human urine for its storage and reuse as flush water. *Science of the Total Environment*, 382(1):159–164, 2007.

[35] A.W. Jeremiasse. *Cathode innovations for enhanced H2 production through microbial electrolysis*. Phd thesis, Wageningen UR, 2011.

136

[36] A.W. Jeremiasse, H.V.M. Hamelers, M. Saakes, and C.J.N. Buisman. Ni foam cathode enables high volumetric h2 production in a microbial electrolysis cell. *International Journal of Hydrogen Energy*, 35(23):12716–12723, 2010.

[37] M. S. M. Jetten, I. Cirpus, B. Kartal, L. van Niftrik, K. T. van de Pas-Schoonen, O. Sliekers, S. Haaijer, W. van der Star, M. Schmid, J. van de Vossenberg, I. Schmidt, H. Harhangi, M. van Loosdrecht, J. G. Kuenen, H. O. den Camp, and M. Strous. 1994-2004: 10 years of research on the anaerobic oxidation of ammonium. *Biochemical Society Transactions*, 33:119–123, 2005.

[38] T. C. Jorgensen and L. R. Weatherley. Ammonia removal from wastewater by ion exchange in the presence of organic contaminants. *Water Research*, 37(8): 1723–1728, 2003.

[39] J. R. Kim, Y. Zuo, J. M. Regan, and B. E. Logan. Analysis of ammonia loss mechanisms in microbial fuel cells treating animal wastewater. *Biotechnology and Bioengineering*, 99(5):1120–1127, 2008.

[40] H. Kirchmann and S. Pettersson. Human urine - chemical-composition and fertilizer use efficiency. *Fertilizer Research*, 40(2):149–154, 1995.

[41] M. Kitano, Y. Inoue, Y. Yamazaki, F. Hayashi, S. Kanbara, S. Matsuishi, T. Yokoyama, S. W. Kim, M. Hara, and H. Hosono. Ammonia synthesis using a stable electride as an electron donor and reversible hydrogen store. *Nature Chemistry*, 4(11):934–940, 2012.

[42] I.W. Koster. Characteristics of the ph-influenced adaptation of methanogenic sludge to ammonium toxicity. *Journal of Chemical Technology and Biotechnology*, 36(10):445–455, 1986.

[43] I.W. Koster and E. Koomen. Ammonia inhibition of the maximum growth rate of hydrogenotrophic methanogens at various ph-levels and temperatures. *Applied Microbiology and Biotechnology*, 28(4):500–505, 1988.

[44] K. Kujawa-Roeleveld and G. Zeeman. Anaerobic treatment in decentralised and source-separation-based sanitation concepts. *Reviews in Environmental Science and Biotechnology*, 5(1):115–139, 2006.

[45] P. Kuntke, M. Geleji, H. Bruning, G. Zeeman, H.V.M. Hamelers, and C.J.N. Buisman. Effects of ammonium concentration and charge exchange on ammonium recovery from high strength wastewater using a microbial fuel cell. *Bioresource Technology*, 102(6):4376–4382, 2011.

[46] P. Kuntke, K. M. Śmiech, H. Bruning, G. Zeeman, M. Saakes, T.H.J.A. Sleutels, H.V.M. Hamelers, and C.J.N. Buisman. Ammonium recovery and energy production from urine by a microbial fuel cell. *Water Research*, 46(8):26272636, 2012.

[47] J. Larminie and A. Dicks. *Fuel Cell Systems Explained*. John Wiley & Sons Ltd, Chichester, West Sussex, England, 2nd edition edition, 2003.

[48] T.A. Larsen and W. Gujer. Separate management of anthropogenic nutrient solutions (human urine). *Water Science and Technology*, 34(3-4):87–94, 1996.

[49] J. B. Lee, K. K. Park, H. M. Eum, and C. W. Lee. Desalination of a thermal power plant wastewater by membrane capacitive deionization. *Desalination*, 196(1-3):125–134, 2006.

[50] H. B. Li, Y. Gao, L. K. Pan, Y. P. Zhang, Y. W. Chen, and Z. Sun. Electrosorptive desalination by carbon nanotubes and nanofibres electrodes and ion-exchange membranes. *Water Research*, 42(20):4923–4928, 2008.

[51] B. B. Lind, Z. Ban, and S. Byden. Nutrient recovery from human urine by struvite crystallization with ammonia adsorption on zeolite and wollastonite. *Bioresource Technology*, 73(2):169–174, 2000.

[52] B. B. Lind, Z. Ban, and S. Byden. Volume reduction and concentration of nutrients in human urine. *Ecological Engineering*, 16(4):561–566, 2001.

[53] B. E. Logan, B. Hamelers, R. A. Rozendal, U. Schroerder, J. Keller, S. Freguia, P. Aelterman, W. Verstraete, and K. Rabaey. Microbial fuel cells: Methodology and technology. *Environmental Science & Technology*, 40(17):5181–5192, 2006.

[54] M. T. Madigan, J. M. Martinko, and J. Parker. *Brock biology of microorganisms*. Prentice Hall, Upper Saddle Ruver, NJ07458, 9 edition, 2000.

[55] M. Maurer, P. Schwegler, and T.A. Larsen. Nutrients in urine: energetic aspects of removal and recovery. *Water Science and Technology*, 48(1):37–46, 2003.

138

[56] M. Maurer, W. Pronk, and T. A. Larsen. Treatment processes for source-separated urine. *Water Research*, 40(17):3151–3166, 2006.

[57] J.W. McGrath and J. P. Quinn. Biological phosphorus removal. In E. Valsami-Jones, editor, *Phosphorus in Environmental Technology - Principles and Application*, pages 272–290. IWA Publishing, London, UK, 2004.

[58] H.L.T. Mobley and R.P. Hausinger. Microbial ureases - significance, regulation, and molecular characterization. *Microbiological Reviews*, 53(1):85–108, 1989.

[59] T. Mueller, B. Walter, A. Wirtz, and A. Burkovski. Ammonium toxicity in bacteria. *Current Microbiology*, 52(5):400–406, 2006.

[60] E. V. Münch and K. Barr. Controlled struvite crystallisation for removing phosphorus from anaerobic digester sidestreams. *Water Research*, 35(1):151–159, 2001.

[61] Joo-Youn Nam, Hyun-Woo Kim, and Hang-Sik Shin. Ammonia inhibition of electricity generation in single-chambered microbial fuel cells. *Journal of Power Sources*, 195(19):6428–6433, 2010.

[62] M. Ni, M. K. H. Leung, and D. Y. C. Leung. Ammonia-fed solid oxide fuel cells for power generation-a review. *International Journal of Energy Research*, 33(11):943–959, 2009.

[63] C. Niewersch, S. Petzet, J. Henkel, T Wintgens, T. Melin, and P. Cornel. Phosphorus recovery from eluated sewage sludge ashes by nanofiltration. In K. Ashley, D. Mavinic, and F. Koch, editors, *International Conference on Nutrient Recovery from Wastewater Streams*, pages 23–44, Vancouver BC, Canada, 2009. IWA Publishing.

[64] E. R. Nightingale. Phenomenological theory of ion solvation - effective radii of hydrated ions. *Journal of Physical Chemistry*, 63(9):1381–1387, 1959.

[65] U.S. Department of the Interior & U.S. Geological Survey. Mineral commodity summaries, phosphate rock 2012, 2012. URL `http://minerals.usgs.gov/minerals/pubs/commodity/phosphate_rock/index.html`. Accessed on: 18 July 2012.

[66] D. Pant, G. Van Bogaert, L. Diels, and K. Vanbroekhoven. A review of the substrates used in microbial fuel cells (mfcs) for sustainable energy production. *Bioresource Technology*, 101(6):1533–1543, 2010.

[67] S.A. Parsons and T.-A. Berry. Chemical phosphorus removal. In E. Valsami-Jones, editor, *Phosphorus in Environmental Technology - Principles and Application*, pages 260–271. IWA Publishing, London, UK, 2004.

[68] T. H. Pham, P. Aelterman, and W. Verstraete. Bioanode performance in bioelectrochemical systems: recent improvements and prospects. *Trends in Biotechnology*, 27(3):168–178, 2009.

[69] T.H. Pham, J.K. Jang, H.S. Moon, I.S. Chang, and B.H. Kim. Improved performance of microbial fuel cell using membrane-electrode assembly. *Journal of Microbiology and Biotechnology*, 15(2):438–441, 2005.

[70] G.K.S. Prakash, F.A. Viva, O. Bretschger, B. Yang, M. El-Naggar, and K. Nealson. Inoculation procedures and characterization of membrane electrode assemblies for microbial fuel cells. *Journal of Power Sources*, 195(1):111–117, 2010.

[71] W. Pronk, M. Biebow, and M. Boller. Electrodialysis for recovering salts from a urine solution containing micropollutants. *Environmental Science & Technology*, 40(7):2414–2420, 2006a.

[72] W. Pronk, H. Palmquist, M. Biebow, and M. Boller. Nanofiltration for the separation of pharmaceuticals from nutrients in source-separated urine. *Water Research*, 40(7):1405–1412, 2006b.

[73] K. Rabaey and W. Verstraete. Microbial fuel cells: novel biotechnology for energy generation. *Trends in Biotechnology*, 23(6):291–298, 2005.

[74] J. Rockström, W. Steffen, K. Noone, A. Persson, F.S. Chapin, E.F. Lambin, T.M. Lenton, M. Scheffer, C. Folke, H.J. Schellnhuber, B. Nykvist, C.A. de Wit, T. Hughes, S. van der Leeuw, H. Rodhe, S. Sörlin, P.K. Snyder, R. Costanza, U. Svedin, M. Falkenmark, L. Karlberg, R.W. Corell, V.J. Fabry, J. Hansen, B. Walker, D. Liverman, K. Richardson, P. Crutzen, and J.A. Foley. A safe operating space for humanity. *Nature*, 461(7263):472–475, 2009.

[75] M. Ronteltap, M. Maurer, and W. Gujer. Struvite precipitation thermodynamics in source-separated urine. *Water Research*, 41(5):977–984, 2007.

[76] M. Ronteltap, M. Maurer, and W. Gujer. The behaviour of pharmaceuticals and heavy metals during struvite precipitation in urine. *Water Research*, 41 (9):1859–1868, 2007.

[77] R.A. Rozendal. *Hydrogen producion through biocatalyzed electrolysis*. PhD thesis, Wageningen University, 2008.

[78] R.A. Rozendal, H.V.M. Hamelers, and C.J.N. Buisman. Effects of membrane cation transport on ph and microbial fuel cell performance. *Environmental Science & Technology*, 40(17):5206–5211, 2006.

[79] R.A. Rozendal, H.V.M. Hamelers, K. Rabaey, J. Keller, and C.J.N. Buisman. Towards practical implementation of bioelectrochemical wastewater treatment. *Trends in biotechnology*, 26(8):450–459, 2008.

[80] R.A. Rozendal, T.H.J.A. Sleutels, H.V.M. Hamelers, and C.J.N. Buisman. Effect of the type of ion exchange membrane on performance, ion transport, and ph in biocatalyzed electrolysis of wastewater. *Water Science and Technology.*, 57(11):1757–1762, 2008.

[81] S. H. Shin, Y. J. Choi, S. H. Na, S. H. Jung, and S. Kim. Development of bipolar plate stack type microbial fuel cells. *Bulletin of the Korean Chemical Society*, 27(2):281–285, 2006.

[82] T. H. J. A. Sleutels, A. Ter Heijne, C. J. N. Buisman, and H. V. M. Hamelers. Bioelectrochemical systems: An outlook for practical applications. *Chemsuschem*, 5(6):1012–1019, 2012.

[83] T.H.J.A. Sleutels, R. Lodder, H. V. M. Hamelers, and C. J. N. Buisman. Improved performance of porous bio-anodes in microbial electrolysis cells by enhancing mass and charge transport. *International Journal of Hydrogen Energy*, 34(24):9655–9661, 2009a.

[84] T.H.J.A. Sleutels, H.V.M. Hamelers, R.A. Rozendal, and C.J.N. Buisman. Ion transport resistance in microbial electrolysis cells with anion and cation ex-

change membranes. *International Journal of Hydrogen Energy*, 34(9):3612–3620, 2009b.

[85] A. Boudghene Stambouli and E. Traversa. Solid oxide fuel cells (sofcs): a review of an environmentally clean and efficient source of energy. *Renewable and Sustainable Energy Reviews*, 6(5):433–455, 2002.

[86] Centraal Bureau voor de Statistiek. Aardgas en elektriciteit; gemiddelde tarieven 1996-2012, 2012. URL `http://statline.cbs.nl/StatWeb/publication/?DM=SLNL&PA=37359/`. Accessed on: 20 August 2012.

[87] V. Stefov, B. Soptrajanov, F. Spirovski, I. Kuzmanovski, H. D. Lutz, and B. Engelen. Infrared and raman spectra of magnesium ammonium phosphate hexahydrate (struvite) and its isomorphous analogues. i. spectra of protiated and partially deuterated magnesium potassium phosphate hexahydrate. *Journal of Molecular Structure*, 689(1-2):1–10, 2004.

[88] V. Stefov, B. Soptrajanov, I. Kuzmanovski, H. D. Lutz, and B. Engelen. Infrared and raman spectra of magnesium ammonium phosphate hexahydrate (struvite) and its isomorphous analogues. iii. spectra of protiated and partially deuterated magnesium ammonium phosphate hexahydrate. *Journal of Molecular Structure*, 752(1-3):60–67, 2005.

[89] OLI system Inc. A guide to using oli analyzer studio, 2009.

[90] G. Tchobanoglous, F. L. Burton, Metcalf, and Inc Eddy. *Wastewater engineering : treatment and reuse.* McGraw-Hill series in civil and environmental engineering. McGraw-Hill, Boston [etc.], 2003. Monograph Wageningen UR Library.

[91] A. Ter Heijne, H.V.M. Hamelers, M. Saakes, and C.J.N. Buisman. Performance of non-porous graphite and titanium-based anodes in microbial fuel cells. *Electrochimica Acta*, 53(18):5697–5703, 2008.

[92] A. Ter Heijne, F. Liu, R. van der Weijden, J. Weijma, C.J.N. Buisman, and H.V.M. Hamelers. Copper recovery combined with electricity production in a microbial fuel cell. *Environmental Science & Technology*, 44(11):4376–4381, 2010.

[93] A. Ter Heijne, F. Liu, L.S. van Rijnsoever, M. Saakes, H.V.M. Hamelers, and C.J.N. Buisman. Performance of a scaled-up microbial fuel cell with iron reduction as the cathode reaction. *Journal of Power Sources*, 196(18):7572–7577, 2011.

[94] V. Tricoli and E.L. Cussler. Ammonia selective hollow fibers. *Journal of Membrane Science*, 104(1-2):19–26, 1995.

[95] K. M. Udert, C. Fux, M. Münster, T. A. Larsen, H. Siegrist, and W. Gujer. Nitrification and autotrophic denitrification of source-separated urine. *Water Science and Technology*, 48(1):119–130, 2003.

[96] K. M. Udert, T. A. Larsen, M. Biebow, and W. Gujer. Urea hydrolysis and precipitation dynamics in a urine-collecting system. *Water Research*, 37(11): 2571–2582, 2003.

[97] K. M. Udert, T. A. Larsen, M. Biebow, and W. Gujer. Urea hydrolysis and precipitation dynamics in a urine-collecting system. *Water Research*, 37(11): 2571–2582, 2003.

[98] K. M. Udert, T. A. Larsen, and W. Gujer. Estimating the precipitation potential in urine-collecting systems. *Water Research*, 37(11):2667–2677, 2003.

[99] K.M. Udert, T.A. Larsen, and W. Gujer. Fate of major compounds in source-separated urine. *Water Science & Technology*, 54(11-12):413–420, 2006.

[100] UN. The world at six billion, 2011. URL `http://www.un.org/esa/population/publications/sixbillion/sixbillion.htm`. Accessed on: 11 May 2011.

[101] E. Valsami-Jones. *Phosphorus in Environmental Technologies: Principles and Applications*. Integrated Environmental Technology Series. IWA Publishing, London UK, 2004.

[102] L.G.J.M. van Dongen, M.S.M. Jetten, and M.C.M van Loosdrecht. Het combineerde sharon/anammoxproces. Technical Report 2000-25, STOWA, 2000.

[103] L.G.J.M. van Dongen, M.S.M. Jetten, and M.C.M van Loosdrecht. The sharon-anammox process for treatment of ammonium rich wastewater. *Water Science and Technology*, 44(1):153–160, 2001.

[104] A.F.M. van Velsen. *Aneaobic digestion of piggery waste*. PhD thesis, Wageningen University, 1981.

[105] A.V. Vorobiev and I.N. Beckman. Ammonia and carbon dioxide permeability through perfluorosulfonic membranes. *Russian Chemical Bulletin*, 51(2):275–281, 2002.

[106] G. Wanders. Quotation from m.a.f. magnesite, 2012. URL `http://www.magnesiumoxide.com/`. received on: 2 May 2012.

[107] T. J. Welgemoed and C. F. Schutte. Capacitive deionization technology (tm) : An alternative desalination solution. *Desalination*, 183(1-3):327–340, 2005.

[108] J. A. Wilsenach. *Treatment of source separated urine and its effects on wastewater systems*. Phd thesis, TU Delft, 2006.

[109] J. A. Wilsenach and M. C. M. Van Loosdrecht. Effects of separate urine collection on advanced nutrient removal processes. *Environmental Science & Technology*, 38(4):1208–1215, 2004.

[110] J. A. Wilsenach, M. Maurer, T. A. Larsen, and M. C. M. van Loosdrecht. From waste treatment to integrated resource management. *Water Science and Technology*, 48(1):1–9, 2003.

[111] J. A. Wilsenach, C. A. H. Schuurbiers, and M. C. M. van Loosdrecht. Phosphate and potassium recovery from source separated urine through struvite precipitation. *Water Research*, 41(2):458–466, 2007.

[112] M. Winker, B. Vinnerås, A. Muskolus, U. Arnold, and J. Clemens. Fertiliser products from new sanitation systems: Their potential values and risks. *Bioresource Technology*, 100(18):4090–4096, 2009.

[113] P. Xu, J. E. Drewes, D. Heil, and G. Wang. Treatment of brackish produced water using carbon aerogel-based capacitive deionization technology. *Water Research*, 42(10-11):2605–2617, 2008.

[114] C. M. Yang, W. H. Choi, B. K. Na, B. W. Cho, and W. I. Cho. Capacitive deionization of nacl solution with carbon aerogel-silicagel composite electrodes. *Desalination*, 174(2):125–133, 2005.

[115] Guo-Long Zang, Guo-Ping Sheng, Wen-Wei Li, Zhong-Hua Tong, Raymond J. Zeng, Chen Shi, and Han-Qing Yu. Nutrient removal and energy production in a urine treatment process using magnesium ammonium phosphate precipitation and a microbial fuel cell technique. *Physical Chemistry Chemical Physics*, 14 (6), 2012.

[116] G. Zeeman. *Mesophilic and psychrophilic digestion of liquid manure*. PhD thesis, Wageningen University, 1991.

[117] F. Zhao, F. Harnisch, U. Schröder, F. Scholz, P. Bogdanoff, and I. Herrmann. Challenges and constraints of using oxygen cathodes in microbial fuel cells. *Environmental Science & Technology*, 40(17):5193–5199, 2006.

[118] R. Zhao, P. M. Biesheuvel, and A. van der Wal. Energy consumption and constant current operation in membrane capacitive deionization. *Energy & Environmental Science*, 5(11):9520–9527, 2012.

Acknowledgements

After 5.5 years of work, a wide range of experiments and countless analyzed (urine) samples finally here it is: My PhD-Thesis! Of course all of this would not have been possible without the contribution of others, which helped, supported and advised me on this adventurous journey. First of all, I would like to thank Cees, Gert-Jan, Grietje, Harry and Johannes, who gave me the chance to pursue this research project at Wetsus after a series of interviews at the Wetsus Water Challenge and at the Sub-department of Environmental Technology of Wageningen University (ETE).

I wish to express my gratitude to my supervisors; Cees as my promotor for our inspiring meetings, during which you sketched the bigger picture, the possibilities and future impact of this research. Grietje and Harry, I am grateful for our discussions in which you helped me finding back reality, the encouragement and the advise on my work. I would like to thank Gert-Jan for many useful discussions during the start of my project and Sybrand for the daily supervision at Wetsus. I would like to especially thank Bert and Michel, although you were not my supervisors, you were always willing to help and support me during my first steps into the fascinating world of bioelectrochemical systems. I would like to thank the Separation at Source theme and the Stowa guiding committee for support and helpful discussions.

Many thanks go to the current and former technical, analytical, administrative and secretarial staff of Wetsus and Wageningen for their support; Wim, Harm, Harry, Jan, Foppe and Ernst for all the help in building setups, organizing/ ordering materials

and answers to my numerous questions. Janneke, Jelmer, Pieter, Mieke, Marianne, Ton and Bob (Wetsus) and Katja, Vinnie and Jean (Wageningen) for their help with countless sample analyses. Trienke, Helena, Linda, Hester, Nynke, Roely, Geke, Albert, Jan, Petra (Wetsus) and Liesbeth, Anita and Ramona (Wageningen); thank you for your support and help.

I would like to thank Bart, Bruno, Tom, Adriaan, Elsemiek, Urania, Annemiek, Alexandra and Rene for their help during my exploration into the world of membrane capacitive deionization and bioelectrochemical systems, respectively. Marthe, Lucía, Natasja, Loes, Andrii and Taina thank you for your help and useful discussions in the Separation at Source theme.

My students; Kealan, Magdolna and Karolina you all performed excellently and I am grateful for your help, hard work and your input during our cooperation. I had great time working with you.

A special thank you to my office mates Perry, Paula, Tim, Maxime, Camiel, Luewton, Claudia D. and Nadine (HW1.05) and Astrid, Martina, Doekle, Maria and Sam (VX0.03) for creating a nice office atmosphere for working and every now and then a small diversion.

Alexandra and Ingo; thank you for being my paranymphs and your help during this last step of my time as PhD Candidate. Ingo; thank you for being a friend, always having the time to listen, to give advise and share your sarcasm. Alexandra; thank you for all your help and being a friend. All this made working and living in Leeuwarden easier (especially in the beginning).

Adam, Adriaan, Agata, Aleid, Ana Marta (and Carsten), Astrid, Bart (and family), Bruno (and Rita), Camiel, Christina (and Pablo), Claudia S., Claudia D. (and Norman), Daniel, Doekle, Dries, Elmar, Elsemiek, Justina, Jos, Kamuran, Lena, Loes, Lina, Lucía, Luewton (and his family), Marthe, Marco, Mariana, Martijn B. (and Jennifer), Martina, Maxime, Nadine (and Eric), Olivier (and Loreline), Odne, Paula, Petra, Piotr, Roel, Tom, Taina, and Urania; thank you for all the good times during and outside the Wetsus working hours.

I also would like to thank all Wetsians and Wageningen colleagues from ETE for creating a great working atmosphere and all the inspiring talks, and help.

I am grateful for the help of the Wetsus LaTeXusers group; Lucía, Ingo, Bart and Martijn W.: your valuable input saved me from some frustration.

My never-ending thanks go to my family for their love and enormous support during

this adventure: my father Andreas, my mother Dagmar, my brother Fabian, my sister Anika, my grandmothers Gisela and Gerda and my Grandfather Lothar (27/01/1931 - 10/02/2011). Also I would like to thank Dirk, Abie and Inge Bruinenberg for the good times.

Sandra, I could not have done it without you and I cannot thank you enough for your love, the encouragement and support.

<div align="right">

Philipp Kuntke

Leeuwarden

March 2013

</div>

About the author

Philipp Kuntke was born on 29 April 1981 in Duisburg, Germany. In 2001 he started his study of Water Science at the University of Duisburg, Germany (since 2003 the University of Duisburg-Essen) in the department of Chemistry. His MSc project New Approaches for Managing a Chloraminated Distribution System focused on the development of an ammonia sensor and disinfection control of a drinking water distribution system. This work was carried out at the Australian Water Quality Centre (AWQC, Adelaide, South Australia) under the supervision of Prof. Dr. H-C Flemming (Uni Du-E) and Dr. C.W.K Chow (AWQC). He graduated in 2006. In 2007 he started research on nutrient and energy recovery from urine as a PhD student at the Sub-department of Environmental Technology, Wageningen University, but was stationed at Wetsus in Leeuwarden. In October of 2011 he started working as a researcher/(pre)postdoc at Wetsus. His focus was the application of bioelectrochemical systems for nutrient and energy recovery, which lead to the ValueFromUrine project funded by Europes 7th Framework Programme. Since October 2012 he works for Wetsus as a researcher in the ValueFromUrine project.

Sense certificate

SENSE

Netherlands Research School for the
Socio-Economic and Natural Sciences of the Environment

C E R T I F I C A T E

The Netherlands Research School for the
Socio-Economic and Natural Sciences of the Environment
(SENSE), declares that

Philipp Kuntke

born on 29 April 1981 in Duisburg, Germany

has successfully fulfilled all requirements of the
Educational Programme of SENSE.

Leeuwarden, 26 April 2013

the Chairman of the SENSE board   the SENSE Director of Education

Prof. dr. Rik Leemans   Dr. Ad van Dommelen

The SENSE Research School has been accredited by the Royal Netherlands Academy of Arts and Sciences (KNAW)

K O N I N K L I J K E   N E D E R L A N D S E
A K A D E M I E   V A N   W E T E N S C H A P P E N

The SENSE Research School declares that **Mr. Philipp Kuntke** has successfully fulfilled all requirements of the Educational PhD Programme of SENSE with a work load of 46 ECTS, including the following activities:

<u>SENSE PhD Courses</u>
o Environmental Research in Context
o Research Context Activity: Co-organizing Wetsus Water Challenge, 28-30 May 2008, Leeuwarden
o Basic Statistics
o Linear Models
o Mixed Linear Models
o Biological Processes for Resource Recovery in Environmental Technology

<u>Other PhD and Advanced MSc Courses</u>
o Electrochemistry
o Principles of Anaerobic Wastewater Treatment
o MATLAB
o Techniques for Writing and Presenting Scientific Papers

<u>Management and Didactic Skills Training</u>
o Writing and coordinating the EU FP7 project proposal *ValueFromUrine*
o Participation in the Wetsus Internal Business Challenge, 2011
o Participation in the Wetsus Rabobank Water Business Challenge, 2011
o Supervision of group work in the MSc course *Biological Processes for Resource Recovery in Environmental Technology*
o Supervision of practicals in the course *BSc Thesis Environmental Technology Part 1: Design Tools*
o Supervision of three MSc theses and one internship

<u>Oral Presentations</u>
o *MCDI as a Tool to Concentrate Nutrients from Urine,* Innovative Techniques for a Sustainable Environment, SENSE Symposium, 19-20 February 2009, Wageningen
o *Resources recovery within 'New Sanitation' - Struvite from black water and urine,* Phosphorus, from excess to shortage - can technology solve the problem? NBV, 18 November 2010, Delft
o *A novel strategy for direct ammonium recovery from wastewater using a microbial fuel cell,* 3rd International Microbial Fuel Cell Conference 2011, 06-08 June 2011, Leeuwarden
o *Ammonium recovery from urine using a microbial fuel cell*, Wetsus Congress 2011, 04 October 2011, Leeuwarden

SENSE Coordinator PhD Education

Drs. Serge Stalpers